**ANKARA YILDIRIM BEYAZIT UNIVERSITY**

**GRADUATE SCHOOL OF NATURAL AND APPLIED SCIENCES**

# FINITE ELEMENT MODELLING OF HYBRID STABILIZATION SYSTEMS FOR THE BILEVEL DISC DEGENERATION OF HUMAN LUMBAR SPINE

**Ph.D. Thesis by**

**Eylül DEMİR**

**Department of Mechanical Engineering**

**September, 2021**

**ANKARA**

# FINITE ELEMENT MODELLING OF HYBRID STABILIZATION SYSTEMS FOR THE BILEVEL DISC DEGENERATION OF HUMAN LUMBAR SPINE

**A Thesis Submitted to**

**The Graduate School of Natural and Applied Sciences of**

**Ankara Yıldırım Beyazıt University**

**In Partial Fulfillment of the Requirements for the Degree of Doctor of Philosophy in Mechanical Engineering, Department of Mechanical Engineering**

**by**

**Eylül DEMİR**

**September, 2021**

**ANKARA**

# Ph.D. THESIS EXAMINATION RESULT FORM

We have read the thesis entitled **"FINITE ELEMENT MODELLING OF HYBRID STABILIZATION SYSTEMS FOR THE BILEVEL DISC DEGENERATION OF HUMAN LUMBAR SPINE"** completed by **Eylül DEMİR** under the supervision of **Assoc. Prof. Dr. İhsan TOKTAŞ** and we certify that in our opinion it is fully adequate, in scope and in quality, as a thesis for the degree of **Philosophy of Doctorate.**

Assoc. Prof. Dr. İhsan TOKTAŞ

**Supervisor**

Prof. Dr. Sadettin ORHAN

**Jury Member**

Prof. Dr. Kürşad DÜNDAR

**Jury Member**

Prof. Dr. Zafer EVİS

**Jury Member**

Prof. Dr. Yasin KİŞİOĞLU

**Jury Member**

Prof. Dr. Sadettin ORHAN

**Director**

Graduate School of Natural and Applied Sciences

# ETHICAL DECLERATION

I hereby declare that, in this thesis which has been prepared in accordance with the Thesis Writing Manual of Graduate School of Natural and Applied Sciences,

- All data, information and documents are obtained in the framework of academic and ethical rules,
- All information, documents and assessments are presented in accordance with scientific ethics and morals,
- All the materials that have been utilized are fully cited and referenced,
- No change has been made on the utilized materials,
- All the works presented are original,

and in any contrary case of above statements, I accept to renounce all my legal rights.

**Date: 05.09.2021**

**Signature:**

**Name & Surname: Eylül DEMİR**

# ACKNOWLEDGEMENTS

Firstly, I would like to express my sincere gratitude to my supervisor Assoc. Prof. Dr. İhsan TOKTAŞ for his tremendous support, advice and motivation during my study. His knowledge and encouragement constituted the milestones of this study. His guidance assisted me all the time of my research and while writing this thesis.

I am also thankful to Prof. Dr. Damien Lacroix and Dr. Andre Castro for their helps and supports during this period. They provided me to access ABAQUS at the University of Sheffield, and University of Lisbon. I would like to thank Peter Eltes providing Computerized Tomography images of this thesis from National Center for Spinal Disorders. Their collaborations and critical contributions are very valuable. This study would have never been completed without their support.

Also, I would like to thank my dear family for their continuous encouragement and my father whose eternal love I will carry deep inside my heart.

**2021, 05 September** **Eylül DEMİR**

# FINITE ELEMENT MODELLING OF HYBRID STABILIZATION SYSTEMS FOR THE BILEVEL DISC DEGENERATION OF HUMAN LUMBAR SPINE


## ABSTRACT

Fusion is a very common treatment for spinal disorders associated with Intervertebral Disc (IVD) degeneration. Dynamic implantation systems have become the preferable solution for Degenerative Disc Disease (DDD) to eliminate the negative effects of fusion prosedure. In this thesis, different commercial Hybrid Stabilization Systems (HSSs) and a new designed HSS named as Mobile-PEEK were analysed and compared to each other for the treatment of bilevel DDD. Finite Element (FE) model of L1-S1 lumbar spine was used in the analyses and Range of Motion (ROM), Intradiscal Pressure (IDP) and von Mises Stress (VMS) in case of intact and implanted spine were calculated as there is no comparison in the literature about the efficiency of these systems. Additionaly, some new combinations of Artifical Disc Replacement (ADR) systems and the dynamic portion of HSSs were analysed to suggest optional treatments of bilevel disc degenerations. Finite Element Analysis (FEA) of the HSSs showed that such systems could be effective for providing some of the natural lumbar spine motion, while reducing the probability for increasing adjacent segment degeneration. Results revealed that the hybrid combination of B-DYN, with a less flexible dynamic portion, and artificial disc showed more mobility than the conventional B-DYN hybrid structure. Additionally, B-DYN+ADR showed no indications for adjacent segment disease and no implant failure. Similarly, Mobile-PEEK may provide valuable indications for future device developments, as it was found to have desirable elastic movement and also low pressure at adjacent segment.



**Keywords:** Lumbar spine, degenerative disc disease, finite element modelling, range of motion, intradiscal pressure, von Mises stress, hybrid stabilization, implant failure, artificial disc replacement.

# İNSAN LOMBER OMURGASININ İKİ SEVİYELİ DİSK DEJENERASYONU İÇİN HİBRİT STABİLİZASYON SİSTEMLERİNİN SONLU ELEMAN MODELLEMESİ


## ÖZ

Füzyon, intervertebral disk (IVD) dejenerasyonu ile ilişkili spinal bozukluklar için çok yaygın bir tedavidir. Dinamik implantasyon sistemleri, füzyon işleminin olumsuz etkilerini ortadan kaldırmak için dejeneratif disk hastalığı (DDD) için tercih edilen çözüm haline gelmiştir. Bu tezde, iki seviyeli dejeneratif disk hastalığının tedavisi için farklı ticari hibrit sistemler (HSSs) ve Mobile-PEEK olarak adlandırılan yeni tasarlanmış bir hibrit sistem analiz edilmiş ve birbirleriyle karşılaştırılmıştır. Analizlerde L1-S1 lomber omurganın Sonlu Eleman (FE) modeli kullanılmış ve literatürde bu sistemlerin etkinliği ile ilgili bir karşılaştırma olmadığı için omurganın sağlıklı ve implante olması durumunda hareket değeri (ROM), disk içi basınç (IDP) ve von Mises gerilmesi (VMS) hesaplanmıştır. Ek olarak, Lomber Disk Protezi (ADR) sisteminin ve hibrit sistemlerin dinamik kısmından oluşan yeni hibrit kombinasyonlar, iki seviyeli disk dejenerasyonlarına opsiyonel tedavi önermek için analiz edilmiştir. Hibrit sistemlerin sonlu elemanlar analizi, bu tür sistemlerin, artan komşu segment dejenerasyonu olasılığını azaltırken, doğal lomber omurga hareketini de korumak için etkili olabileceğini göstermiştir. Sonuçlar, daha az esnek bir dinamik parçaya sahip olan B-DYN implantı ile yapay disk hibrit kombinasyonunun, geleneksel B-DYN hibrit yapısından daha fazla hareketlilik gösterdiğini ortaya koymuştur. Ek olarak; B-DYN, komşu segment hastalığı için herhangi bir endikasyon ve hiçbir implant başarısızlığı göstermemiştir. Benzer şekilde, Mobile-PEEK, arzu edilen esneklik ve komşu segmentte düşük basınca sahip olduğu tespit edildiğinden, gelecekteki ürün tasarımları için önemli girdiler sağlayabilir.



**Anahtar Kelimeler:** Lomber omurga, dejeneratif disk hastalığı, sonlu eleman modellemesi, hareket değeri, disk içi basınç, von Mises gerilmesi, hibrit stabilizasyon, implant başarısızlığı, lomber disk protezi.

# CONTENTS

# NOMENCLATURE

| | |
|---|---|
| ADR | Artificial Disc Replacement |
| ASD | Adjacent Segment Disease |
| ALIF | Anterior Lumbar Interbody Fusion |
| ALL | Anterior Longitudinal Ligament |
| CL | Capsular Ligament |
| COMI | The Core Outcome Measures Index |
| CT | Computerized Tomography |
| DDD | Degenerative Disc Disease |
| DTO | Dynesys Transition Optima |
| FEA | Finite Element Analysis |
| HSS | Hybrid Stabilization System |
| IDP | Intradiscal Pressure |
| ISL | Interspinous Ligament |
| ITL | Intertransverse Ligament |
| IVD | Intervertebral Disc |
| LF | Ligamentum Flavum |
| ODI | Oswestry Disability Index |
| PCU | Polycarbonate urethane |
| PEEK | Polyetheretherketone |
| PET | Polyethylene terephthalate |
| PLL | Posterior longitudinal ligament |
| QCT | The Quantitative Computed Tomography |
| ROM | Range of Motion |
| SSL | Supraspinous Ligament |
| STL | Stereolithography |
| VAS | Visual Analog Scale |
| VMS | von Mises Stress |

## LIST OF TABLES

## LIST OF FIGURES

# CHAPTER 1 - INTRODUCTION

## 1.1 Literature Summary

Low back pain is the second most common disorder and can be attributed to Degenerative Disc Disease (DDD) in general [1]. Although serious ones require surgical procedures, mild DDD can be treated by bed rest and physiotherapy exercises [2]. Fusion surgeries for the spinal disorders have been used since early 1900s [1]. This technique joins two or more vertebrae stabilized by rigid rods and artificially eliminates the mobility at fused levels, as the Intervertebral Disc (IVD) is removed. Besides having benefits like providing spinal stability and relieving back pain, fusion has some important disadvantages, i.e. it causes excessive motion at the adjacent levels that may lead to re-interventions and pseudoarthrosis [2-5]. Clinical reports showed that Adjacent Segment Disease (ASD) can occur after fusion activity in the range of 12.2% to %35 [6,7]. To overcome this issue, dynamic stabilizations systems that allow partial mobility at implanted level and reduce the risk of ASD have been offered as alternatives to traditional spinal fusion techniques [8,9]. However, the long-term effects, reliability and complications are still unknown for most dynamic implants, so even the prevention of hypermobility at adjacent segment is not yet guaranteed [6].

In multilevel DDD, Hybrid Stabilization Systems (HSS) may be useful to protect the adjacent segment from excessive spinal fusion mobility [10,11]. HSS involves fusion with rigid instrumentation at extreme DDD level and non-fusion with dynamic stabilization at mild DDD level. Severe DDD levels are fused and implanted with rigid rods. The symptoms of the adjacent segment are not extreme enough to warrant arthrodesis, so dynamic implantation is favoured and this stage is preserved from hypermobility [12]. HSSs are very restricted in clinical applications and numerical analysis and further studies are needed. Most research on conventional fusion therapies with rigid fixations and dynamic stabilizations can be found at one stage, but there is a little longer-term information about HSS. In other words, due to the lack of definitive evidence, the clinical and numerical importance of HSS are still uncertain.

Artificial Disc Replacement (ADR) can also be an alternative to fusion for the therapy of severe DDD, in order to eliminate the total immobilization of given levels. ADR is a surgical method that removes the degenerated IVD and replaces it with an artificial disc, restoring the intervertebral space height while reconstructing the lumbosacral curve and minimizing the risk of ASD. In fact, this method allows for the preservation of the mobility [13,14]. Different HSSs which are composed of artificial discs and posterior/anterior implants have implemented to the selected patients suffering from multilevel DDD [1,15,16]. Bertagnoli et al. [16] stated that a number of clinical studies using artificial disc and posterior constructions at the same time provided different perspectives and promising outcomes. Patient selection is a critical issue at this point. However, short-, intermediate-, and long-term effects of hybrid IVD replacement systems should be investigated [1,15,16]. ADR systems have been used for mono and bilevel DDD, but there are limited numerical and clinical studies subjected to anterior and posterior implantations at the same time. In case of bilevel DDD, hybrid implantation is an effective method to ensure spinal stability [12, 17].

## 1.2 Purpose of the Thesis

In this thesis, the general aim is to bring a different perspectives to surgeons for the treatment of bilevel DDD. Eight different hybrid stabilization systems were modelled and analysed. Results are presented in a comparative manner, and advantages of these systems are disscussed in terms of The Range of Motion (ROM), Intradiscal Pressure (IDP) and Von Mises Stress (VMS).

## 1.3 Original Contribution

Sophisticated computer techniques for both geometric reconstruction and stress analysis have become common methods for a detailed research into lumbar spine biomechanics. Computerized tomography (CT) images were used to create three-dimensional (3D) models. Thus, essential features for the simulation of anatomical components were saved. Original contributions of this thesis can be counted as follows:

- 3D model reconstruction of lumbar spine was obtained using CT images of a patient, by considering the real anatomy of human lumbar spine,
- The Finite Element (FE) approach which has become a preferable choice for predictions of spinal stability in intact or implantation cases, was used to provide insight into tissues that can not be reached through *in vivo* and/or *in vitro* experiments,
- Mechanical results provided by FE models are comparable with *in vivo* and *in vitro* studies,
- Different stabilization perspectives were offered with a cost effective method for pre-operation planning of the surgeons,
- A new hybrid system was proposed and results may provide valuable indications for future device developments.

# CHAPTER 2 - BACKGROUND

## 2.1. Human Lumbar Spine Anatomy

The lumbar vertebral segment comprises of five vertebra, which are named by their areas in the intact spine. From upward to downward, they are named as the cervical, thoracic, lumbar, sacrum, coccyx vertebra (Figure 2.1). Lumbar region bears the upper body weight and also gives motion to upper body. Degeneration in segments including ligaments, intervertebral discs, muscles, facets etc. can lead to low back pain. The lumbar vertebra (L1-L5) conveying most of the body weight is the most affected region and major stresses arise over it.

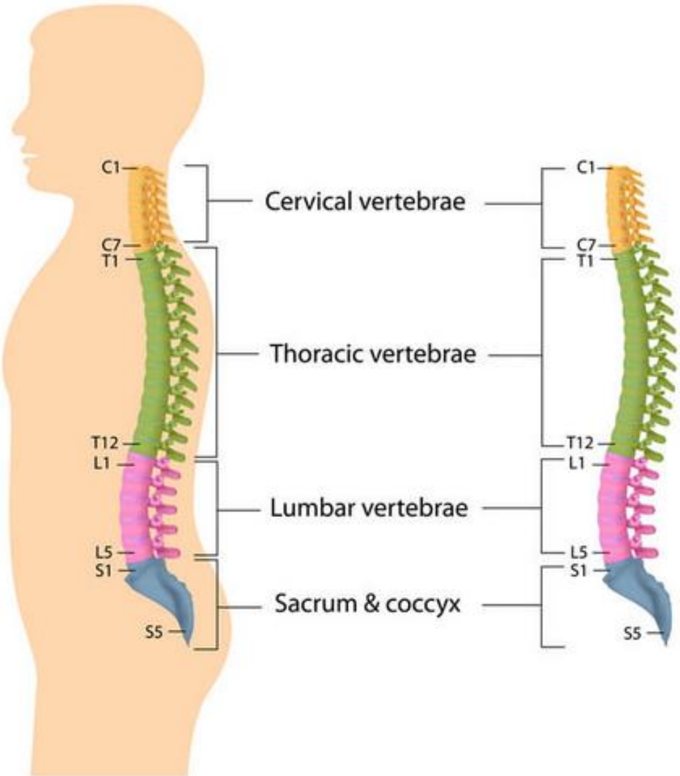


**Figure 2.1** Human spine structure [18]

### 2.1.1 Structure of Lumbar Vertebra

Biomechanical properties of the lumbar spine are dependent on the integrity of all subsystems [19]. The functional portions of a lumbar vertebra may be counted as vertebral body, the pedicles and the posterior elements as seen in Figure 2.2. Although each of these portions has its own function, each of them promotes the whole integrated function [20]. The load bearing part of the lumbar vertebra is the vertebral body. This part consists of two sections as cortical and cancellous bones, which support dynamic load-bearing and light weight structure [20]. The facet joints, are the joints formed between the superior and inferior articular processes of adjacent vertebrae. These cartilage-covered facets provide a locking mechanism [19] that allow motion in flexion, extension and lateral bending properly, however, restrict anterior translation or shear of the vertebrae and also limit the axial rotation [21].

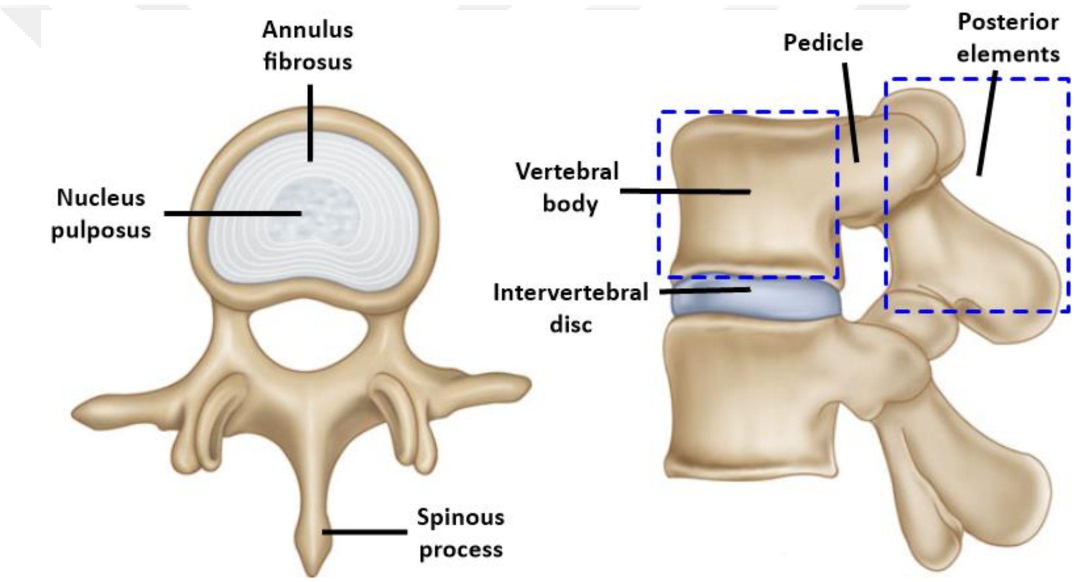


**Figure 2.2** Anatomical parts of vertebra [22]

### 2.1.2 Intervertebral Disc (IVD)

IVD consisting of annulus fibrosus and nucleus pulposus is a soft tissue structure which enables both rotations (flexion-extension, lateral bending, and axial rotation) and translations (cranial-caudal, medial-lateral, and anterior-posterior) of the vertebra [23]. IVDs have three different segments: (i) annulus fibrosus formed from concentric collagen fibers, (ii) nucleus pulposus composed of water, proteoglycans and collagen and (iii) cartilage endplates. The annulus fibrosus has lamellar structure and covers the nucleus pulposus. Nucleus pulposus can absorb the impact energy of the spine under motion [24]. A cartilage endplate, which joins the vertebral body and intervertebral disc, supports a nutritional way to the intervertebral disc [19]. The intervertebral disc enables nearly 40% to 50% of torque strength, while the posterior elements and the interspinous ligaments secure the rest of it [25].

### 2.1.3 Ligaments

Ligaments of the lumbar spine enable passive tensile resistance under loading. Seven different ligaments exist over the spine and provide stability depending on the strength and arrangement. DDD reduce the tension of the ligaments, thus causes to decrease the fuctionality of them in providing stability of translation and rotation [19]. Ligaments in real anatomy can be counted as follows: anterior longitudinal ligament (ALL), posterior longitudinal ligament (PLL), ligamentum flavum (LF), intertransverse ligament (ITL), interspinous ligament (ISL), supraspinous ligament (SSL), capsular ligament (CL). Ligaments covering lumbar spine can be seen in Figure 2.3.

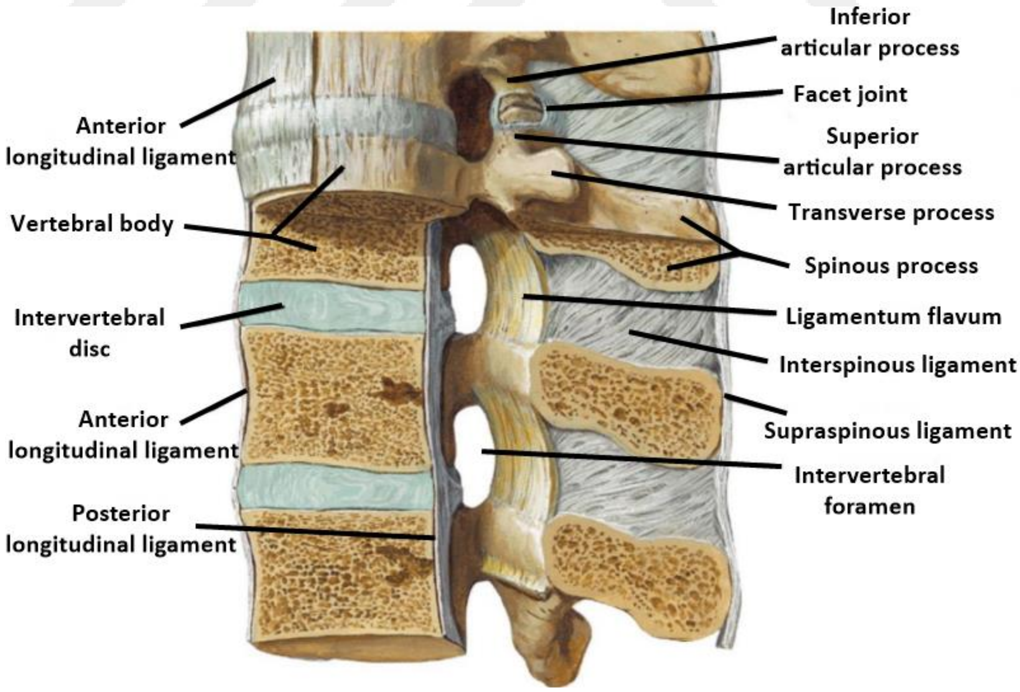


**Figure 2.3** Ligaments of lumbar spine [26]

## 2.2 Kinematics of Spine

The vertebral column has six degrees of freedom around X, Y, and Z axes as seen in Figure 2.4. There are rotations around these axes as follows:

- Rotation around the X-axis: Flexion–Extension
- Rotation around the Y-axis: Right and Left Axial Rotation
- Rotation around the Z-axis: Right and Left Lateral Bending.

In addition, lumbar spine has translational displacements along three axes. The movements can occur by means of disc and facet joints [27].

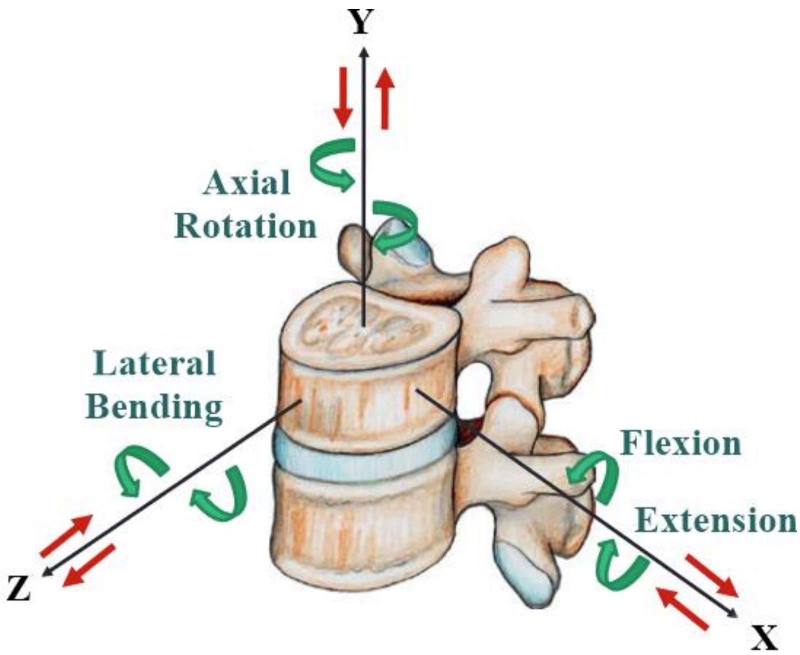


**Figure 2.4** Kinematics of lumbar spine [27]

## 2.3 Degenerative Disc Disease (DDD)

Principal functionalities of the IVD provide joint mobility and transmit axial loads between the vertebrae. Together with the vertebrae, the disc resists almost 80% of the compressive force in standing [19]. Several theories about the formation of DDD are mechanical, age-related, chemical, autoimmune, hereditary, and genetic factors [28]. Injury or degenerative processes affect the natural balance and lead to a transfer in undesirable loads to the spinal structures. By this way, pain or dysfunction occurs.

Degenerative diseases change the mechanical properties of IVD [19]. A degenerated IVD diminishes the capacity of shock absorption and the disc becomes less flexible due to the misfortune liquid within it [29]. A reduction in water substance of the core pulposus with intervertebral plate degeneration leads to changes within the fabric properties of the core pulposus from fluid-like behavior to solid-like behavior [30] that can cause the increment stress in annulus part [31]. Besides, abnormal motion, transverse and sagittal translation, increased loads over facets may occur with DDD [32]. In Figure 2.5, DDD is presented.

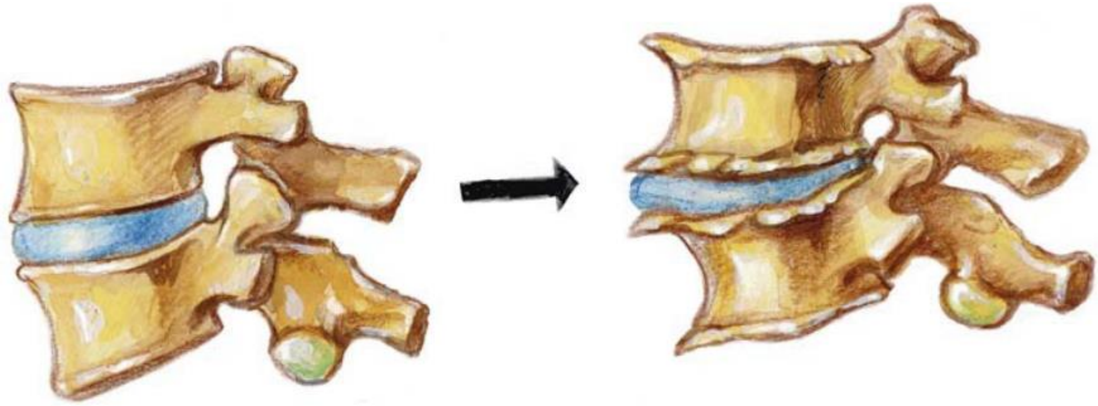

**Figure 2.5** Degenerative disc disease [33]

### 2.3.1. Surgical Treatments

Three primary surgical treatments are discussed as follows: decompression, fusion and nonfusion. Conservative therapies such as traction, exercise, heat therapy or joint mobilization are preferred for treatment in the early stages of low back pain. For other patients who do not have regular everyday activities, surgery is recommended.

### 2.3.2. Decompression Surgery

Surgical decompression is a type of treatment caused by decreases in the height of the disc, disc herniation and spinal stenosis [34]. With the latest advances in biotechnology, spinal decompression has become a cost-effective non-surgical treatment for treating herniated disc and degenerative disc disease, which is one of the leading causes of back pain [35]. This non-surgical treatment for herniated and degenerative disc disease works on the affected spinal segments by significantly reducing the pressure within the disc [36]. The decompression, unloading the intervertebral disc (Figure 2.6) and lumbar facet joints, have been proven to be an effective method for the treatment of degenerative and herniated disc diseases by generating and maintaining negative pressure in the intervertebral disc space [35].

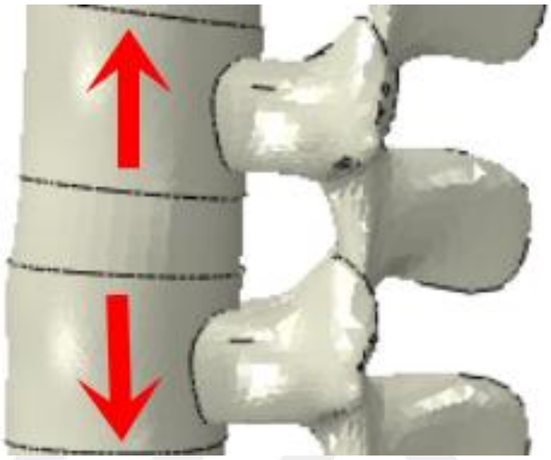

**Figure 2.6** Decompression of intervertebral disc

### 2.3.3. Fusion Surgery

For the treatment of DDD, fusion surgery is also used to replace bone, restore alignment, retain position and avoid motion in the treatment of fractures. With spinal instrumentation containing rods, screws, hooks, and wires or bone grafts only, this technique aims to provide spinal stability as seen in Figure 2.7 (a). The core theory of this procedure relies on the development of the bone at various stages of the spine. During surgery, bone grafts are inserted around the spine and the body then repair the grafts over several months, binding or "welding" the vertebra together. This technique may be preferred in the case of treatment of broken vertebra, correction of deformity (spinal curves or slippages), removal of pain, treatment of instability, and treatment of some herniated cervical discs. A few years after the fusion surgery, it is considered that adjacent segments may be influenced [6,37]. Possible excessive motion at adjacent segment is illustrated in Figure 2.7 (b).

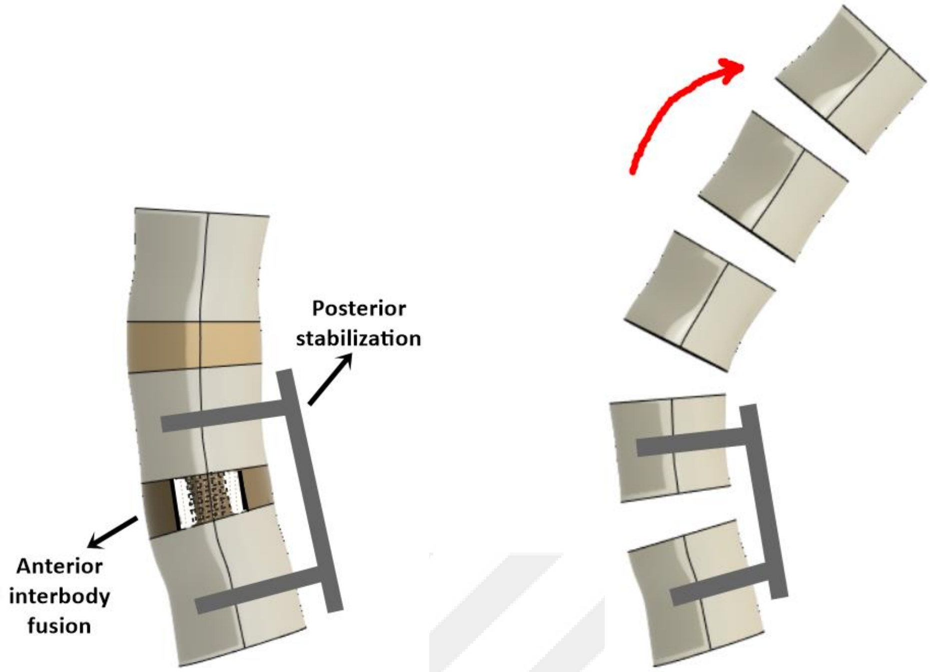


(a) (b)

**Figure 2.7** (a) Anterior interbody fusion + Posterior stabilization, (b) Motion at adjacent level after rigid implantation

Load sharing with implants reduces the load transmitted through the vertabrae and thus reduces the pressure in the vertebra. Rigid implantation also causes the adjacent segments to overload and contributes to their degeneration by raising stress [38,39]. In addition, lumbosacral surgery showed elevated intradical pressure at adjacent levels [6,40]. The disadvantages of this approach are operation time, pseudarthrosis, and fatigue failure of implantation systems [41].

### 2.3.4. Non-fusion Surgery

As high as %35 to 45%, ASD caused by rigid implanted fusion has been stated [7]. Many studies have shown that fusion surgery will cause subsequent mechanical and physiological changes, hypermobility at adjacent level, loss of motion, and intervertebral rotation center changes [42,43]. The solution to these problems could be semi-rigid rod fixation, which has also been used for dynamic stabilization of the unstable segment [44].

### *2.3.4.1. Artificial Disc Replacement Systems*

Artificial Disc Replacement (ADR) provides dynamic stabilization for the treatments of disc diseases. In this part, a commercial artificial disc named as LP-ESP was handled.

- **LP-ESP Artificial Disc**

The lumbar IVD prosthesis LP-ESP (from lumbar prosthesis–elastic spine pad, developed by FH Ortho Inc., Chicago, IL, USA) has six degrees of freedom about three different axes, with the elastic components between the Titanium endplates being able to mimic the annulus fibrosus and the nucleus pulposus of the human IVD [17]. In order to mimic the natural lumbar disc and allow the spine to function as though the replacement disc were natural in all circumstances, the LP-ESP disc prosthesis was created (Figure 2.8).

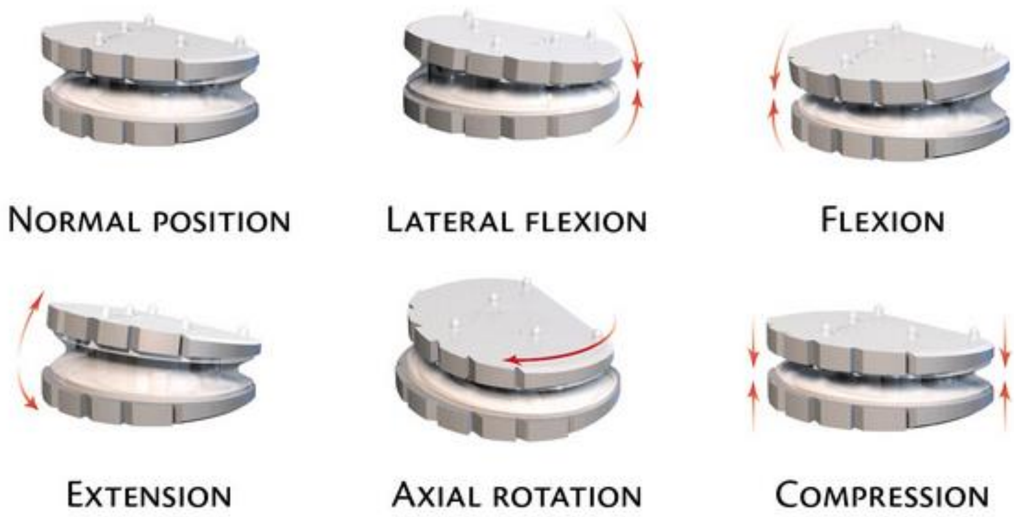


**Figure 2.8** LP-ESP artificial disc [45]

Titanium endplates and hydroxyapatite coating are the composition of the LP-ESP ® lumbar prosthesis, the inner core (Silicone nucleus) and the outer core (Polycarbonate urethane annulus). Lazennec et al. [46] stated that good adaptation and mobility were observed in terms of sagittal balance after 2-years follow-up with this device. There was no record of implantation failure or complications during this period. Lazennec et al. [47] then published a study with the clinical outcomes of 120 patients implanted with LP-ESP disc after 7-years follow-up. Back pain, implant functionality, mobility and sagittal balance were found to be favorable. In another study of Lazennec et al. [48], 61 patients were followed for 5 years and the outcomes were comparable to previously published studies. Gan et al. [15] treated an athlete undergoing a hybrid procedure with LP-ESP disc at L4-L5 level and anterior lumbar interbody fusion (ALIF) at L5-S1 level. This athlete was able to go back in activity after 16 weeks. In addition, the Oswestry Disability Index (ODI) was reduced from 9 to 1 and the visual analog scale (VAS) scores degraded from 62% to 12%.

#### *2.3.4.2 Dynamic Stabilization Systems*

Dynamic pedicle-based systems support flexibility of the motion segment and dissipation of mechanical forces over the spine [49]. These devices use more compatible materials (such as nitinol, polymers, or polyether ether ketone [PEEK]) or design changes. It is believed that they can maintain or restore load sharing characteristics to the level of a complete spine with less protection against stress [50]. Pedicle based posterior dynamic stabilization system is based on the principles of the traditional pedicle screw rigid rod system used for spinal fusion. The pedicle-based systems can be used by surgeons and maintain the integrity of posterior ligaments and facet joints [51]. Because the inherent characteristics of intervertebral motion are retained, pedicle screws can be used to promote graft fusion [52], or as an independent system for non-fusion surgery [53]. Load distribution in case of dynamic implantation is seen in Figure 2.9.

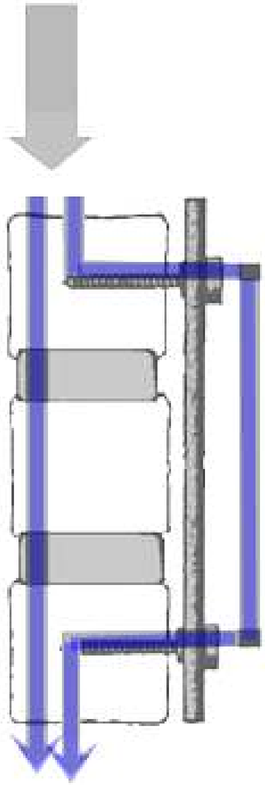

**Figure 2.9** Load distribution after implantation [53]

### *2.3.4.3 Hybrid Systems*

For multilevel degenerative spinal disease, hybrid systems can be an efficient process. One level of severe disc degeneration requires fusion, the adjacent level has only disease symptoms and must be dynamically implanted without fusion [12,54]. An example of multilevel disc degeneration is given in Figure 2.10. In hybrid applications, rigid implant is used to fuse at the injured or degenerated segment, extending the dynamic stabilization at a level above or below the fused segment. The goal of mixed applications is to preventively limit the pressure on the level above or below the fusion, and to prevent the development of adjacent levels of disease [11]. In this thesis, simplified models of the most recent HSSs were used, the commercially available Dynesys Transition Optima (Zimmer-Biomet Spine, Denver, USA), CD Horizon BalanC$^{TM}$ (Medtronic, Minneapolis, USA) and B-DYN (S14 Implants, Pessac, France) HSSs were compared with each other. These systems have different geometrical designs and material properties that the details will be given in Chapter 3. The primary objective of this analysis is to test the ROM, intradiscal pressure (IDP) variations at index and adjacent levels and stress distributions of three simplified HSS models.

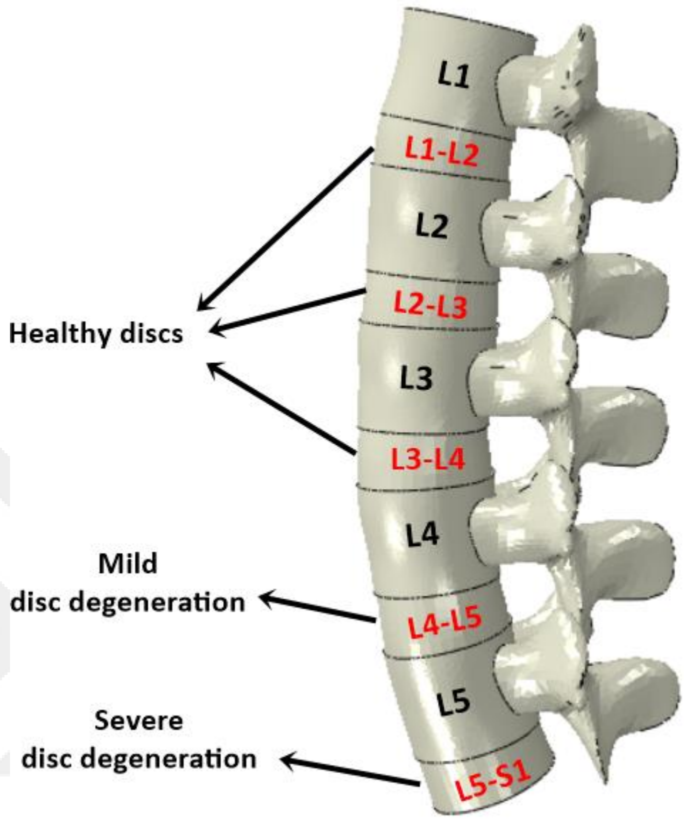


**Figure 2.10** Bilevel disc degeneration

- **Dynesys Transition Optima (DTO) Hybrid System**

Dynesys Transition Optima (DTO) hybrid system incorporates the conventional spinal fusion surgical approach with the dynamic stabilization theory, using versatile materials to stabilize the spine while retaining anatomical structures. To stabilize the spine as an adjunct to fusion, the device uses three components: The system is anchored to the spine by Titanium screws, the PolyCarbonate Urethane (PCU) spacers restrict spinal extension, the PolyEthylene Terephthalate (PET) cord acts as a tension band to restrict spinal flexion. The safety and efficacy of this device for the intended use of spinal stabilization without fusion have not been developed. This system is intended for use only when bone graft fusion is done at all stages of the instrumentation as seen in Figure 2.11 (a).

- **B-DYN Hybrid System**

B-DYN allows to reduce the intradiscal pressure and facet loads. B-DYN system can be considered as a spinal cushion. Using a single visco-elastic damping technology using silicone spacer in its dynamic part, B-DYN is suggested for the treatment of degenerative lumbar pathologies undergoing alterations such as disc disease, lumbar stenosis, lumbar instability, and avoidance of adjacent syndromes. Rigid part consists of rigid rods made of Titanium as seen in Figure 2.11 (b).

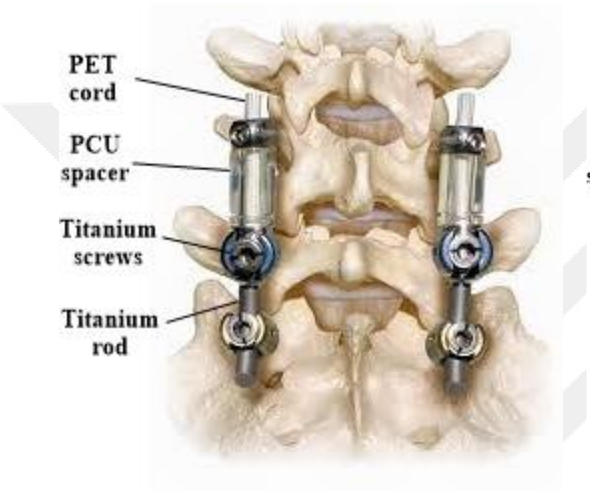


(a)

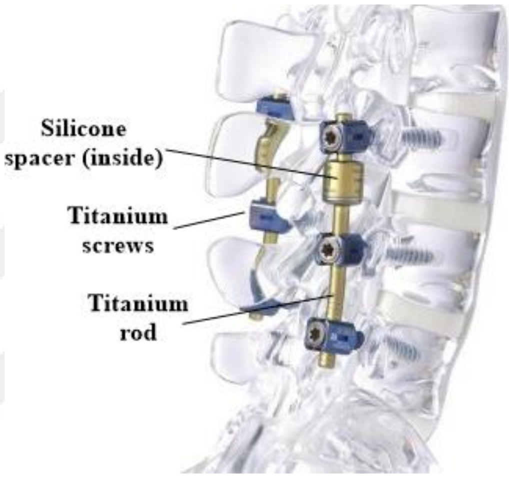


(b)

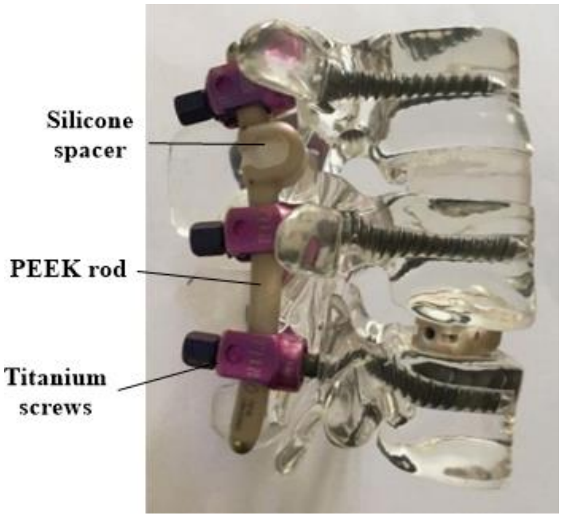


(c)

**Figure 2.11** Commercially available HSSs a) DTO [54], (b) B-DYN [55], (c) BalanC [56]

- **CD Horizon BalanCTM Hybrid System**

CD Horizon BalanC$^{TM}$ system, which is abbreviated as BalanC, is a neutral stabilization comprising of PEEK and silicone materials. In treating multilevel spinal diseases involving fusion at one or more levels and neutral stabilization (non-fusion) at the adjacent level for common spine disorders such as spinal stenosis and early stage degenerative disc disease. In its dynamic part, the BalanC rod is made of silicone and PEEK, while the fusion part is entirely made of PEEK (Figure 2.11 (c)). In order to preserve motion, the dynamic component is built to create a transitional zone between the fused and mobile segments.

- **Literature Review of HSSs**

Hybrid stabilization systems subjected to some studies are presented in Table 2.1. BalanC was subjected to the *in vivo* [54,56] and *in vitro* [57] studies. Oikonomidis et al. [56] revealed that implant failure occured by 18% while ASD commenced by 15%. Pain scale was found low. However, authors did not offer to use a dynamic implantation adjacent to rigid instrumentation. In comparison to Oikonomidis et al. [56], Herren et al. [57] and Formica et al. [58] offered that PEEK based hybrid system may have biomechanical advantages. DTO hybrid system was mostly used one. Kashkoush et al. [54] and Schwarzenbach et al. [4] suggested that DTO system was safe and feasible. In addititon, risk of failure was found similar to conventional rigid systems. Lee et al. [17] revealed that ROM was preserved, reasonable outcomes were obtained and ASD may be delayed in case of hybrid implantation. The findings of another study [59] agreed that DTO hybrid systems are promising in terms of screw loosening, implant failure, safety and clinical outcomes. Maserati et al. [12] stated that DTO system diminished the risk of ASD, however, further research was needed. Another hybrid system named as Isobar TTL was tested *in vivo* [3,60,61] studies. Hudson et al. [3] found that results were encouraging for 2 years follow-up, but long term studies should be studied to obtain more certain outcomes in terms of ASD. In another study, Isobar TTL hybrid system has good clinical outcomes after 2 years, however, ASD and degeneration at index level continued. The number of FE studies are very limited. FE may be an easy way to predict the possible effects of implantation systems and to compare the *in vivo* and *in vitro* studies.

**Table 2.1** Literature review of hybrid stabilization systems

| Study Type | Device | Condition | Treatment | Parameters | Reference |
|---|---|---|---|---|---|
| Experimental (*in vivo*) | BalanC | 22 patients, 2 years follow-up | TLIF, PLIF | VAS, COMI | Oikonomidis et al. [56] |
| Experimental (in vitro) | BalanC and rigid rod | 5 cadavers<br>L3-L4 with rigid<br>L3-L5 with hybrid | Disectomy, polymethyl methacrylate (PMMA) resin | ROM | Herren et al. [57] |
| Experimental (*in vivo*) | DTO | 66 patients, 5 years follow-up | Discectomy, laminectomy, facectomy | Interbody cage migration, infection and screw breakage | Kashkoush et al. [54] |
| Experimental (*in vivo*) | DTO and Nflex | 15 patients with hybrid group<br>10 patients with fusion group | Laminectomy, decompression, facetectomy, discectomy and interbody fusion | ROM, ODI, VAS | Lee et al. [17] |
| Experimental (*in vivo*) | DTO and rigid | 30 patients | Laminectomy, fusion | ODI, VAS | Baioni et al. [59] |
| Experimental (*in vivo*) | BalanC | 41 patients, 2 years follow-up | TLIF, PLIF and ALIF | ODI , VAS | Formica et al. [58] |
| Experimental (*in vivo*) | Isobar TTL | 36 patiens, 2 years follow-up | | ROM, disc height, VAS, ODI | Fu et. al. [60] |
| Experimental (*in vivo*) | Universal Clamp UC | 150 patients | PLIF, decompression | ODI, lordosis, fusion rate | Tegos et al. [62] |
| Experimental (*in vivo*) | S4 Aesculap AG dynamic system and rigid fixation | Up to 3 years follow-up | PLIF | ODI, COMI | Siewe et al. [63] |
| Exprimental (*in vivo*) | Isobar TTL | 6 cadavers<br>Intact, injured (L4-L5 laminectomy) and instrumented (L4-L5 with TTL) | Laminectomy, facetectomy, PLIF | ROM, IDP, facet joint load | Barrey et al. [61] |

| | | | | | |
|---|---|---|---|---|---|
| Experimental (*in vivo*) | DIAM interspinous device, Winglock interspinous device, B-DYN, PEEK Optima rods | 20 patients, 2 years follow-up | TLIF, PLIF | Adjacent segment disease | Castelli et al. [64] |
| Experimental (*in vitro*) | Allospine Dynesys Transition | 6 human cadavers<br>Intact, single level fixation (L5-S1), single level + dynamic fixation (L4-S1), two level fixation (L4-S1) | Dissection of the intervertebral disc, anterior bone cement block and an anterior wire fixation | ROM | Strube et al. [65] |
| Experimental (*in vivo*) | Dynesys hybrid system | 28 patients, 2 years follow-up | Laminectomy, foraminectomy, discectomy, PLIF | ROM, VAS, ODI | Tsai et al. [66] |
| Experimental (*in vivo*) | Rigid and Isobar TTL | 28 patients | Laminectomy, hemilaminectomy, discectomy | VAS, ODI, lordosis, flexion extension, disc height | Hudson et al. [3] |
| Experimental (*in vivo*) | Maverick ADR and pyramid plate | 80 Patients | ALIF<br>TDR | VAS, ODI | Aunoble et al. [1] |
| Experimental (*in vivo*) | DTO | 24 patients, 22 months follow-up | TLIF | VAS, disc degeneration | Maserati et al. [12] |
| Experimental (*in vivo*) | Dynesys hybrid system | 31 patients | Discectomy, nucleotomy, decompression, PLIF | VAS, ODI | Schwarzenbach et al. [4] |
| Experimental (*in vivo*) | Dynesys hybrid system | 32 patients, 2 years follow-up | PLIF | Disc height, disc degeneration | Kumar et al. [67] |
| Experimental (*in vitro*) | Hybrid system | 13 human cadavers (L1-S1)<br>L3-L4 fused<br>L2-L3 dynamic stabilization | | ROM | Cheng et al. [68] |
| Experimental (*in vivo*) | ProDisc ADR, Maverick ADR and Dynesys | 7 patients | Discectomy, laminectomy | VAS, positioning of the implants | Bertagnoli et al. [16] |

TLIF:Transforaminal Lumbar Interbody Fusion, PLIF:Posterior Lumbar Interbody Fusion, ALIF:Anterior Lumbar Interbody Fusion, VAS:Visual Analogue Scale, ODI:Oswestry Low Back Pain, COMI:The Core Outcome Measure Index, ADR:Artificial Disc Replacement

# CHAPTER 3 - MATERIALS AND METHODS

## 3.1 Reconstruction from CT images

The lumbar spine is composed of five lumbar vertebrae (L1-L5) that are connected by facet joints, and each pair of vertebrae are separated by an IVD. In addition, seven different ligaments spread over the lumbar spine. IVD, facet joints, and ligaments are the most important load transformation segments of the lumbar spine and mechanical properties of these parts play an important role on the spinal stability. Ligaments and discs have soft and flexible structures, when compared to the vertebral bodies [69].

The Quantitative Computed Tomography (QCT) images of a 39 years old female subject with two level disc degeneration at L4-S1 (Pfirmann grade III on L4-L5 and Pfirmann grade IV on L5-S1) were obtained from a Hitachi Presto CT machine (National Center for Spinal Disorders of Budapest, Hungary). CT images were reconstructed 1.25 mm slice thickness for a voxel size of 0.6 mm × 0.6 mm × 0.6 mm. Vertebral body and posterior elements were directly segmented from the CT images [70]. 3D Slicer, free open-source software, was used in processing of CT images. Reconstruction steps of the lumbar spine are given in Figure 3.1.

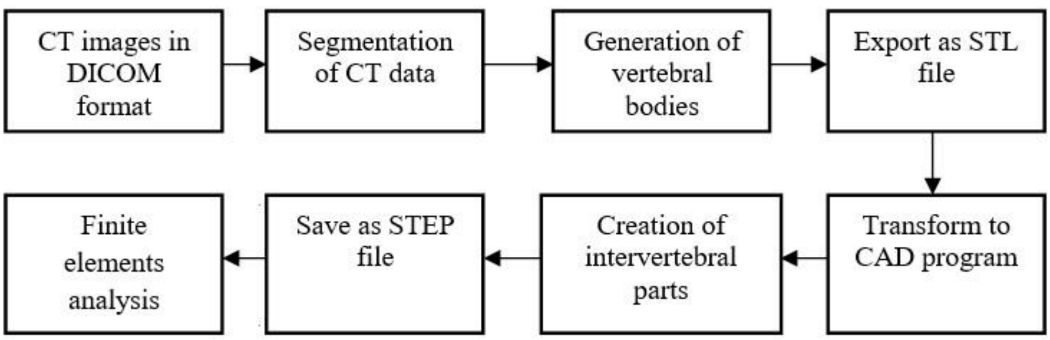


**Figure 3.1** Flow chart of the reconstruction of lumbar spine

After exporting the model in STL (Stereolithography) format (Figure 3.2), CAD program named as Fusion 360 (Autodesk, USA) was used for further processing (Figure 3.3). In Fusion 360, smoother surface was obtained and finally 0.5 mm cortical thickness [70] was created over cancellous bone. A simplified model of S1 was created as a cubic solid [9].

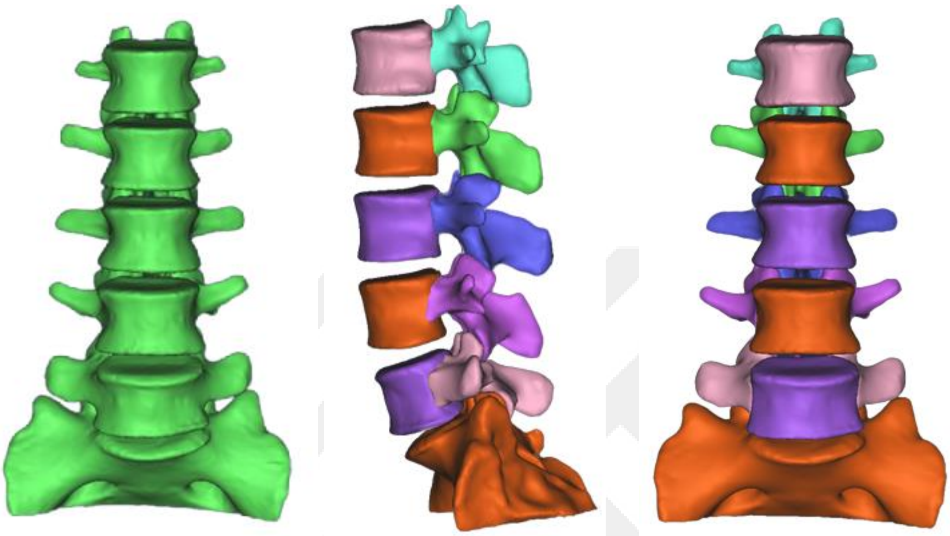

**Figure 3.2** STL format of lumbar spine

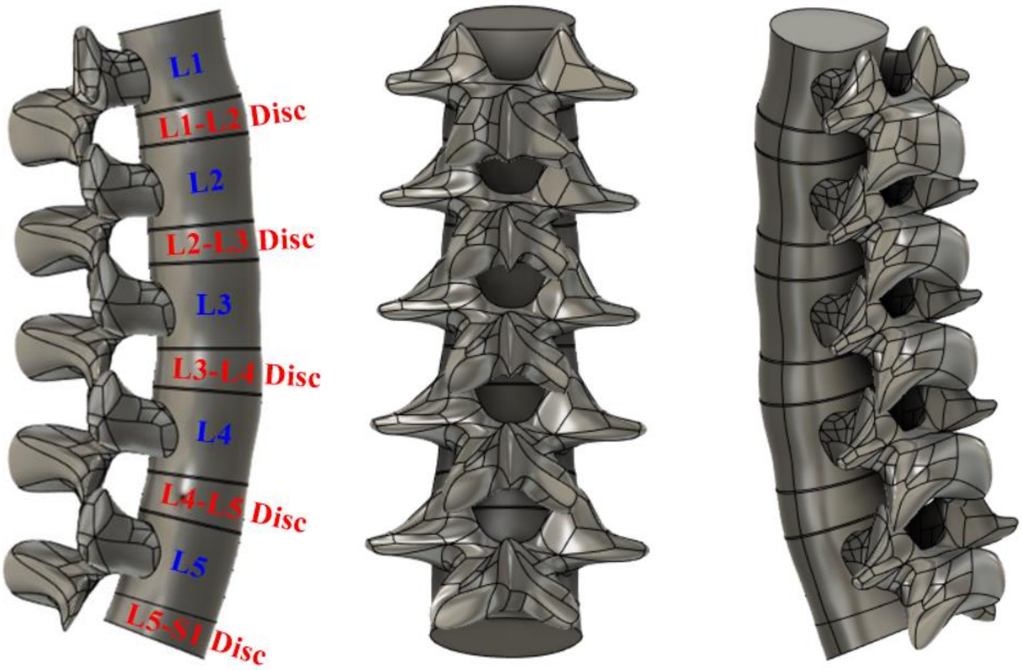


**Figure 3.3** 3D model of lumbar spine

The IVDs are divided into four parts: Nucleus Pulposus, Annulus Fibrosus, Inferior Endplate and Superior Endplate [71]. The nucleus pulposus was 30-50% of the total IVD volume [37] and thickness of the cartilage endplates was 0.6 mm [51]. Lumbar spine has seven different ligaments in real anatomy as following: Anterior Longitudinal Ligament (ALL), Posterior Longitudinal Ligament (PLL), Ligamentum Flavum (LF), Intertransverse Ligament (ITL), Interspinous Ligament (ISL), Supraspinous Ligament (SSL), Capsular Ligament (CL).

## 3.2 FE Model creation

Spinal ligaments have a restriction effect on spinal motion. Each ligament with linear elastic and tension only behavior was modelled in ABAQUS(R) 6.14 (Dassault Systèmes Simulia Corp., USA). Although ligaments represent nonlinear elastic behaviour in reality, they were created in a simplier way. Material properties and cross-sectional areas were adopted from literature as given in Table 3.1. Besides, Figure 3.4 (a) represented all sections of lumbar spine to which the material properties assigned.

**Table 3.1** Material properties of lumbar spine and hybrid stabilization systems

| Material | Modulus of Elasticiy (MPa) | Poisson ratio, v | Reference |
|---|---|---|---|
| **Cortical bone** | 12000 | 0.3 | Shin et al. [72] |
| **Cancellous bone** | 100 | 0.2 | |
| **Posterior elements** | 3500 | 0.25 | Rohlman et al. [73] |
| **Annulus fibrosus** | 8.4 | 0.45 | Shin et al. [72] |
| **Nucleus pulposus** | 1 | 0.49 | |
| **Endplate** | 24 | 0.4 | |
| **Facet Cartilage** | Hyperelastic Neo-Hookean C10=2, D1=0 | | Noailly et al. [74] |
| **ALL**<br>**PLL**<br>**LF**<br>**ITL**<br>**ISL**<br>**SSL**<br>**CL** | 20<br>20<br>19.5<br>58.7<br>11.6<br>15<br>32.9 | | Zhong et al. [75] |
| **PCU** | 68.4 | 0.4 | Liu et al. [76] |
| **PET** | 1500 | 0.4 | |
| **Ti alloy (Ti-6Al-4V)** | 110000 | 0.3 | |
| **Silicone** | 50 | 0.49 | https://www.azom.com [77] |
| **PEEK** | 3500 | 0.3 | Biswas et al. [78] |

### 3.2.1 Modelling of Hybrid Systems

Three different HSSs were created from the commercially available models used in clinical treatments. All of them have rigid part and dynamic part. First system has similar mechanical design with Dynesys Transition Optima (DTO) HSS whose dynamic part is composed of PCU spacer, Polyethylene Terephthalate (PET) cord and rigid part is composed of Titanium rods as seen in Figure 3.4 (b). Second one represents the similar mechanical properties with BalanC HSS that is made of C shaped silicone spacer and PEEK in its dynamic portion, while the fusion portion is entirely made of PEEK as given in Figure 3.4 (c). The third one is similar to B-DYN system having viscoelastic damping technology in dynamic part (Figure 3.4 (d)). Rods are made of Titanium for both rigid and dynamic portions. Titanium screws had a mean diameter of 5.5 mm and rigid rod had diameter of 6 mm. Screw lengths were 45 mm. The thread on the pedicle screws was underestimated [76,79-81] to reduce the computational weight of the models. The tie constraint was created between the pedicle screws and the vertebrae to be permanently bonded together by full constraint.

Three dimensional solid model of ADR system was created by imitating the mechanical properties of LP-ESP disc. LP-ESP model has Titanium endplates, PCU and silicone sections as seen in Figure 3.5 (a). The elastic components between Titanium endplates mimic the annulus and the nucleus part of real human disc.

AutoCAD Fusion 360 (Autodesk, USA) program was used for modeling of the implant components whose dimensions were taken from the product catalogues. Fusion mass properties were assigned the same as posterior elements [82]. Linear isotropic material properties were assigned to all the segments. For mesh sensivity, three different mesh densities as coarse (17557 nodes, 50036 elements), medium (57238 nodes, 131756 elements) and fine (101886 nodes, 183031 elements) were analysed. The model comprising coarse elements was disregarded since it caused an excessive element distortion. Under flexion, extension and lateral bending, mesh density affected the ROM values by max. 5%. Therefore, medium mesh was preferred for analyses. Total number of elements over the implanted spine was approximately 161,000 comprising tetrahedral and hexahedral element types. S1 segment was fixed [65,83,84]. Pure moments were applied from superior surface of L1 vertebra as 7.5 and 10 Nm to be able to validate the model by comparing with literature datas. For the implanted model, L4-L5 level was implanted dynamically and L5-S1 level was subjected to mono-segmental fusion and fixed with the rigid stabilization. Facet joint interactions were defined as surface to surface frictionless, hard contact. General static analysis option was selected for a time period of 1 second. ROM values under different moments, flexion (FL), extension (EXT), lateral bending (LB) and axial rotation (AR), were calculated and IVD pressures and stress distribution over the implants were investigated. For validation the computed ROM and IDP values were compared with *in vitro* and FE studies. Table 3.2 summarises the HSSs and ADR combinations.

**Table 3.2** Hybrid combinations

| **Stabilization type** | **Stabilization level** | | **Mono-segmental Fusion** |
|---|---|---|---|
| | **L4-L5** | **L5-S1** | |
| **B-DYN HSS** | B-DYN dynamic portion | B-DYN rigid portion | L5-S1 |
| **BalanC HSS** | BalanC dynamic portion | BalanC rigid portion | L5-S1 |
| **DTO HSS** | DTO dynamic portion | DTO rigid portion | L5-S1 |
| **Mobile-PEEK HSS** | Mobile-PEEK dynamic portion | Mobile-PEEK rigid portion | L5-S1 |
| **Dynesys + LP-ESP ADR** | Dynesys dynamic portion | ADR | - |
| **BalanC + LP-ESP ADR** | BalanC dynamic portion | ADR | - |
| **B-DYN + LP-ESP ADR** | B-DYN dynamic portion | ADR | - |
| **Mobile-PEEK + LP-ESP ADR** | Mobile-PEEK dynamic portion | ADR | - |

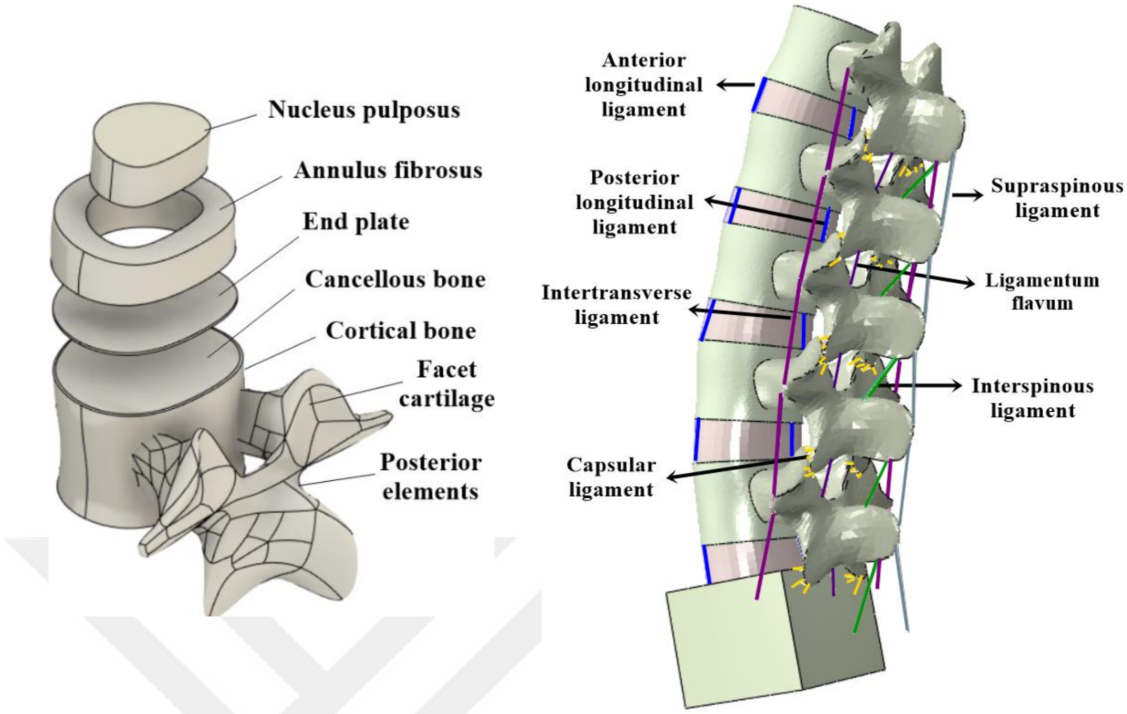
Nucleus pulposus
Annulus fibrosus
End plate
Cancellous bone
Cortical bone
Facet cartilage
Posterior elements
Anterior longitudinal ligament
Posterior longitudinal ligament
Intertransverse ligament
Capsular ligament
Supraspinous ligament
Ligamentum flavum
Interspinous ligament

a)

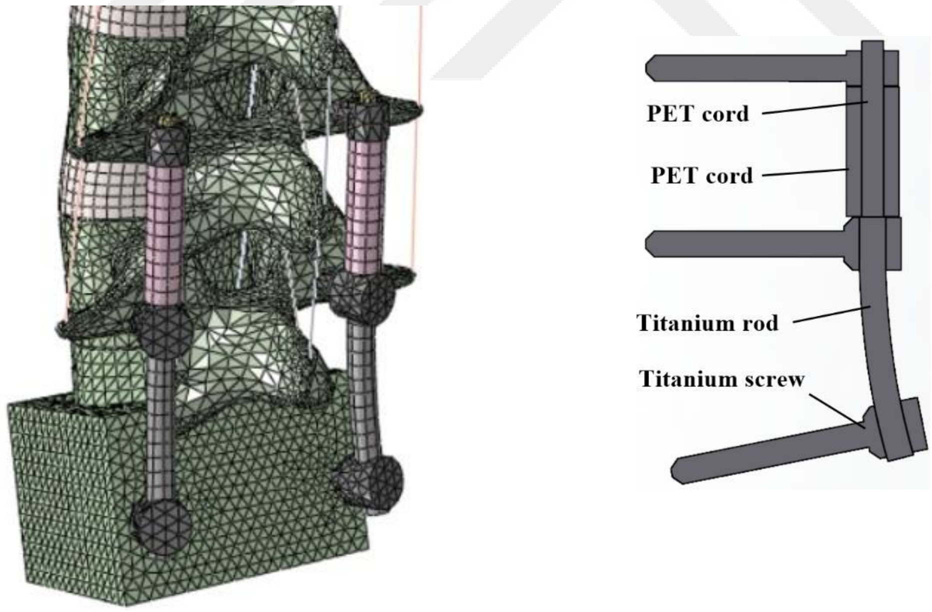
PET cord
PET cord
Titanium rod
Titanium screw

b)

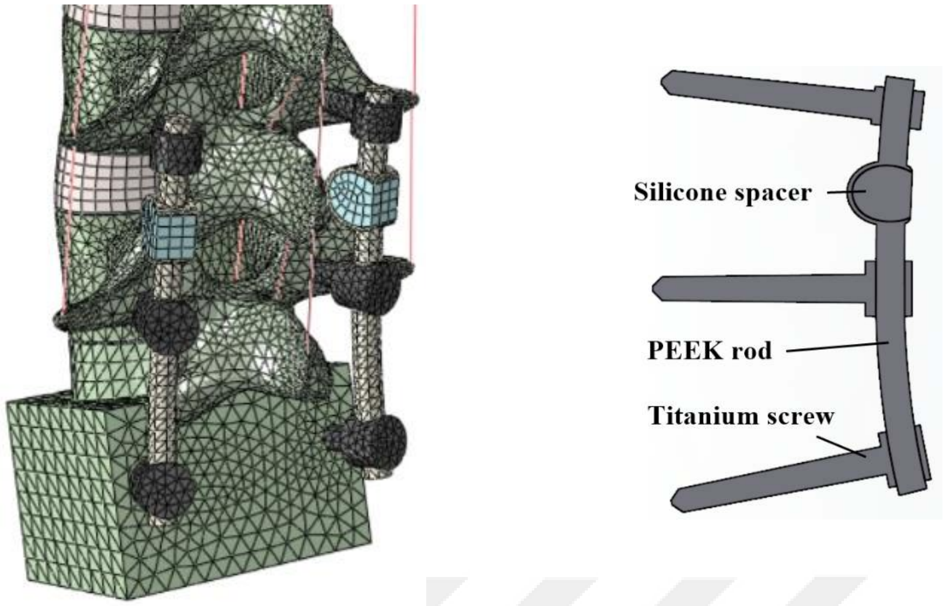
Silicone spacer
PEEK rod
Titanium screw

c)

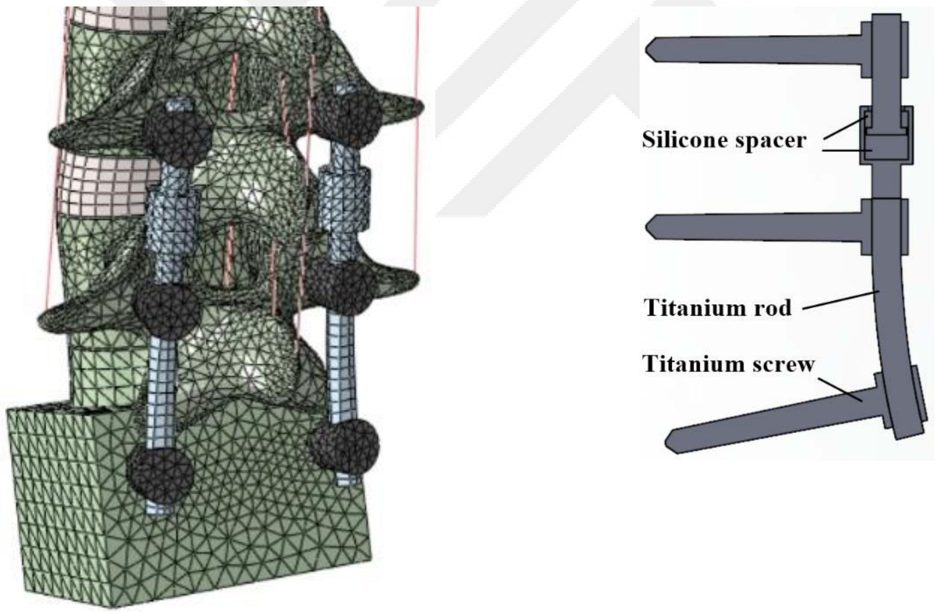
Silicone spacer
Titanium rod
Titanium screw

d)

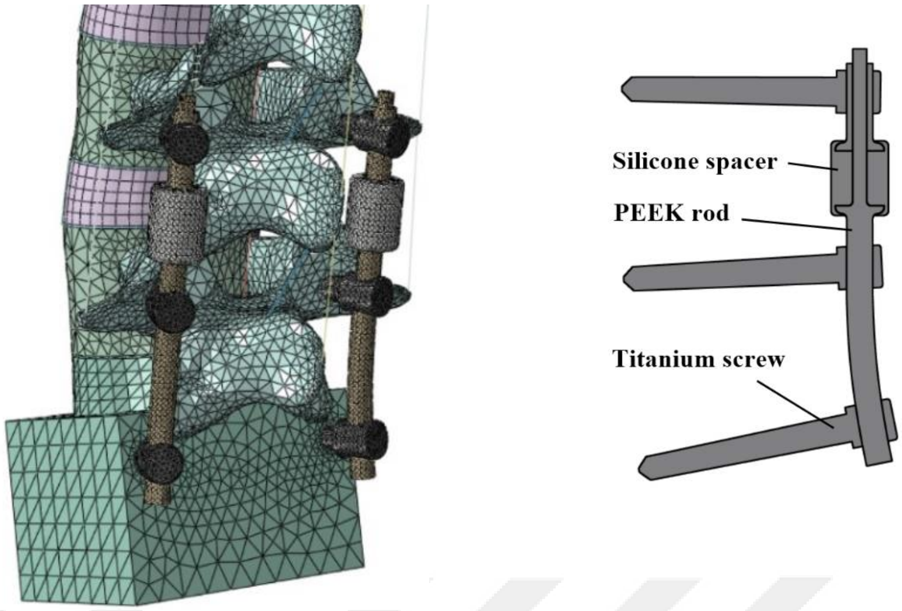


e)

**Figure 3.4** Intact and implanted spine a) Intact spine, b) DTO, c) BalanC, d) B-DYN, e) Mobile-PEEK (New design)

Bertagnoli et al. [16] suggested further studies needed for more accurate evaluations and patient selections for multilevel treatments using ADR and rods. By considering the limited *in vivo* studies subjected to both posterior and anterior stabilization systems, new hybrid combinations consisting of ADR and dynamic rods were modelled and implanted to the model. LP-ESP ADR mimicking the real human disc was combined with the dynamic parts of Dynesys, BalanC, B-DYN and Mobile-PEEK as given in Figure 3.5 (a-d). The general aim of these combinations is not to lose the motion completely at both degenerated level by avoiding the harmful effects of fusion process. S1 was modelled in a simplified way differently to provide the compatibility with ADR, however, the output datas do not change due to the S1 is fixed structure and the results are independent from S1 geometry. Intervertebral disc with ALL and PLL at L5-S1 level were removed to be able to replace with LP-ESP disc. Table 3.2 gives the details about each implanted levels.

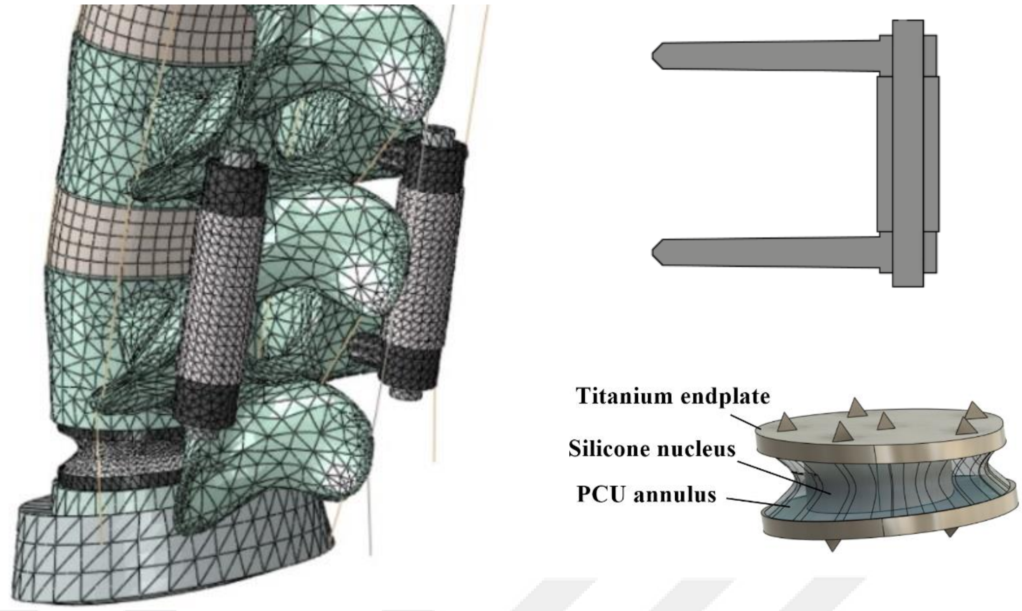
Titanium endplate
Silicone nucleus
PCU annulus

a)

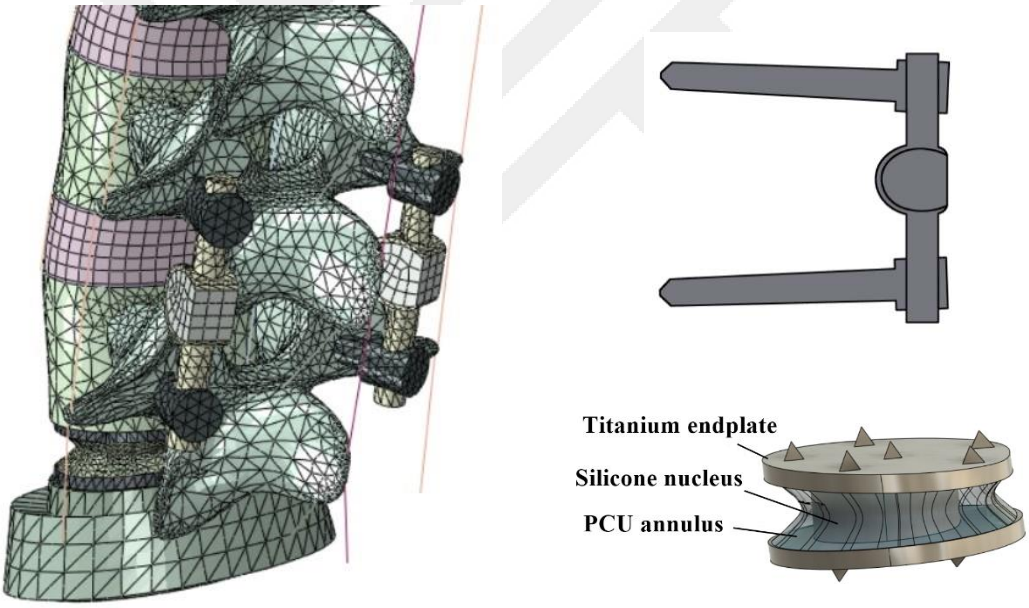
Titanium endplate
Silicone nucleus
PCU annulus

b)

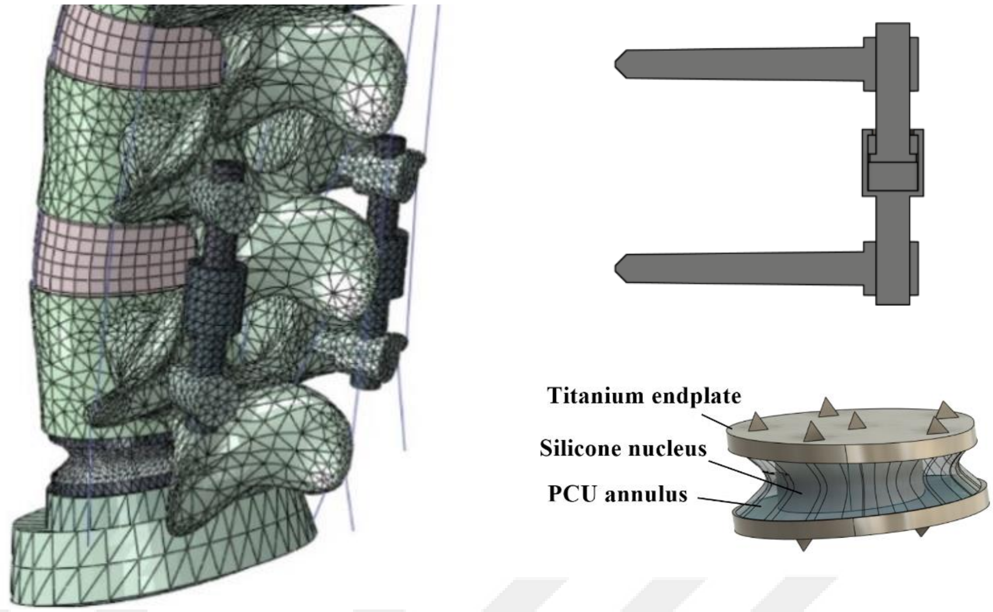


c)

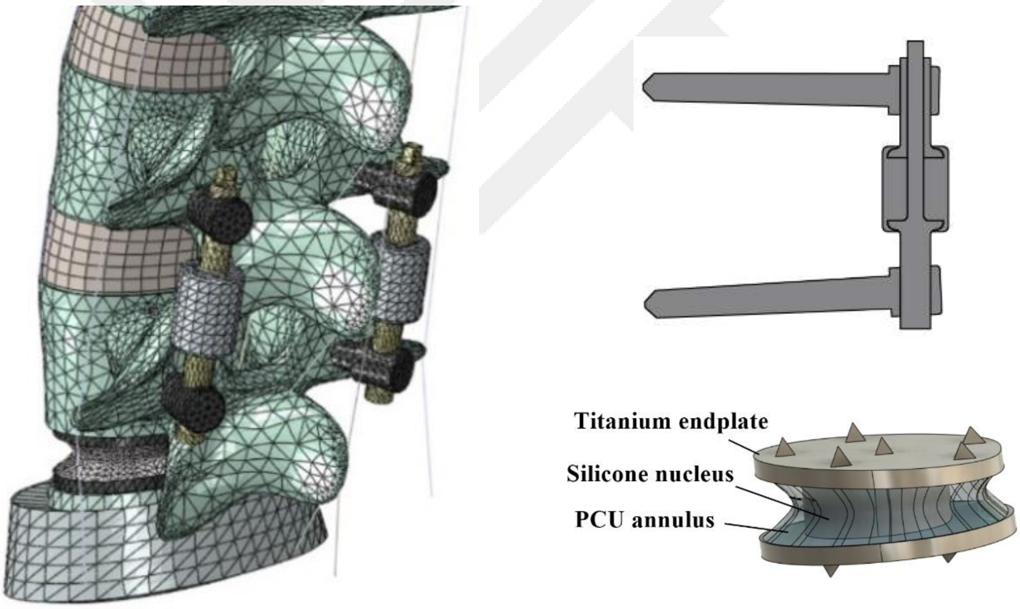


d)

**Figure 3.5** a) 1 Level Dynesys + ADR, b) 1 Level BalanC + ADR, c) 1 level B-DYN + ADR, d) 1 Level Mobile-PEEK + ADR

### 3.2.2 A New Hybrid Design

A new hybrid design was modelled by inspring CD Horizon Agile™ (Medtronic Sofamor Danek, Inc. Memphis, TN) that was first used in late 2006 and withdrawn from the market due to its tendency to failure, shearing and cable breaks. Agile consisted of pre-curved, lordotic Titanium rods with a Titanium cable and PCU bumper. In new design, named as Mobile-PEEK, PEEK rod and silicone spacer was used instead of Titanium alloy and PCU, respectively. Besides, floating Ti cable was replaced with thicker square shaped PEEK rod to resist the axial rotation and reduce the probability to the breakage as seen in Figure 3.4. (e). Figure 3.6 explains how Mobile-PEEK allows motion under loading. Superior PEEK rod can move both along and around inferior PEEK. Silicon spacer act as a viscoelastic damper. New hybrid model named as Mobile-PEEK was designed to increase the mobility at index level and reduce the hypermobility at the adjacent level. Axial rotation has still been an unsolved phenomena because of the design and material properties of dynamic systems. Squared shaped PEEK rod was recommended to resist the axial motion. Implant failure has been another important point that has to be taken into account. Square structure and thickness were designed to enhance the strength against bending moments. Rods were made from PEEK material to ensure the flexibility. Silicon spacer has the ability of absorbtion under different loading conditions.

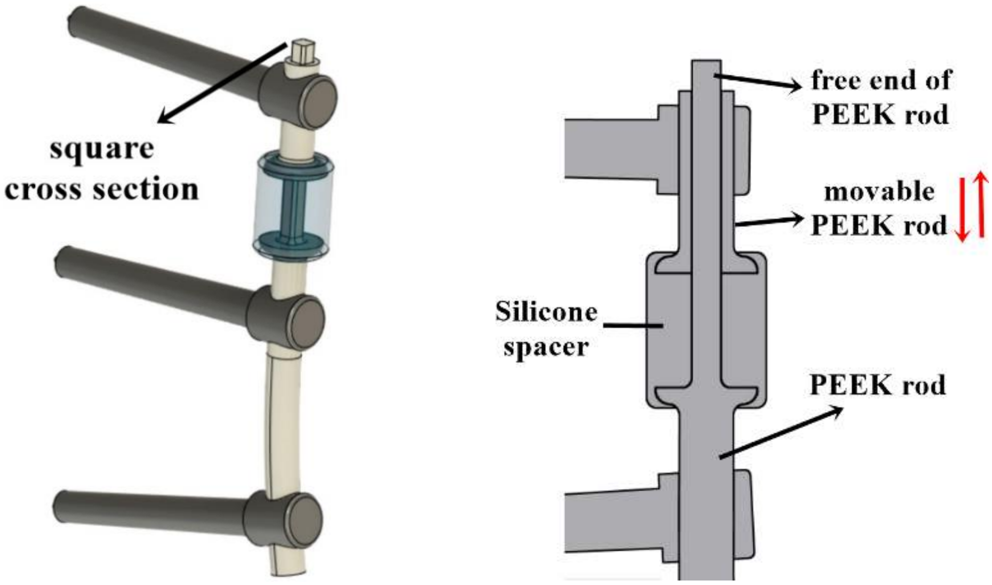


**Figure 3.6** Mobile-PEEK in details

## 3.3 Mass-Spring Model of Lumbar Spine (L1-L5)

A two dimensional rigid body model given in Fig 3.7 was suggested by Keller et al. [85] and used in this thesis to see the kinematic results and to make a comparison with FEA results. The model consisting of five lumbar vertebrae (L1-L5) and intervertebral discs were denoted with mass, massless springs and damping elements. Mass referred to vertebra, whereas massless spring and damping element referred to intervertebral disc. 10 Nm flexion moment was applied from the superior plate of L1 vertebra. Sacrum (S1) was fixed. Each rotational degrees of vertebraes (L1-L5) under loading were predicted and ROM values was calculated by using them.

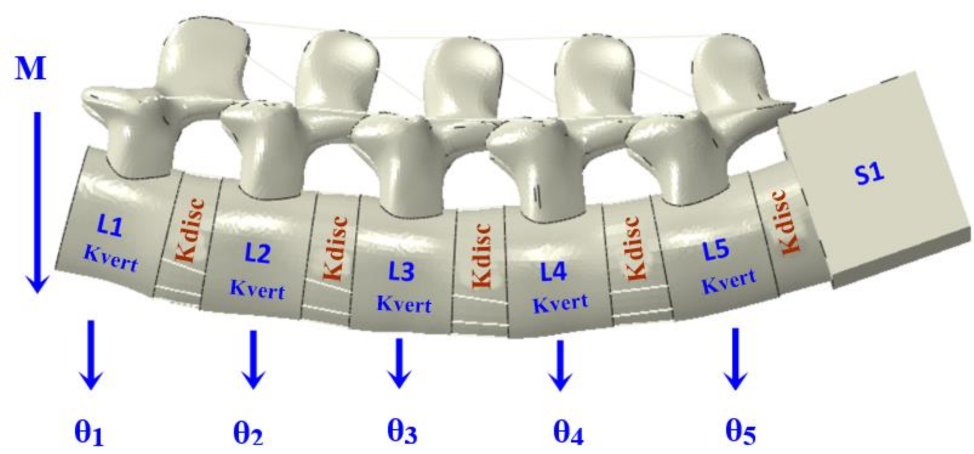


(a)

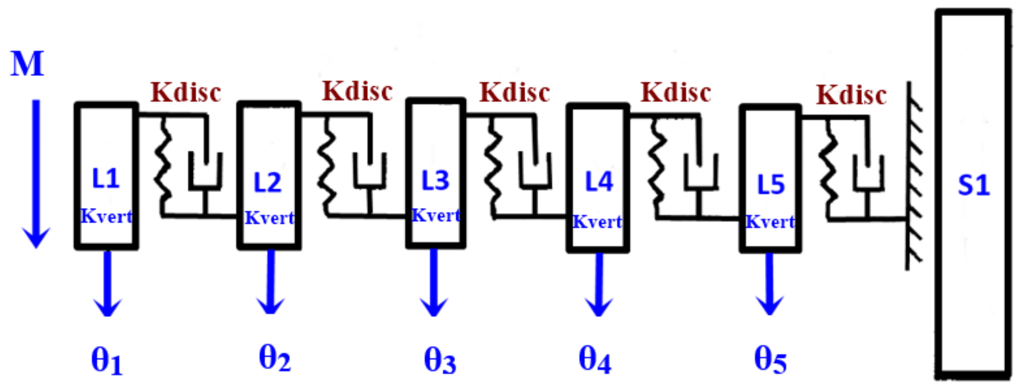


(b)

**Figure 3.7** Mass-spring model creation a) Vertebral body and discs of real anatomy b) Mass-spring model of lumbar spine (L1-L5) [85]

Matrix representation of general equation of translational motion used in Keller's study [85] is given in Equation 3.1:

$$[M]\ \{\ddot{x}\}+[C]\ \{\dot{x}\}+[K]\ \{x\}=\{F\} \tag{3.1}$$

where [M] is the mass matrix, [C] is the viscous damping matrix, [K] is the stiffness matrix, {F} is force vector (column matrix) and {x} is the resulting displacement vector. In this thesis, general equation of rotational motion was used as seen in Equation 3.2:

$$[J]\ \{\ddot{\theta}\}+[C]\ \{\dot{\theta}\}+[K]\ \{\theta\}=\{M\} \tag{3.2}$$

where [J] is the Mass Moment of Inertia matrix, [C] is the viscous damping matrix, [K] is the rotational stiffness matrix, {M} is moment and {θ} is the rotational displacement vector. The mass-spring model was developed in Simulink as seen in Figure 3.8 and rotational degree of each vertebra was predicted by using Equation 3.2. Rotational stiffness coefficient values of vertebra and disc were calculated by using Equation 3.3;

$$k = EI/L \tag{3.3}$$

where $E$ is Modulus of Elasticity, $I$ is Moment of Inertia and $L$ is the length of anatomical part (vertebra or disc). Both vertebra and disc were considered as a composite material including different sections. Therefore, $E$ of vertebra was calculated by regarding the volume fractions of cortical and cancellous bones as given in Equation 3.4. $E$ of intervertebral disc was calculated in a similar way by using volume fractions of nucleus pulposus and annulus fibrosus.

$$E_{composite} = E_x\,\mathrm{V}_X + E_y\,\mathrm{V}_y \quad , \quad V_x + V_y = 1 \tag{3.4}$$

where volume is denoted as $V$, $x$ and $y$ are the variables referring different anatomical sections. Adjacent vertebra and disc were considered as two springs in series and equivalent rotational stiffness value ($k$) was calculated as given in Equation 3.5:

$$1/k_{eq} = 1/k_{vertebra} + 1/k_{disc} \tag{3.5}$$

The sagittal rotational plane motion under flexion moment was predicted by solving the equations in Simulink, and compared FEA results. The problem can be solved for lateral and axial bending, however, the aim of this example is to offer a simplified mathematical model for current FE model. In this mathematical model, posterior elements were also included to the vertebral body and mass properties and mechanical properties were taken into consideration. Ligaments and end plates were excluded from the model. Table 3.3 gives the values used for the Equation 3.2. Modulus of Elasticity values was taken from Table 3.1. Volume, length and Moment of Inertia values were taken from Fusion 360. Damping coefficient was taken as 0.15 [85,86].

**Table 3.3** Mass-spring model variables used in Simulink model

| | **Cortical bone** | **Cancellous bone** | **Nucleus pulposus** | **Annulus fibrosus** |
|---|---|---|---|---|
| **Volume, V ($m^3$)** | $1591 \times 10^{-9}$ | $46098 \times 10^{-9}$ | $5019 \times 10^{-9}$ | $7816 \times 10^{-9}$ |
| **Modulus of Elasticiy, E (Pa)** | $12000 \times 10^{6}$ | $100 \times 10^{6}$ | $1 \times 10^{6}$ | $8.4 \times 10^{6}$ |
| **Length, L (m)** | $27 \times 10^{-3}$ | | $10 \times 10^{-3}$ | |
| **Moment of Inertia, I ($m^4$)** | $0.91 \times 10^{-6}$ | | $0.02 \times 10^{-6}$ | |

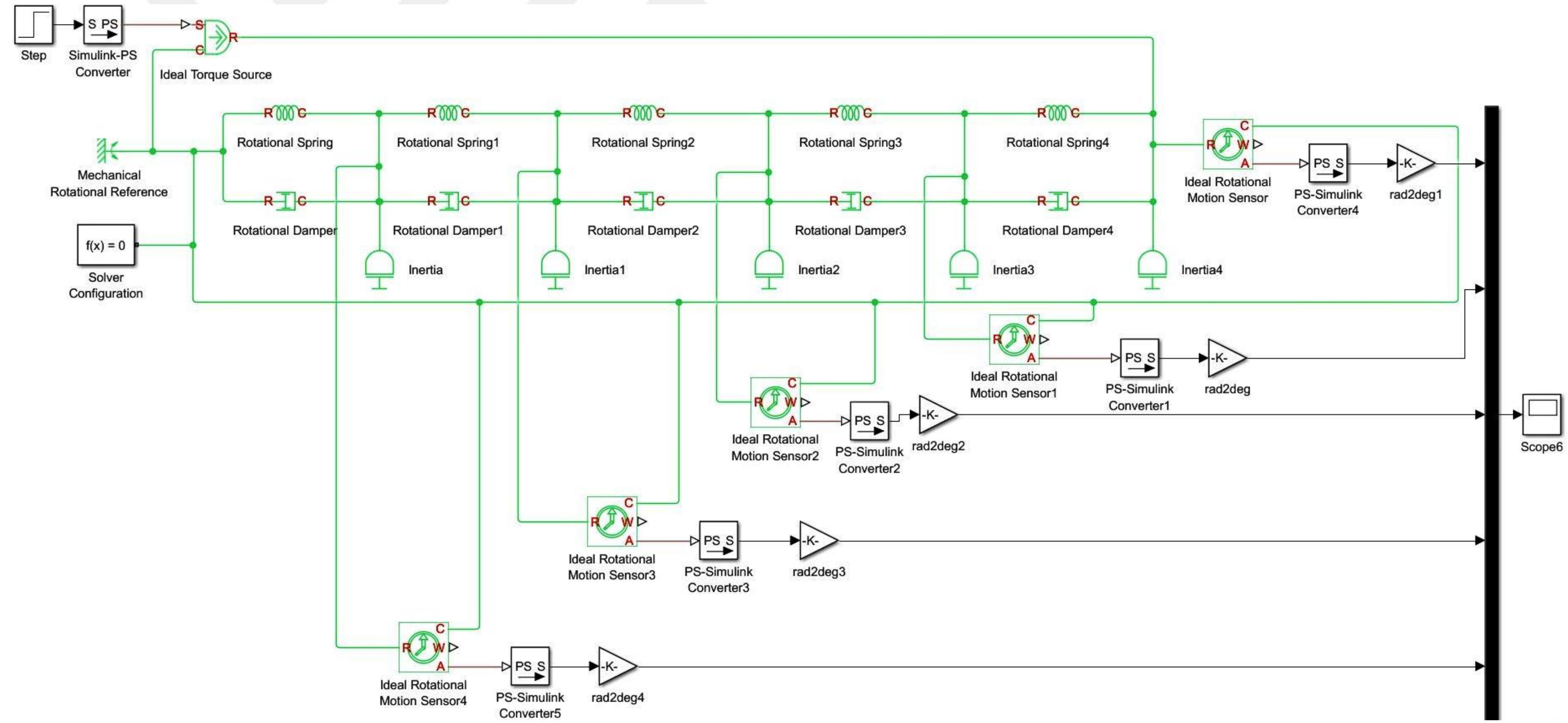


**Figure 3.8** Two dimensional development of lumbar spine kinematics using Simulink model

# CHAPTER 4 - RESULTS

## 4.1 ROM Analysis of Finite Element Model of Intact Spine

Human lumbar spine has six degrees of freedom along and around x, y and z axes (Figure 4.1 (a)). Kinematic response of lumbar spinal units under flexion, extension, lateral bending and axial rotation is seen in Figure 4.1 (b-e), respectively. Rotational degrees under 10 Nm different loading conditions were obtained from simulation program. The difference of the rotations of two adjacent vertebrae issued the ROM values of each intervertebral disc (e.g. Rotation (L4) – Rotation (L5) is L4-L5 ROM). Predicted ROM values were given in Table 4.1. According to the results, mobility increased from L1 to S1 for all loading cases. Mobility values were found the highest for flexion and the lowest for axial rotation. Ligaments have tension-only behavior, therefore flexion is restricted by all ligaments except ALL, whereas extension is limited by only ALL and facet contacts. Under lateral bending and axial rotation, the ligaments and facet contacts restrict the motion depending on the bending moment direction.

**Table 4.1** ROM values of intact spine under 10 Nm pure moment

<table>
<tr><th></th><th>L1-L2</th><th>L2-L3</th><th>L3-L4</th><th>L4-L5</th><th>L5-S1</th><th>Model</th></tr>
<tr><th>Flexion (degree)</th><td>3.9</td><td>4.1</td><td>4.7</td><td>5.2</td><td>6.4</td><td rowspan="4">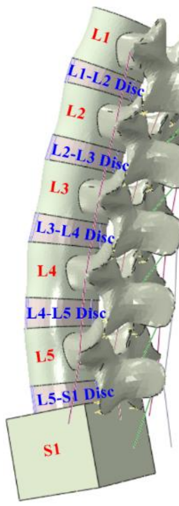
</td></tr>
<tr><th>Extension (degree)</th><td>3.4</td><td>3.0</td><td>3.7</td><td>4.7</td><td>4.2</td></tr>
<tr><th>Lateral Bending (degree)</th><td>4.1</td><td>4.1</td><td>4.5</td><td>4.0</td><td>5.0</td></tr>
<tr><th>Axial Rotation (degree)</th><td>1.5</td><td>1.6</td><td>1.5</td><td>2.1</td><td>2.1</td></tr>
</table>

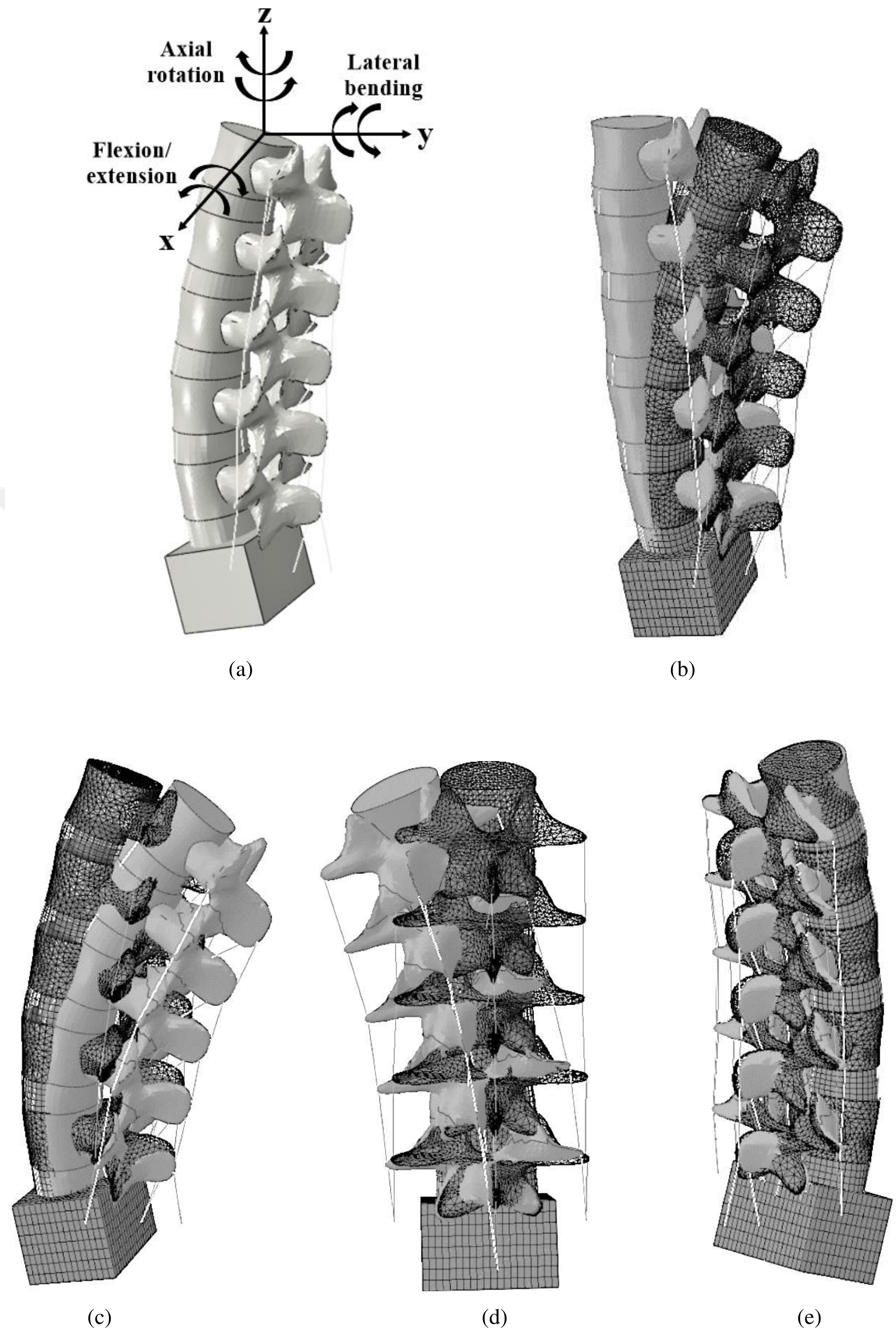


**Figure 4.1** Lumbar spine model under different loadings conditions (a) Rotations around three different axes (b) Flexion (c) Extension (d) Lateral bending (e) Axial rotation

### 4.1.1 Validation of Finite Element Model of Intact Spine

#### *4.1.1.1 Comparison with In vitro Studies*

It was aimed to compare the results of the intact spine with *in vitro* studies conducted by Yamamoto et al. [87] and Schmoelz et al. [88] who used pure bending moments of 10 Nm without any compressive load similar with this thesis. L1-L5 segments of the spine were tested Yamamoto et al. [87] while Schmoelz et al. [88] used only L2-L4 segments. When considering L2-L3 and L3-L4 levels, my model results are more compatible with Schmoelz et al. [88] under flexion, extension, lateral bending and axial rotation. Yamamoto's values [87] are slightly higher than current findings at all lumbar levels. ROM values are represented in Table 4.2.

**Table 4.2** ROM comparison with in vitro studies

| | **Intervertebral discs** | | | | **Reference** | **Model** |
|---|---|---|---|---|---|---|
| | **L1-L2** | **L2-L3** | **L3-L4** | **L4-L5** | | |
| **Flexion (degree)** | 3.9 | 4.1 | 4.7 | 5.2 | This thesis | 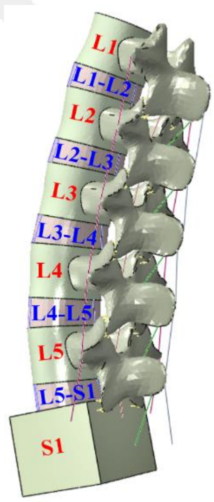 |
| | 5.8±0.6 | 6.5±0.3 | 7.5±0.8 | 8.9±0.7 | Yamamoto et al. [87] | |
| | - | 4.3±1.0 | 5.0±1.0 | - | Schmoelz et al. [88] | |
| **Extension (degree)** | 3.4 | 3.0 | 3.7 | 4.7 | This thesis | |
| | 4.3±0.5 | 4.3±0.3 | 3.7±0.3 | 5.8±0.4 | Yamamoto et al. [87] | |
| | - | 4.6 ± 2.2 | 4.0±1.3 | - | Schmoelz et al. [88] | |
| **Lateral Bending (degree)** | 4.1 | 4.1 | 4.5 | 4.0 | This thesis | |
| | 5.2±0.4 (R)<br>4.7±0.4 (L) | 7.0±0.6 (R)<br>7.0±0.6 (L) | 5.8±0.5 (R)<br>5.7±0.3 (L) | 5.9±0.5 (R)<br>5.5±0.5 (L) | Yamamoto et al.[87] | |
| | - | 5.4 ± 2.2 | 4.7 ± 2.0 | - | Schmoelz et al. [88] | |
| **Axial Rotation (degree)** | 1.5 | 1.6 | 1.5 | 2.1 | This thesis | |
| | 2.0±0.6 (R)<br>2.6±0.5 (L) | 3.0±0.4 (R)<br>2.2±0.4 (L) | 2.5±0.4 (R)<br>2.7±0.4 (L) | 2.7±0.5 (R)<br>1.7±0.3 (L) | Yamamoto et al. [87] | |
| | - | 1.0 ± 1.0 | 1.0±0.6 | - | Schmoelz et al.[88] | |

#### *4.1.1.2 Comparison with In vivo and FE Studies*

In the second step of the validation, ROM values were compared with the study carried out by Dreischarf et al. [89]. They collected well-established eight FE models in the literature and applied 7.5 Nm pure moments around three different axes. The total movement of L1-L5 body was handled. These eight models were arbitrarily numbered from 1 to 8 and represented in Figure 4.2. The details of mechanical and geometrical properties and employed data for validation were given in the study [89]. L5 was fixed for the Model 3 and Model 4, whereas S1 was fixed for other six Models.

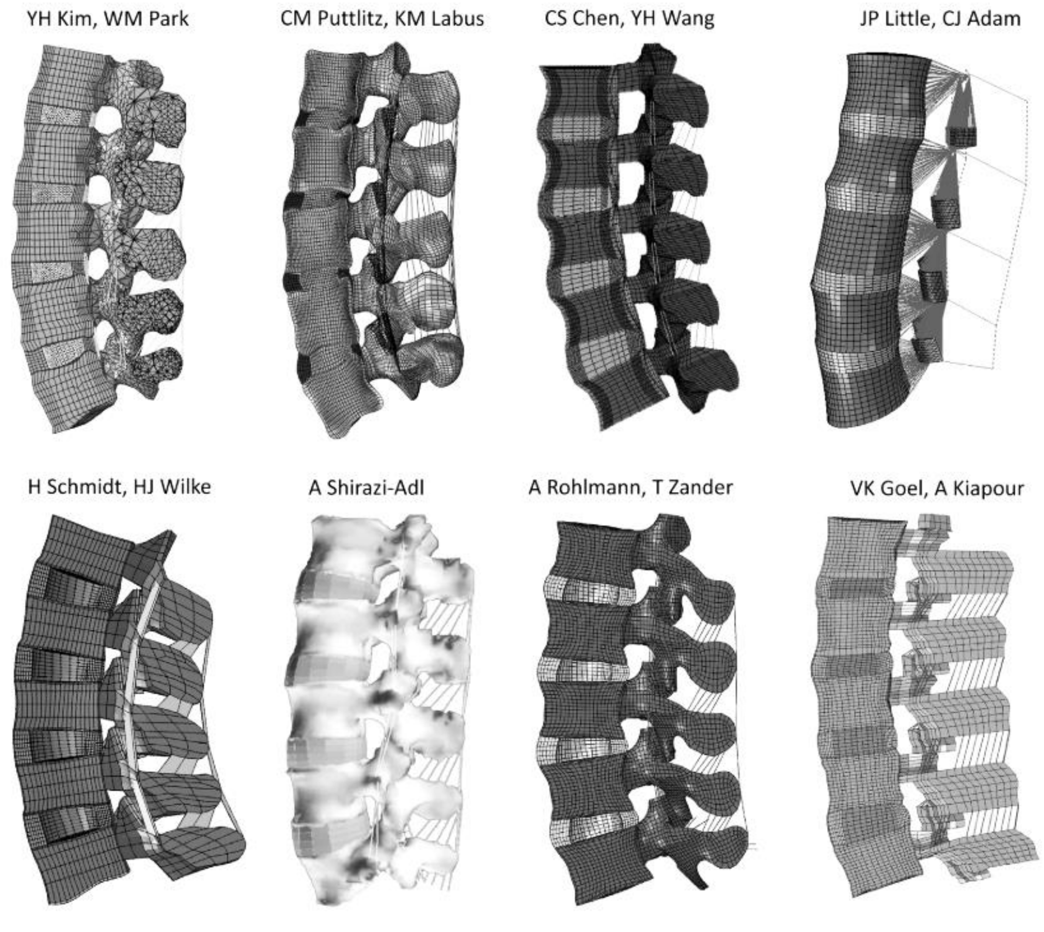


**Figure 4.2** Eight different FE model used in Dreiscarf's study [89]

In Figure 4.3, blue bar gives the predicted ROM in this thesis. The red one represents median ROM values of *in vivo* study performed by Rohlmann et al. [90]. ROM values were obtained from ten human cadaveric lumbar spines loaded with 7.5 Nm pure moment. The green bar denotes the median value of ROM values under flexion-extension, lateral bending (right+left) and axial rotation (right+left) for eight different FE models represented in Figure 4.2. Current model performs 33° where median value of the FE models is approximately 34° with a range of 24°- 41° and *in vitro* tests perform 31° in the range of 23.5°- 37° during flexion-extension. My model performs a movement of 33° where median value of the FE models perform about 35° in the range of 25°- 41° and *in vitro* tests shows 34° in the range of 23°- 44.5° in both of right and left lateral bending. The model studied in this thesis represents a rotation of 12° where median value of the FE models perform about 17° in the range of 11° - 22° and *in vitro* tests shows 12° in the range of 10°- 19.5° in both of right and left axial rotation.

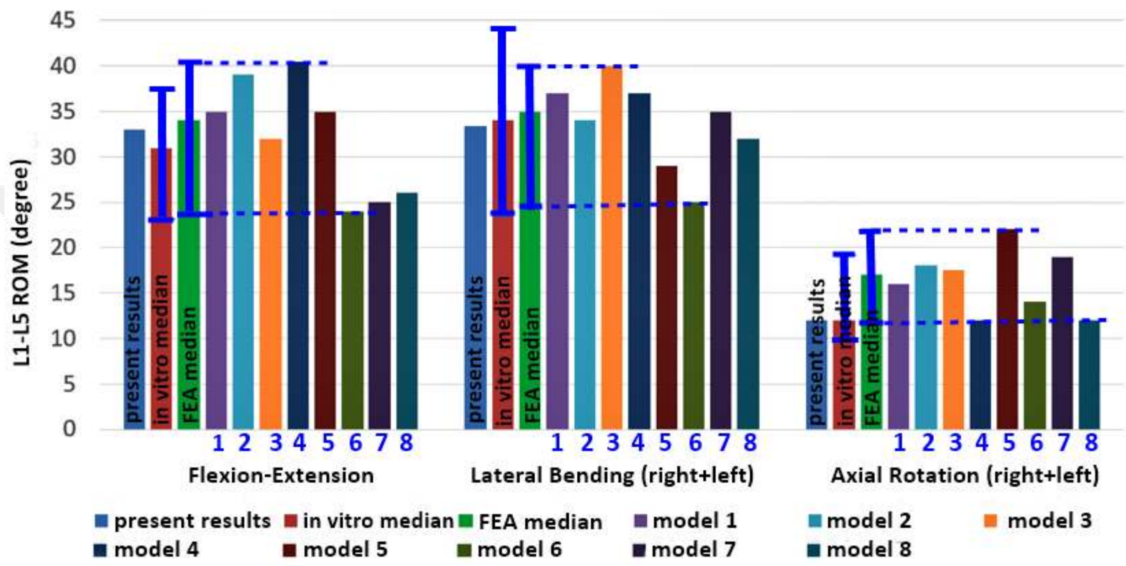


**Figure 4.3** Comparison of ROM values under 7.5 Nm pure moment (Adapted from Dreischarf et al. [89])

### *4.1.1.3 Comparison with Mass-Spring Model Results*

In mass-spring model, the problem was solved for only flexion. Rotational degrees of each vertebra (L1-L5) during flexion were measured and the graphical representation of results are seen in Figure 4.4. As expected, movements increased from L5 to L1, however there was no significant difference between intervertebral rotation when ROMs were compared with FEA results. ROM values were predicted in a similar way used for FEA. Each intervertebral motion were obtained from the difference of two adjacent vertebrae.

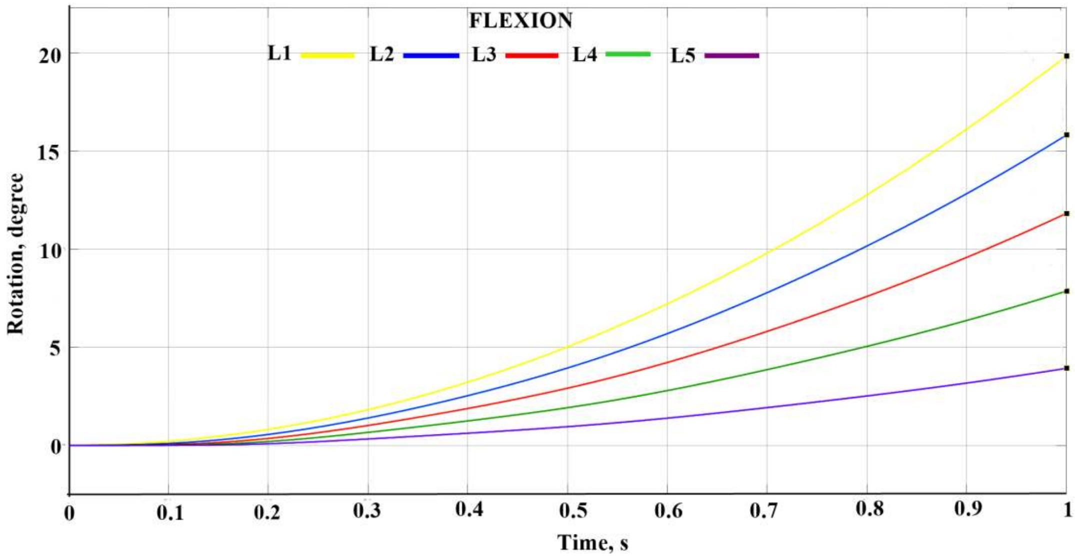


**Figure 4.4** Rotation values of mass-spring model

ROM results were compared in Table 4.3. The movements at levels of L1-L2 and L2-L3 were found very close to ecah other for both mass-spring and FE models. All intervertebral levels had almost same mobility for mass-spring model and 4 degrees of rotation. However, intervertebral motion differs at L1-L2 disc level and L5-S1 disc level in my FE model. L1-L2 had 64% of L5-S1 motion in my FE model whereas L1-L2 had 53% of L5-S1 motion in Yamamoto' study [87]. The different anatomical parts of human lumbar spine triggers the nonlinear motion. In mass-spring model, ligaments having an important effect in spinal motion were underestimated. The motion difference between FE model and mass-spring model were calculated as 40% at L5-S1 disc, 23% at L4-L5 disc, 15% at L3-L4 disc.

**Table 4.3** ROM comparison of mass-spring model and FEA results

| | | ROM values under Flexion | |
|---|---|---|---|
| | | **FEA model (degree)** | **Mass-spring model (degree)** |
| **Intervertebral disc** | **L1-L2** | 3.9 | 4 |
| | **L2-L3** | 4.1 | 4 |
| | **L3-L4** | 4.7 | 4 |
| | **L4-L5** | 5.2 | 4 |
| | **L5-S1** | 6.4 | 3.9 |

## 4.2 ROM Analysis of Implanted Spine

There are limited FEA, *in vitro* and *in vivo* studies subjected to hybrid stabilization systems examining the variation of ROM values. When implanted with hybrid systems, motion at L4-L5 level during flexion decreased significantly with respect to the intact case as shown in Figure 4.5, however was not lost completely. There were not any dramatical changes at L1-L2 and L2-L3 discs. Any hypermobility was not detected at level (L3-L4) adjacent to the dynamic implantation.

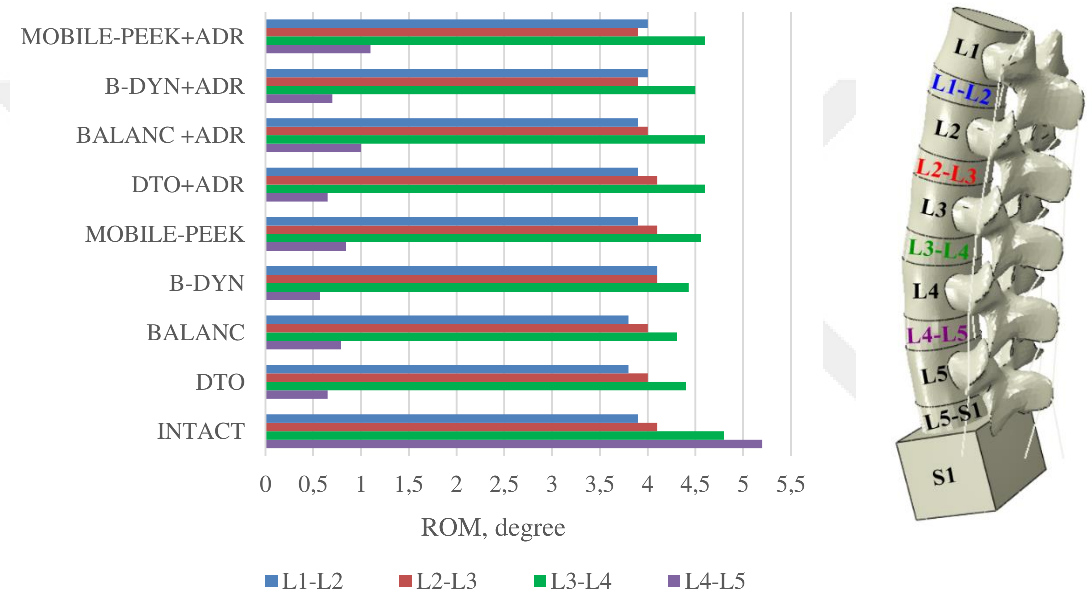


**Figure 4.5** ROM values of L1-L5 in flexion

In case of implantation, there were not any dramatical changes in ROM of L1-L2 and L2-L3 discs during extension. The alterations in ROM of the adjacent level (L3-L4) were around 5% and the hypermobility was considered as negligible. At L4-L5 level, ROM values diminished as expected. Graphical representation of ROM values are shown in Figure 4.6.

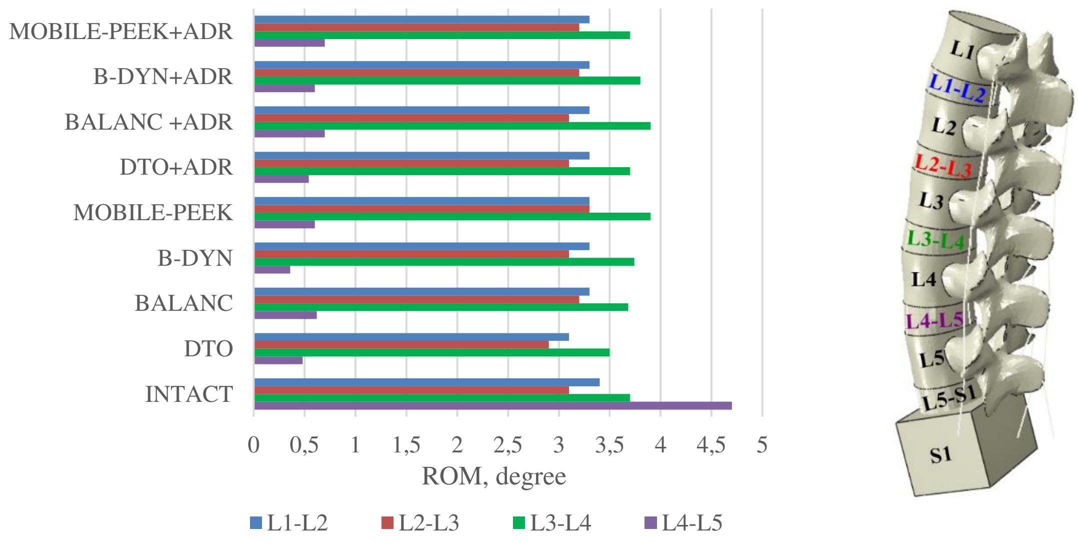


**Figure 4.6** ROM values of L1-L5 in extension

Under lateral bending motion, comparable ROM values are shown in Figure 4.7. Increment in ROM of L1-L2 disc was found by 7% in case of BalanC implantation. Other increments that were lower than 5% were underestimated at this level. Any hypermobility was detected at L2-L3 level. ROMs of Mobile-PEEK and DTO exceeded the intact case by 2% at L3-L4 level, however, it is considered as insignificant. As expected, ROM values of L4-L5 level were lower than the intact case, but it was not completely lost.

During axial rotation, ROM values increased by 40% for B-DYN, by 33% for BalanC and BalanC+ADR, by 16% for DTO+ADR and Mobile-PEEK+ADR, by 13% for DTO at L1-L2 level. Any dramatical change was not detected for Mobile-PEEK and B-DYN+ADR. ROM was also increased by 15% for BalanC, B-DYN and DTO+ADR, by 12% for DTO, BalanC+ADR and Mobile-PEEK+ADR at L2-L3 level. At the adjacent level (L3-L4), ROM increased by 42% for BalanC+ADR, by 28% for BalanC, by 21% for B-DYN and Mobile-PEEK+ADR, by 14% for DTO+ADR, by 7% for DTO. Mobile-PEEK and B-DYN+ADR did not cause any hypermobility at the adjacent level. Mobility at L4-L5 level was preserved more than other loading conditions, however, ROM values did not exceed the values of the intact case. The results are shown graphically in Figure 4.8.

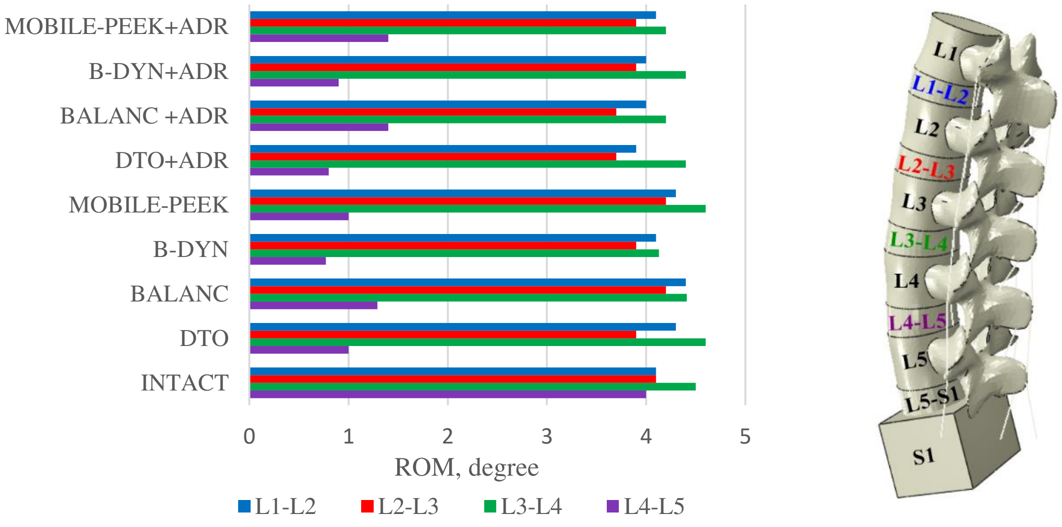


**Figure 4.7** ROM values of L1-L5 in lateral bending

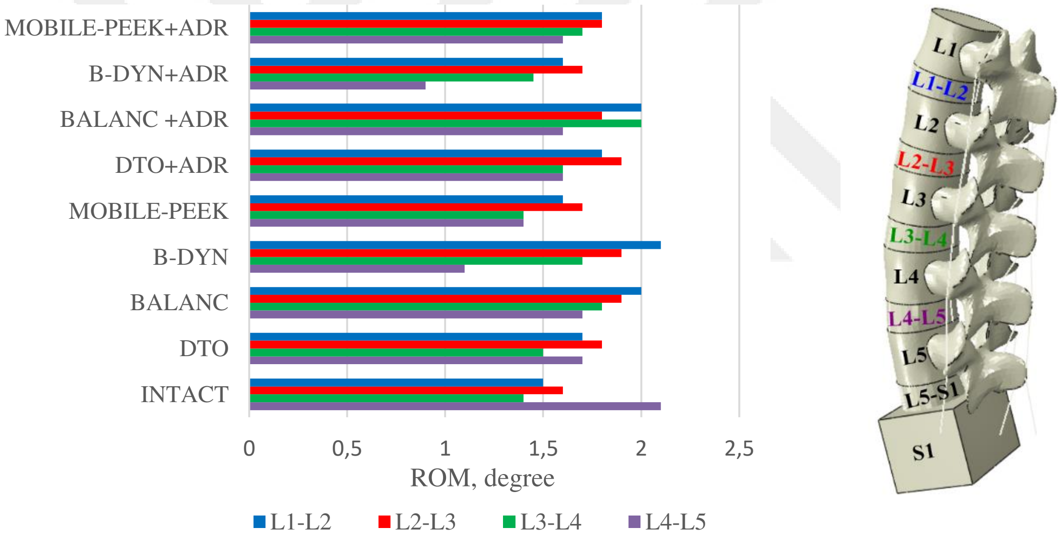


**Figure 4.8** ROM values of L1-L5 in axial rotation

Table 4.4 gives the predicted ROM values at the adjacent level (L3-L4) and the increment percentages in mobility when compared to the intact case. During flexion, ROM values were found lower than the intact spine. During extension, mobility was higher 3% for B-DYN, and 5% for BalanC+ADR that both might be considered as insignificant. Increment during lateral bending was found 2% for DTO and Mobile-PEEK that this value was underestimated. ROM was increased the highest by 42% for BalanC+ADR whereas Mobile-PEEK and B-DYN+ADR did not cause any increment in ROM at the adjacent level.

**Table 4.4** ROM values at the adjacent level

| | | ADJACENT LEVEL (L3-L4 disc) | | | Model |
|---|---|---|---|---|---|
| | | Intact ROM | Instrumented case ROM | Increment % | |
| FLEXION | B-DYN | 4.7 | 4.4 | - | 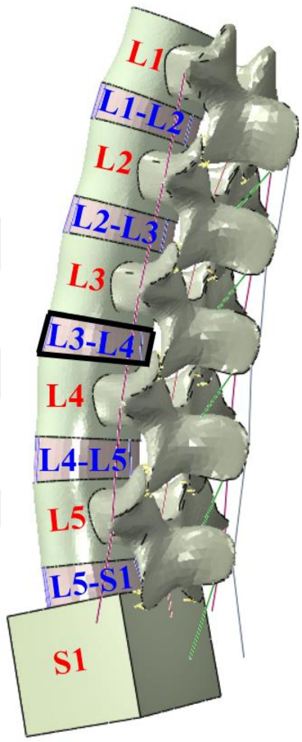 |
| | BalanC | | 4.3 | - | |
| | DTO | | 4.4 | - | |
| | Mobile-PEEK | | 4.6 | - | |
| | B-DYN+ADR | | 4.5 | - | |
| | BalanC+ADR | | 4.6 | - | |
| | Dynesys+ADR | | 4.6 | - | |
| | Mobile-PEEK+ADR | | 4.6 | - | |
| EXTENSION | B-DYN | 3.7 | 3.8 | 3 | |
| | BalanC | | 3.6 | - | |
| | DTO | | 3.5 | - | |
| | Mobile-PEEK | | 3.7 | - | |
| | B-DYN+ADR | | 3.7 | - | |
| | BalanC+ADR | | 3.9 | 5 | |
| | Dynesys+ADR | | 3.7 | - | |
| | Mobile-PEEK+ADR | | 3.7 | - | |
| LATERAL BENDING | B-DYN | 4.5 | 4.2 | - | |
| | BalanC | | 4.5 | - | |
| | DTO | | 4.6 | 2 | |
| | Mobile-PEEK | | 4.6 | 2 | |
| | B-DYN+ADR | | 4.4 | - | |
| | BalanC+ADR | | 4.2 | - | |
| | Dynesys+ADR | | 4.4 | - | |
| | Mobile-PEEK+ADR | | 4.2 | - | |
| AXIAL ROTATION | B-DYN | 1.4 | 1.7 | 21 | |
| | BalanC | | 1.8 | 28 | |
| | DTO | | 1.5 | **7** | |
| | Mobile-PEEK | | 1.4 | - | |
| | B-DYN+ADR | | 1.4 | - | |
| | BalanC+ADR | | 2 | 42 | |
| | Dynesys+ADR | | 1.6 | 14 | |
| | Mobile-PEEK+ADR | | 1.7 | 21 | |



In this thesis, L4-L5 and L5-S1 levels can be named as superior and inferior index level, respectively. Mobility of superior index level (L4-L5) was not completely lost in all implantation cases while inferior index level (L5-S1) did not perform any mobility when mono-segmental fusion procedure was carried out. Disc replacement method preserved motion at this level. The predicted ROM values at superior index level (L3-L4) and the increment percentages in motion were represented in Table 4.5.

During flexion, B-DYN showed the least mobility by 12%, whereas Mobile-PEEK+ADR preserved the motion at most by 21%. During extension, BalanC+ADR and Mobile-PEEK+ADR saved 15% of the motion. B-DYN behaved as the most rigid implant similarly and preserved 8% of the motion. During lateral bending, Dynesys+ADR was found the most rigid implant by 20% of the motion preservation, whereas BalanC+ADR and Mobile-PEEK maintained 35% of the mobility. Axial rotation was able to be restricted less than other rotational directions. B-DYN+ADR behaved more stiff than other HSSs and ROM was saved by 43%. BalanC and DTO were the most flexible and preserved 81% of the motion.

**Table 4.5** ROM values of index level

| | | SUPERIOR INDEX LEVEL L4-L5 | | | |
|---|---|---|---|---|---|
| | | **Intact ROM (degree)** | **Instrumented ROM (degree)** | **Motion preservation %** | **Model** |
| **FLEXION** | B-DYN | 5.2 | 0.6 | 12 | 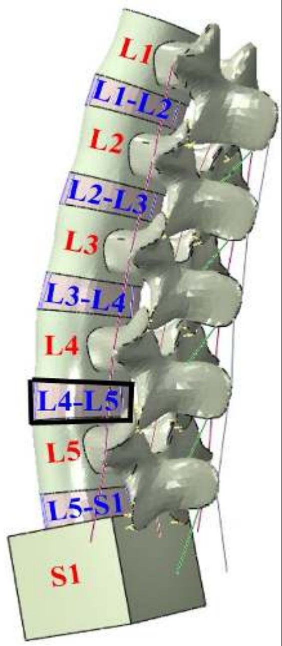 |
| | BalanC | | 0.8 | 15 | |
| | DTO | | 0.65 | 13 | |
| | Mobile-PEEK | | 0.8 | 15 | |
| | B-DYN+ADR | | 0.7 | 13 | |
| | BalanC+ADR | | 1 | 19 | |
| | Dynesys+ADR | | 0.7 | 13 | |
| | Mobile-PEEK+ADR | | 1.1 | 21 | |
| **EXTENSION** | B-DYN | 4.7 | 0.36 | 8 | |
| | BalanC | | 0.6 | 13 | |
| | DTO | | 0.48 | 10 | |
| | Mobile-PEEK | | 0.6 | 13 | |
| | B-DYN+ADR | | 0.6 | 13 | |
| | BalanC+ADR | | 0.7 | 15 | |
| | Dynesys+ADR | | 0.6 | 13 | |
| | Mobile-PEEK+ADR | | 0.7 | 15 | |
| **LATERAL BENDING** | B-DYN | 4.0 | 0.95 | 24 | |
| | BalanC | | 1.3 | 33 | |
| | DTO | | 1.0 | 25 | |
| | Mobile-PEEK | | 1.0 | 25 | |
| | B-DYN+ADR | | 0.9 | 23 | |
| | BalanC+ADR | | 1.4 | 35 | |
| | Dynesys+ADR | | 0.8 | 20 | |
| | Mobile-PEEK+ADR | | 1.4 | 35 | |
| **AXIAL ROTATION** | B-DYN | 2.1 | 1.1 | 52 | |
| | BalanC | | 1.7 | 81 | |
| | DTO | | 1.7 | 81 | |
| | Mobile-PEEK | | 1.4 | 66 | |
| | B-DYN+ADR | | 0.9 | 43 | |
| | BalanC+ADR | | 1.6 | 76 | |
| | Dynesys+ADR | | 1.6 | 76 | |
| | Mobile-PEEK+ADR | | 1.6 | 76 | |

## 4.3 Intradiscal Pressure (IDP) Analysis of Intact and Implanted Spine

IDP values of nucleus pulposus for intact and implanted case were evaluated. IDPs at superior index level (L4-L5) and the adjacent level (L3-L4) of the intact spine were predicted under pure moment of 10 Nm without any follower load. Figure 4.9 shows the IDPs at superior index level (L4-L5) and Figure 4.10 represents the IDPs at the adjacent level (L3-L4). In order to compare with *in vitro* studies, only nucleus part was handled [91-93]. The predicted IDPs at superior index level (L4-L5) of intact spine were determined as 0.27 MPa, 0.36 MPa, 0.39 MPa and 0.12 MPa in flexion, extension, lateral bending and axial rotation, respectively. As expected, HSSs reduced the IDP at superior index level (L4-L5) due to the decreasing load over it.

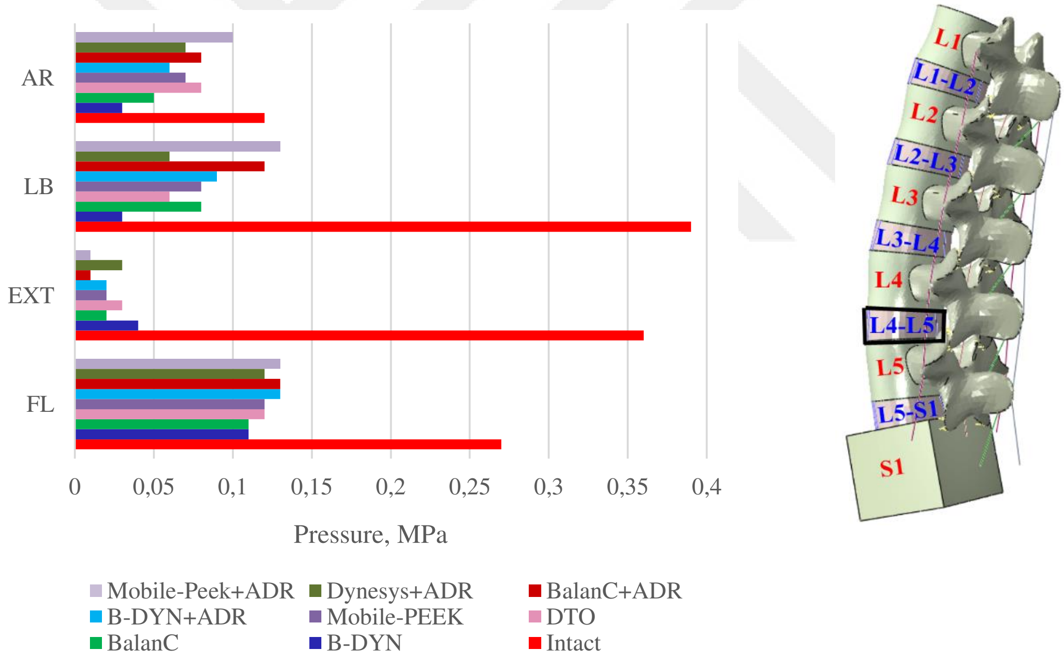


**Figure 4.9** IDPs at superior index level (L4-L5 disc)

The minimum IDP value was found around 0.11 MPa for B-DYN and BalanC implantation during flexion, however any significant difference in IDP did not arise for different HSSs. Minimum IDP value was obtained as 0.01 MPa for BalanC+ADR and Mobile-PEEK+ADR in extension. Minimum IDP values in lateral bending and axial rotation were predicted as 0.03 MPa for B-DYN.

The IDP of the adjacent level (L3-L4) should be taken into account since it is known that high levels of IDP may induce ASD in course of time [68,94]. The maximum IDPs were found as 0.29 MPa, 0.36 MPa, 0.36 MPa and 0.11 MPa in flexion, extension, lateral bending and axial rotation, respectively. No excessive IDP values were detected under flexion and lateral bending. In extension, B-DYN+ADR and Mobile-PEEK+ADR caused the increment by 2.7% that is negligible, whereas BalanC+ADR led to increment by 8%. In axial rotation, BalanC+ADR raised IDP by 18%.

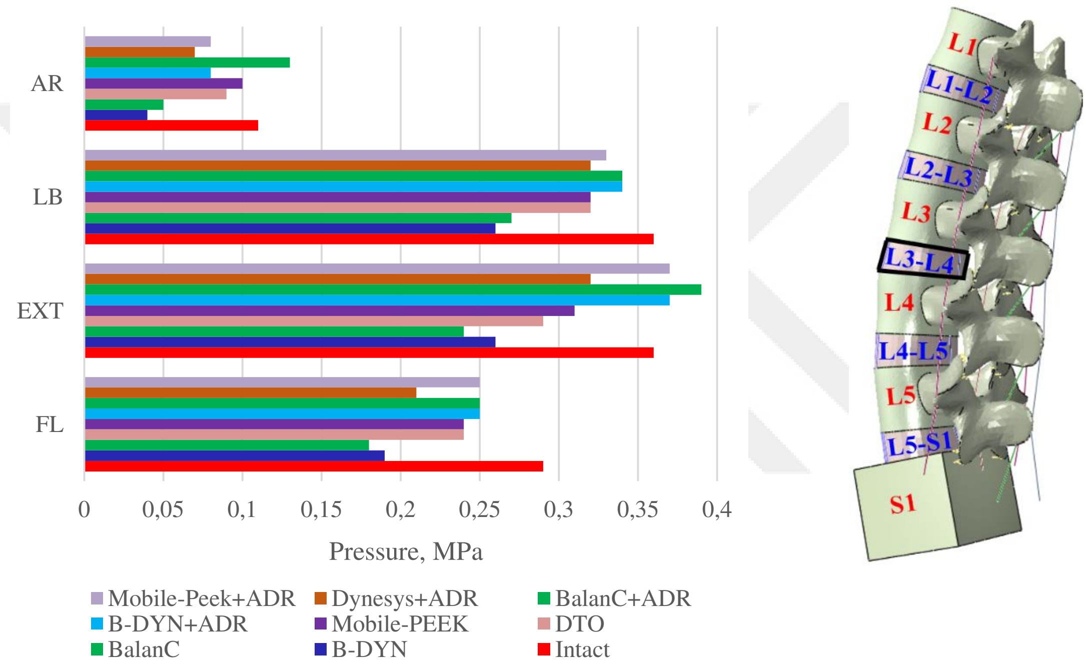


**Figure 4.10** IDPs at the adjacent level (L3-L4 disc)

Pressure distribution at the adjacent level (L3-L4) is given in Figure 4.11. In FL, the anterior part of nucleus pulposus was exposed to compression while posterior part was exposed to tension. In extension, the state changed reverse and compression emerged over the posterior regions. IDPs changed according to the right or left rotation in lateral bending and axial rotation. B-DYN and BalanC showed lower IDPs at the adjacent level (L3-L4) even in combination with ADR. IDPs were found to be lower relatively during axial rotation as the disc was not loaded axially.

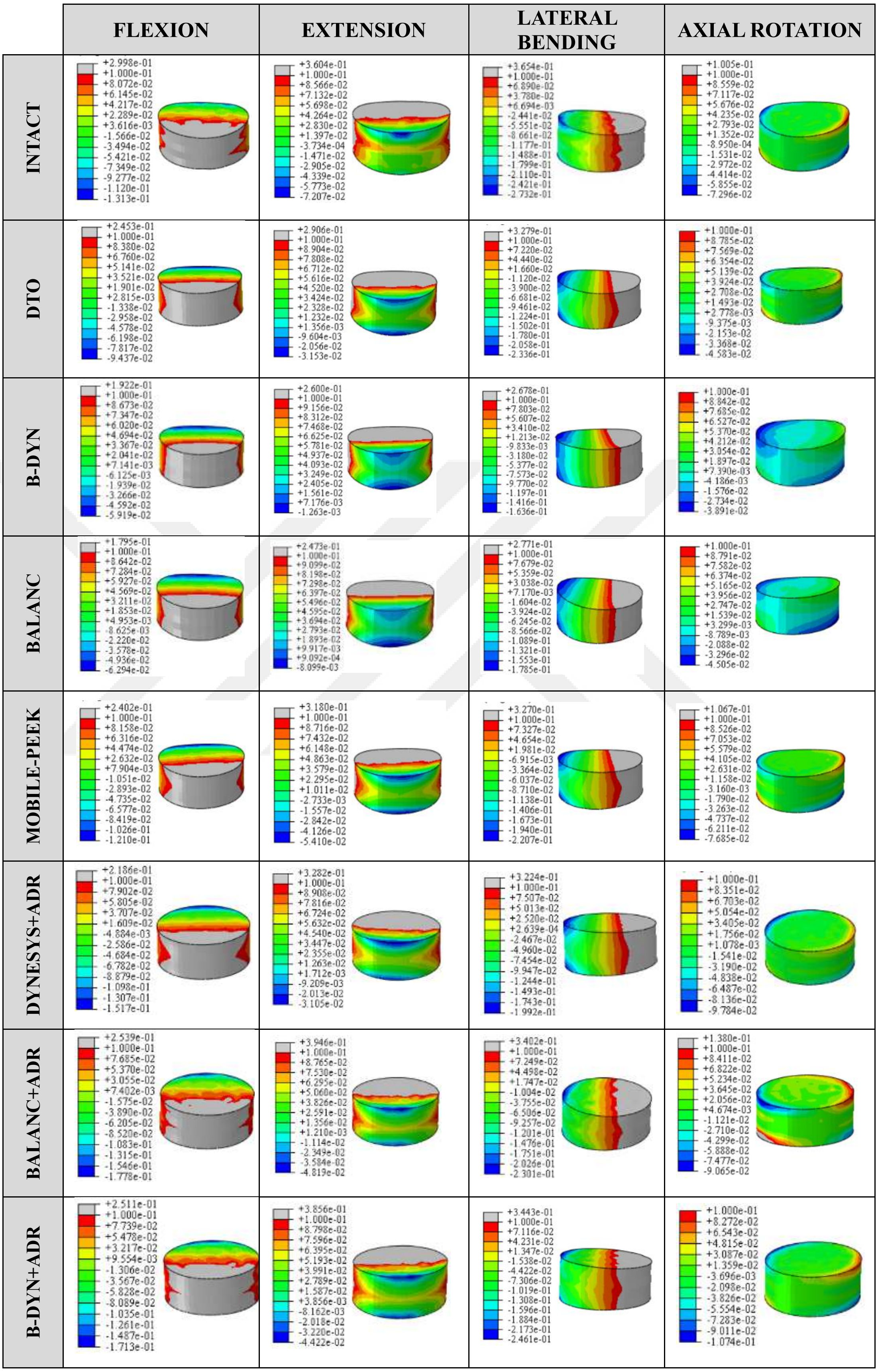
FLEXION
EXTENSION
LATERAL BENDING
AXIAL ROTATION
INTACT
DTO
B-DYN
BALANC
MOBILE-PEEK
DYNESYS+ADR
BALANC+ADR
B-DYN+ADR

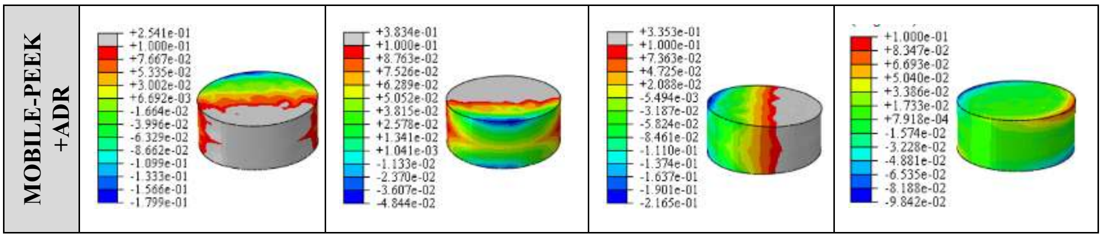


**Figure 4.11** IDPs on nucleus of adjacent level (L3-L4) disc

## 4.4 Stress Analysis of Annulus Fibrosus

Stress distributions over annulus fibrosus are given in Figure 4.12 for the adjacent level (L3-L4). In flexion, anterior part of nucleus was exposed to compressive stress while posterior part was exposed to tensile stress. In extension, the state changed reverse and compressive stress emerged over the posterior regions. Von Mises stress (VMS) distribution changed according to the right or left rotation in lateral bending and axial rotation. In lateral bending, stress values were higher than other loading conditions. VMS were found lowest in axial rotation since the disc was not loaded axially. DTO, Mobile-PEEK and Dynesys+ADR led to the increment in VMS during flexion, extension, lateral bending and minimal change during axial rotation.

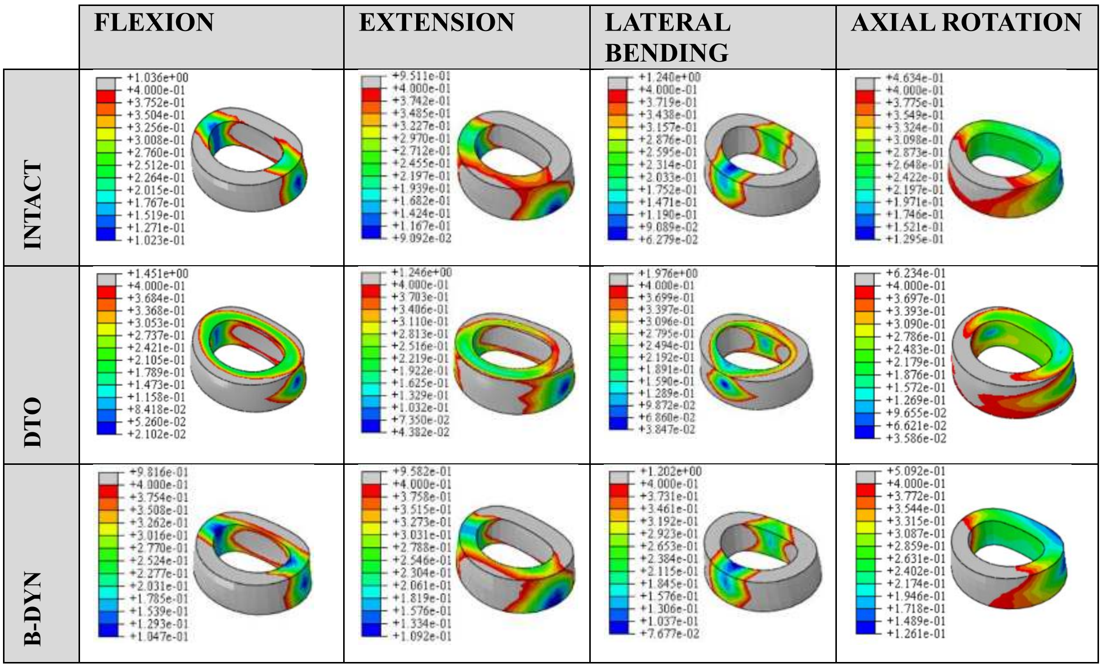

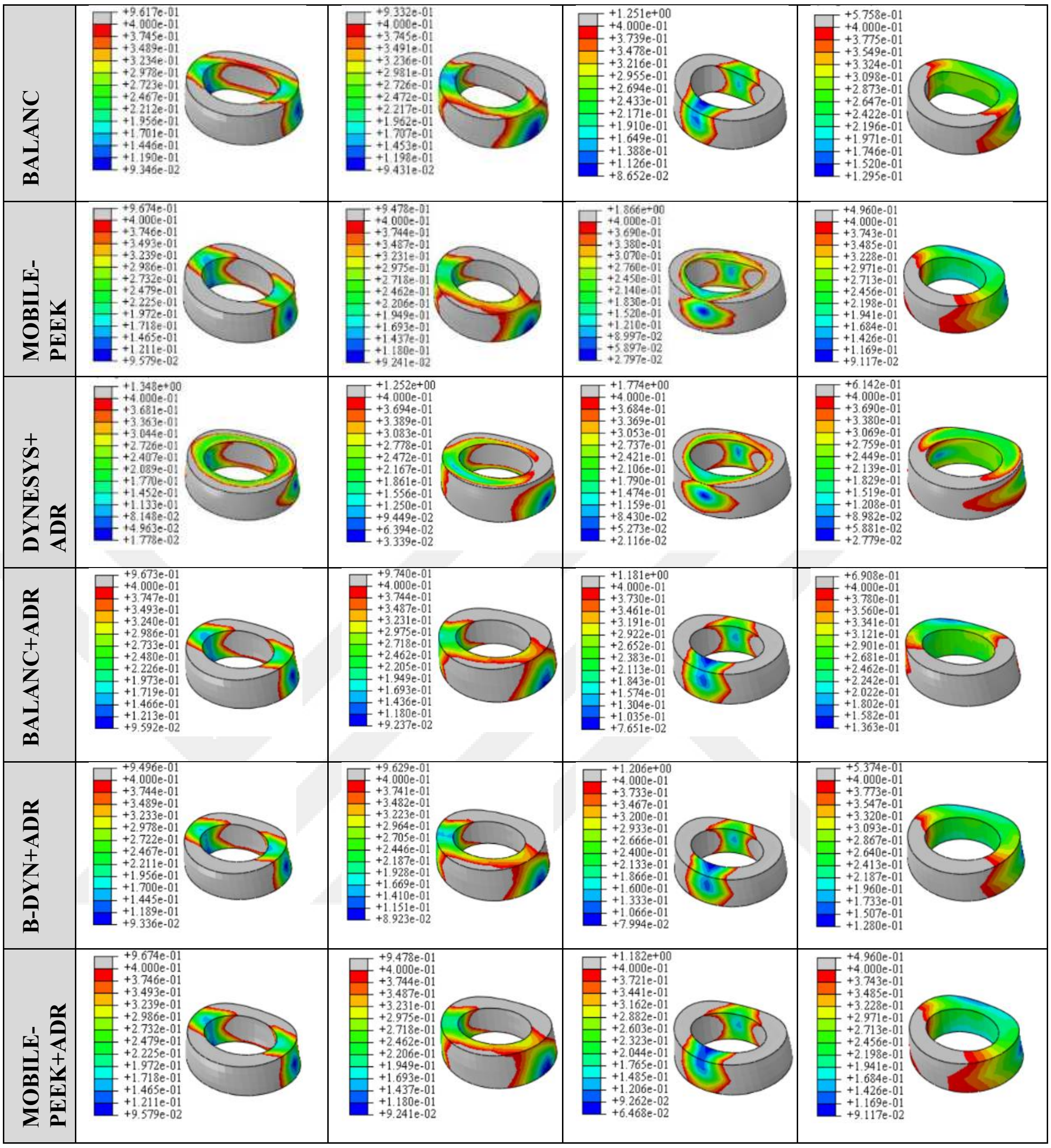


**Figure 4.12** VMS values over annulus of L3-L4 IVD

## 4.5 Stress Analysis of Hybrid Systems

Risk of fracture (RF) value was calculated to be able to compare the stress distribution over stabilization systems. RF is the ratio between the maximum VMS and the yield strength of the implant materials as seen in Equation 4.1. $\sigma_{VMS}$ denoted von Mises stress and $\sigma_{YS}$ denoted yield strength. Yield point was taken as 795 MPa for Titanium [95] and 90 MPa for PEEK [96].

$$RF = \sigma_{VMS}/\sigma_{\mathrm{YS}}100 \tag{4.1}$$

For DTO rods, critical area was found as mating surface between Ti rod and screw that stress rate was significantly high as given in Figure 4.13. Maximum VMS was evaluated over C shape of BalanC that was relatively thinner. Similarly, maximum VMS distributed over Ti rods of B-DYN system where the wall thickness is thinner. When screws of HSSs were handled, B-DYN, having a little more rigidity than others, was also exposed to the highest stress levels. In addition, the regions under stresses were close to the posterior elements of spine; consequently, screw heads and Ti rods were affected more. DTO had lower VMS than DTO and Mobile-PEEK.

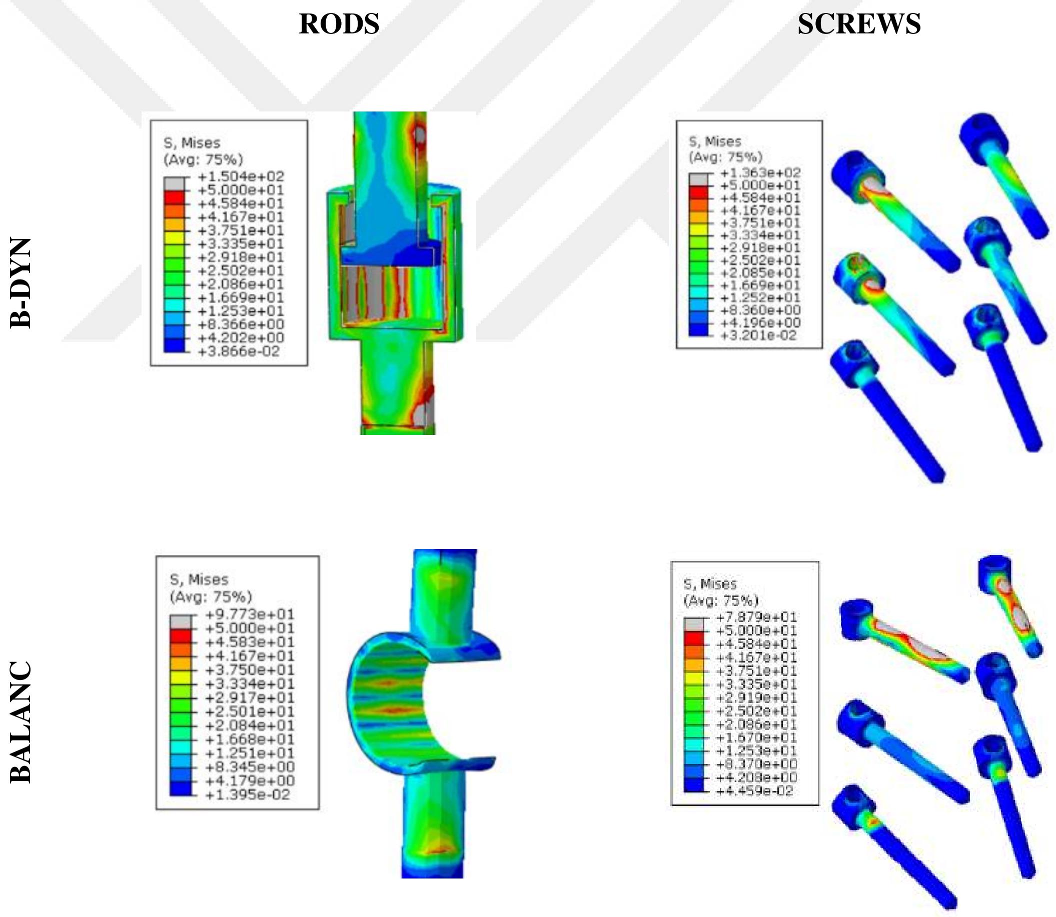

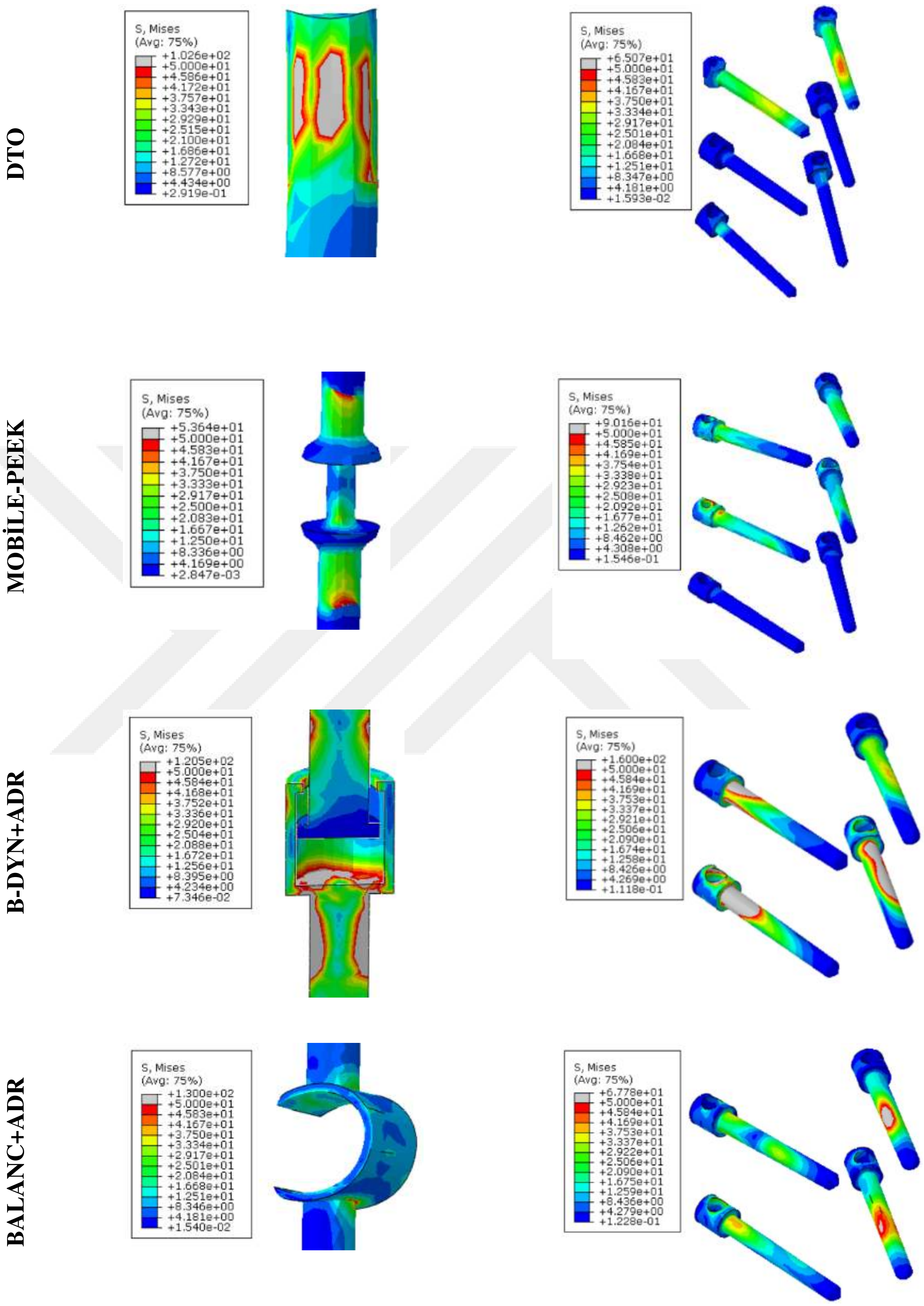
DTO
S, Mises
(Avg: 75%)
+1.026e+02
+5.000e+01
+4.586e+01
+4.172e+01
+3.757e+01
+3.343e+01
+2.929e+01
+2.515e+01
+2.100e+01
+1.686e+01
+1.272e+01
+8.577e+00
+4.434e+00
+2.919e-01
S, Mises
(Avg: 75%)
+6.507e+01
+5.000e+01
+4.583e+01
+4.167e+01
+3.750e+01
+3.334e+01
+2.917e+01
+2.501e+01
+2.084e+01
+1.668e+01
+1.251e+01
+8.347e+00
+4.181e+00
+1.593e-02
MOBİLE-PEEK
S, Mises
(Avg: 75%)
+5.364e+01
+5.000e+01
+4.583e+01
+4.167e+01
+3.750e+01
+3.333e+01
+2.917e+01
+2.500e+01
+2.083e+01
+1.667e+01
+1.250e+01
+8.336e+00
+4.169e+00
+2.847e-03
S, Mises
(Avg: 75%)
+9.016e+01
+5.000e+01
+4.585e+01
+4.169e+01
+3.754e+01
+3.338e+01
+2.923e+01
+2.508e+01
+2.092e+01
+1.677e+01
+1.262e+01
+8.462e+00
+4.308e+00
+1.546e-01
B-DYN+ADR
S, Mises
(Avg: 75%)
+1.205e+02
+5.000e+01
+4.584e+01
+4.168e+01
+3.752e+01
+3.336e+01
+2.920e+01
+2.504e+01
+2.088e+01
+1.672e+01
+1.256e+01
+8.395e+00
+4.234e+00
+7.346e-02
S, Mises
(Avg: 75%)
+1.600e+02
+5.000e+01
+4.584e+01
+4.169e+01
+3.753e+01
+3.337e+01
+2.921e+01
+2.506e+01
+2.090e+01
+1.674e+01
+1.258e+01
+8.426e+00
+4.269e+00
+1.118e-01
BALANC+ADR
S, Mises
(Avg: 75%)
+1.300e+02
+5.000e+01
+4.583e+01
+4.167e+01
+3.750e+01
+3.334e+01
+2.917e+01
+2.501e+01
+2.084e+01
+1.668e+01
+1.251e+01
+8.346e+00
+4.181e+00
+1.540e-02
S, Mises
(Avg: 75%)
+6.778e+01
+5.000e+01
+4.584e+01
+4.169e+01
+3.753e+01
+3.337e+01
+2.922e+01
+2.506e+01
+2.090e+01
+1.675e+01
+1.259e+01
+8.436e+00
+4.279e+00
+1.228e-01

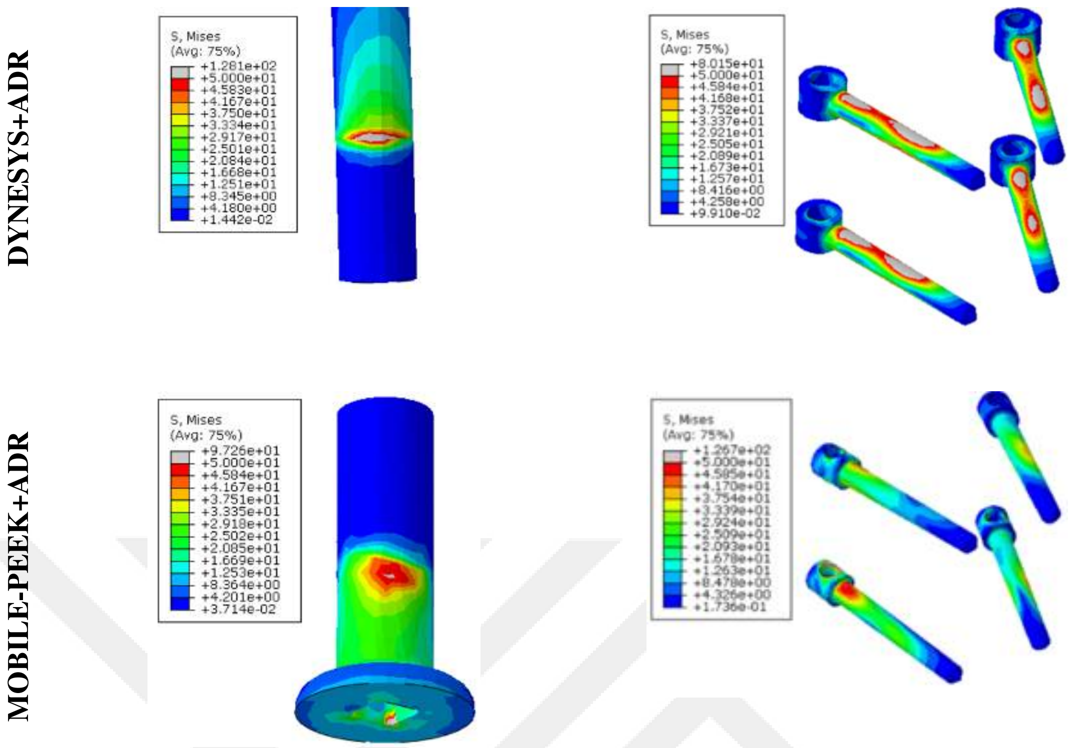


**Figure 4.13** Max VMS on rods and screws of hybrid combinations

### 4.5.1 Von Mises Stresses over Rods

Maximum VMS over rods was evaluated according to the different material properties. Figure 4.14 shows the graphical representation of VMS values for rods. In flexion, maximum VMS was 66 MPa for BalanC+ADR and RF was 73%. In extension, maximum VMS occured for BalanC+ADR and RF was 75%. In lateral bending, maximum VMS was found as 130 MPa for BalanC+ADR where RF was extremely high as 144%.

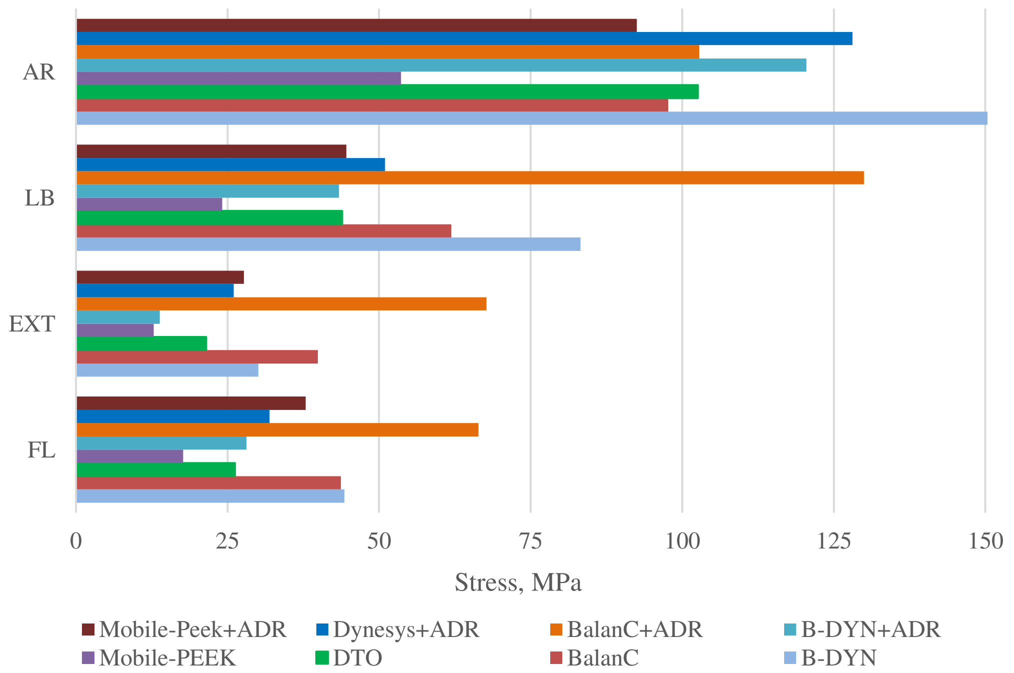


**Figure 4.14** Max VMS on rods

VMS reached to larger values in axial rotation that 150 MPa, 102 MPa, 120 MPa, 128 MPa were evaluated for B-DYN, DTO, B-DYN+ADR and Dynesys+ADR, respectively. However, these values did not exceed the yield point of the Titanium material and RFs were calculated as 19% for B-DYN, 13% for DTO, 15% for B-DYN+ADR and 16% for Dynesys+ADR. VMSs were evaluated as 97 MPa, 53 MPa, 102 MPa and 92 MPa for BalanC, Mobile-PEEK, BalanC+ADR and Mobile-PEEK+ADR, respectively. The risk of fractures were calculated extremely high as 107% for BalanC, 58% for Mobile-PEEK, 113% for BalanC+ADR and 102% for Mobile-PEEK+ADR. BalanC, BalanC+ADR and Mobile-PEEK+ADR systems were prone to failure since VMS values surpassed the $\sigma_{YS}$of PEEK material.

### 4.5.2 Von Mises Stresses over Screws

Maximum VMS over screws were predicted and shown in Figure 4.15. In flexion, extension and lateral bending, low RF values were found since VMS values remained rather less than the yield point of Titanium screws. The maximum RFs were found about 7%, 8% and 10% for flexion, extension and lateral bending, respectively. In axial rotation, maximum VMS of B-DYN+ADR screws was found as 160 MPa where RF was 20%.

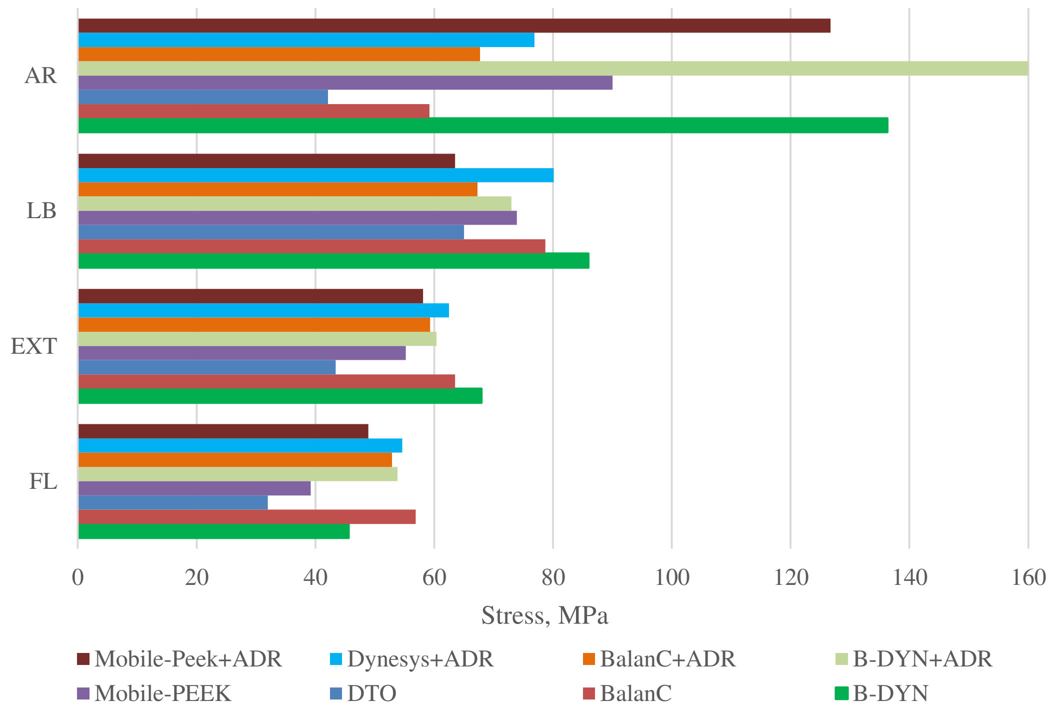


**Figure 4.15** Max VMS on screws

## 4.6 Assessments of ROM, IDP and VMS Results

Table 4.6 summarizes the kinetic and kinematic results obtained in this thesis. Mobility rates at the adjacent level (L3-L4) were found favourable in flexion, extension and lateral bending since any dramatical increments in motion were not observed. In axial rotation, Mobile-PEEK and B-DYN+ADR HSSs did not cause any excessive motion which might degenerative disc disease at this level in time. ROM at superior index level (L4-L5) gave idea about the rigidity of HSSs. Low, medium, high degrees were assigned with respect to the ROM values when compared to each other. The most rigid HSS was B-DYN and DTO in flexion and extension, Dynesys+ADR in lateral bending, B-DYN+ADR in axial rotation. The most flexible HSS was Mobile-PEEK+ADR in flexion, extension and lateral bending, BalanC and DTO in axial rotation.

IDP values were found reasonable in flexion and lateral bending at the adjacent level (L3-L4). BalanC+ADR caused to raise IDP in lateral bending and axial rotation. Any risk of fracture was observed under flexion and extension. BalanC+ADR was prone to the failure during lateral bending. BalanC, BalanC+ADR and Mobile-PEEK+ADR tended to the breakage due to the high stress concentration over their PEEK rods during axial loading.

**Table 4.6** Summary of ROM, IDP and VMS results

| Implantation system | ROM at adjacent level (L3-L4) | | | | ROM at superior index level (L4-L5) | | | | IDP at adjacent level (L3-L4) | | | | VMS on implant components | | | |
|---|---|---|---|---|---|---|---|---|---|---|---|---|---|---|---|---|
| | **FL** | **EX** | **LB** | **AR** | **FL** | **EX** | **LB** | **AR** | **FL** | **EX** | **LB** | **AR** | **FL** | **EX** | **LB** | **AR** |
| **B-DYN** | + | + | + | - | L | L | M | M | + | + | + | + | + | + | + | + |
| **BalanC** | + | + | + | - | M | M | H | H | + | + | + | + | + | + | + | - |
| **DTO** | + | + | + | - | L | L | M | H | + | + | + | + | + | + | + | + |
| **Mobile-PEEK** | + | + | + | + | M | M | M | H | + | + | + | + | + | + | + | + |
| **B-DYN+ADR** | + | + | + | + | M | M | M | M | + | + | + | + | + | + | + | + |
| **BalanC+ADR** | + | + | + | - | H | M | H | H | + | - | + | - | + | + | - | - |
| **Dynesys+ADR** | + | + | + | - | M | M | M | H | + | + | + | + | + | + | + | + |
| **Mobile-PEEK+ADR** | + | + | + | - | H | M | H | H | + | + | + | + | + | + | + | - |

FL:Flexion, EXT:Extension, LB:Lateral Bending, AR:Axial Rotation, L:Low, M:Medium, H:High, (+): Positive effect, (-): Negative effect

# CHAPTER 5 - DISCUSSION

It is possible to say that as the distance to the sacrum increases, a progressive movement of the vertebral bodies is increased under bending moments. At the same time, the IVD motion decreases from L5 to L1. ROM values of intact spine were found to be reasonable according to the literature. ROMs arose in the range of experimental study of Schmoelz et al. [88] where only L2-L4 segments were tested. Yamamoto's results [87] showed more flexible behavior than my model in all rotational directions. However, Eberlein et al. [97] stated that ROM values during flexion were found to be lower than experimental results. To strengthen the validation process, collected data from Dreischarf et al. [86] were included for comparison under 7.5 Nm pure moments. Values of my model were remained within the range of either other participating FE models in Dreischarf's study [89] and in vitro test values [90] in terms of flexion-extension, lateral bending (right+left) and axial rotation (right+left).

In third step of validation, a mass-spring model was created and the problem of rotational motion was solved. When compared with FE results, mobility at levels of L1-L2 and L2-L3 were found very close to each other for both mass-spring and FE models. However, all IVD had almost same mobility for mass-spring model. Intervertebral motion differs from L1 to S1 in real anatomy as revelaed in my model and also Yamamoto' study [87]. This can be explained that FE method is capable of considering the different anatomical, translations/rotations at the same time and evaluate the much more complex equations. Mass-spring model had simpler model and the ligaments covering lumbar spine in real anatomy were underestimated. Ligaments have important effects on the mobility of the lumbar spine. Besides, mechanical properties of L1-L5 vertebrae and intervertebral discs were assumed the same that any ROM difference between L1-L5 discs did not occur. The differences in results can be attributed to these simplifications and assumptions. Additionally, mass-spring model had a damping effect during motion. However, mass-spring model gave rotational motion of L1-S1 that was comparable with FE and *in vitro* results.

Fusion has been considered as a gold standard for the treatment of spinal diseases [3,4]. However, adjacent segment disease occured in case of spinal fusion process that speeds up the degeneration at superior or inferior discs [98-100]. Aunoble et al. [1] suggested that the HSS can be an alternative to the multilevel treatments of spine. Nevertheless, long term clinical studies and following-up are very important for supporting the certain assessments [3,12] and the patient selection is also a critical factor for the good functional outcomes and desired achievements [54]. Lee et al. [17] compared the ROM values of DTO and Nflex systems implanted to the patients who were suffering from spondylolisthesis and severe disc narrowing. They found out that hybrid surgery could maintain the intersegmental motion and delaying adjacent segment disease. Clinical outcomes conducted by Baioni et al. [59] obtained the satisfactory results after 5-year follow-up and found that adjacent segment disease rate was as low as 10%. Maserati et al. [12] investigated the Visual Analogue Scale (VAS) in case of using DTO for arthrodesis with rigid and stabilized dynamically at adjacent level for 24 patients. Their findings were promising in terms of alleviating pain and degenerative disc disease.

In another study, the effects of one level and two-level implantation with DTO device was studied. DTO device was found to limit the ROM at one level. When DTO was used in a hybrid construct, it was found less rigid than rigid fixation [68]. Strube et al. [65] suggested replacing a DTO system adjacent to a single-level fusion, thus adjacent level can be prevented from hypermobility by load-sharing and also limiting ROM of this implanted level. Formica et al. [58] get good clinical outcomes after two year follow-up forty-one patients implanted BalanC who were suffering from one level lumbar degenerative disc disease and initial disc degeneration at the adjacent level. No misalignment of lumbar lordosis or descending of intradiscal height was detected. Herren et al. [57] tested five human cadaveric lumbar spines (L2 to L5) instrumented with BalanC under 7.5 Nm bending moments and besides, compared with one level rigid rod. They revealed that axial rotation was found less restricted. They also stated that BalanC did not lead to any notable effects at adjacent segment under flexion-extension and axial rotation while lateral motion increased by 15%.

Niosi et al. [101] and Cheng et al. [68] carried out *in vitro* studies examining ROMs of implanted spine with Dynesys by applying 7.5 Nm and 6 Nm bending moments, respectively. Niosi et al [101] found that the mobility under flexion, extension and lateral bending could be saved as 27%, 33%, 26%, respectively. Axial rotation capability remained as 76% which is higher than other rotational directions. In this thesis, DTO preserved 13%, 10%, 25% and 81% of motion at superior index level (L4-L5) during flexion, extension, lateral bending and axial rotation, respectively. Dynesys+ADR saved 13%, 13%, 20% and 76% of motion at superior index level (L4-L5) during flexion, extension, lateral bending and axial rotation, respectively. When results were compared to Niosi's study [101], mobility preservation in flexion-extension was found lower in this thesis while the values during lateral bending and axial rotation were close to each other. Cheng et al. [68] showed that 26% of the mobility of both flexion and extension was saved while 41% of lateral bending and 85% of axial motion was preserved. It was seen that motion restriction in axial rotation was similar with my model and Niosi's study [101]. Herren et al. [57] found that the preservation of the motion was found as 36% in flexion-extension, 38% in lateral bending and 82% in axial rotation at the implanted level dynamically (L3-L4). In this thesis, 15%, 13%, 33% and 81% of mobility in case of BalanC implantation were conserved in flexion, extension, lateral bending and axial rotation, respectively. Any dramatical increment was not detected in case of implantation with BalanC+ADR. My results were found compatible with Herren et al. [57] in all loading directions.

One level LP-ESP artificial disc was implemented to the patients to evaluate the sagittal balance and implant functionality [15,46-48]. Lazennec et al. [47] showed that the mean L4-L5 ROM was 4.6º and the mean L5-S1 ROM was 2.7º in case of implantation where the mean L4-L5 ROM was 4.5º and the mean L5-S1 ROM was 2.5º for sagittal motion of the healthy group. In this thesis, ROM of L5-S1 level implanted with LP-ESP was found as 2.5º and this result was consistent with both results of natural lumbar spine motion and Lazennec's study [47]. Lazennec et al. [48] did not find any ASD after 5 years follow-up in case of monosegmental disc replacement with LP-ESP. This was attributed to the viscoelastic nature of LP-ESP disc having no fixed center of rotation. Current study used dynamic implantation superior to LP-ESP disc, therefore it is not possible to provide any supportive data that consonant with this thesis [51].

The outputs of this thesis showed that no excessive motion occurs at the adjacent level (L3-L4) of hybrid systems during flexion and lateral bending while all ADR combinations except Mobile-PEEK and B-DYN+ADR led to the increment in mobility under axial loading. BalanC+ADR and BalanC showed undesirable higher value in axial rotation than the intact case, which may induce adjacent segment disease. ADR involved in hybrid systems provided more flexible structure at superior index level (L4-L5). However, IDP values were not negatively affected, particularly BalanC+ADR caused increment by %8 in extension and 18% in axial rotataion, which may cause the formation of ASD in the time.

L4-L5 and L5-S1 are the most affected segments of the DDD [71]. Rohlmann et al. [91] calculated IDP of L4-L5 level as 0.1 MPa for FL, 0.15 MPa for EXT, 0.1 MPa for LB and 0.08 MPa for AR under 7.5 Nm and 3.75 Nm pure moments. Wilke et al. [92] found higher values than Rohlmann's study [91] under the same moment. Approximately 0.39 MPa for FL and 0.33 MPa for EXT were obtained where L2-L3 and L4-L5 segments were included to tests. Heuer et al. [93] evaluated the IDP of L4-L5 segment as 0.35 MPa where the highest pressure was 0.40 MPa under 10 Nm FL moment. In the same way, 0.16 MPa was found under EXT where the maximum value was 0.36 MPa. In this thesis, IDP was 0.27 MPa for FL, 0.36 MPa for EXT, 0.39 MPa for LB and 0.12 MPa for AR at L4-L5 level under 10 Nm pure moments. To compare the previous studies, the findings seemed to be reasonable, however, Rohlmann's [91] results were remained lower than others.

This thesis showed that VMSs of LP-ESP disc components was quite low and implant failure was not anticipated in agreement with Lazennec et al [46]. Nevertheless, the risk of failure may become a problem for dynamic portions in HSS. The rods of new modified design Mobile-PEEK were exposed to lower stress than other HSS including PEEK rods. Contrary to this, when PEEK is involved in combination with ADR, VMS went up significantly. HSSs such as Dynesys+ADR and B-DYN+ADR, which have more rigidity at their dynamic portion, were found more applicable than others by taking into account IDP and VMS on rods. It can be due to the ADR flexibility, which created undesired motion at the adjacent levels.

In addition, the regions under stresses were close to the posterior elements of spine; consequently, screw heads and Ti rods were affected more. This can be attributed to the low load-sharing capability of B-DYN and loading on the posterior elements is higher than vertebral bodies. On the contrary, BalanC involves more flexible rods and has more load-sharing capability over vertebral bodies. Therefore, stress increased along and towards to the end of the screws. It was seen that instrumenting more spine levels with longer rods reduced both the rod stress and the ROM of the spine model. Increasing the number of screws could help reduce the screw force since load was distributed to more screws.  Axial loading generally produced the largest von Mises stress over implants and screw-bone interaction. Kashkoush et al. [54] investigated developed infections, screw breakages and interbody cage migrations over 66 patients implanted with the DTO system for the treatment of disc herniation and spinal stenosis. Results indicated that the DTO system was reliable and viable technique and there was no higher wound infection or implant failure than conventional systems. It was found that DTO provides relatively less motion in dynamic portion than BalanC, and did not create any significant change in mobility but reduction in IDP at adjacent segment. RF was evaluated as low as 11% for Ti rods and 7% for Ti screws, i.e., there results are compliant with Kashkoush's study [54]. Therefore, the induction of ASD or implant failure are still questionable under the current findings. Oikonomidis et al. [56] found ASD rate of 15% and detected high implant failure (18%) in case of using BalanC. In current study, rods were found to be prone to breakage that this outcome is in agreement with Oikonomidis's study [56]. To the author's best knowledge, number of clinical or numerical studies of B-DYN system is very limited, therefore further clinical studies are needed for more accurate agreements.

Excessive (micro-) mobility and high IVD pressures are undesired phenomena, which very frequently lead to ASD and increment in motion at the adjacent level under AR. However, reasonable lower values of IDP and negligible increments (except AR) in

ROM at adjacent segment were considered as acceptable conditions to prevent or delay ASD, at least for HSS implantation at L4-S1 levels. Even axial rotation may be an important point to consider, i.e., it is possible to say that the residual mobility was still in the moderate range suggested by *in vitro* studies. In addition, higher tendency to breakage of PEEK rod should also be considered within the product development process.

Mobility rates of Mobile-PEEK are comparable with BalanC, but Mobile-PEEK may be preferable with regards to reduction in VMS emerging on the system and reduction of excessive motion at the adjacent level during axial rotation as well. B-DYN+ADR may be introduced as an alternative to Mobile-PEEK in terms of desirable ROM and IDP and VMS ensuring a safe functionality. Even though B-DYN, B-DYN+ADR, DTO and Dynesys+ADR provided more limited mobility at implanted levels, these HSSs of which components are made from Ti presented a durable structure under loading. The reliability of PEEK rods have been still questionable, since the safety factor of a system may be indicative even the VMS remains under the yielding point. Oikonomidis et al. [56] found ASD rate of 15% and revealed high implant failure (18%) with BalanC used, being the outcomes of the current study in terms of implant failure in agreement with that reference. BalanC, BalanC +ADR and Mobile-PEEK+ADR presented higher possibility to break, therefore these combinations could not be proved as reliable solutions.

There are some limitations in the present study. Long term clinical studies which use HSS are essential to obtain more realistic reasoning. Linear-isotropic material properties were applied to the model, since this thesis aimed to establish a biomechanical comparison of the implanted spine models under loading, instead of focusing on material behavior. As so, using linear-isotropic properties may be considered as a reasonable approach, even though the constitutive modeling of the spine is much more complex. The risk of fractures of HSSs were predicted under only static loading. Additionally, HSSs should be tested under cycling loading conditions to evaluate fatigue failure risk of these systems.

# CHAPTER 6 - CONCLUSIONS

This thesis brings a new complete lumbar spine FE model (L1-S1) based on CT data, which is useful for further FE lumbar spine studies. 3D model of a patient was cretaed by considering the real anatomy of human lumbar spine. The most important findings were generated when different HSSs were implanted to the L4-S1 levels: it was shown here that L4-L5 level was dynamically stabilized, not losing all of its natural motion. In addition, IDP was lower for this level, due to decreasing loads for all rotations. This resulted in not having a substantial IDP increment at L3-L4 level after stabilization, as it would be expected by the lighter restrictions imposed on L4-L5 in comparison with rigid fixation. L5-S1 level still had no mobility after disc removal and mono-segmental fusion process. For the HSSs consisting of artificial disc, L5-S1 did not lose its motion. Kinetic (VMS) and kinematical analyses (ROM and IDP) were conducted and compared to literature studies. Current results showed that some important points that should be taken into consideration.

With regard to ROM values;

- ➢ The most rigid hybrid systems were B-DYN and DTO in flexion and extension, Dynesys+ADR in lateral bending, B-DYN+ADR in axial rotation.
- ➢ The most flexible hybrid system was Mobile-PEEK+ADR in flexion, extension and lateral bending, BalanC and DTO in axial rotation.
- ➢ DTO was the most common hybrid systems subjected to the studies and this system can ensure a viable and reliable solution even considering that hypermobility was still a problem for this system at the adjacent level in axial loading.
- ➢ Mobile-PEEK and B-DYN+ADR had no negative effects at the adjacent level; therefore, these systems can be a viable and reliable solution for multilevel disc degeneration.
- ➢ B-DYN, B-DYN+ADR, DTO and Dynesys+ADR including Ti rods behaved like rigid systems, however, they are more reliable in terms of adjacent segment disease.

- B-DYN and DTO involved in the combination with artificial disc behaved more flexible.
- BalanC and Mobile-PEEK, which are more flexible, created undesired motion at the adjacent levels.
- Hypermobility was still a problem at the adjacent level in axial loading, however, Mobile-PEEK and B-DYN+ADR did not cause to rise in motion during axial rotation.
- FEA of the HSSs selected for this work showed that such systems could be effective for maintaining some of the natural lumbar spine motion while reducing the probability for accelerating the adjacent level degeneration.
- The differences in results between mass-spring model and FE model can be attributed to the simplifications and assumptions used in solving of mass-spring problem. Additionally, since mass-spring model had a damping effect during motion.

With regard to IDP;

- HSSs reduced the IDP at superior index level (L4-L5) due to the decreasing load over it.
- BalanC+ADR led to increment in extension and axial rotation at the adjacent level (L3-L4).
- There were no negative effect on IDP of the adjacent level (L3-L4) disc after implantation with HSS.

With regard to VMS;

- B-DYN, B-DYN+ADR, DTO and Dynesys+ADR including Ti rods was found like rigid systems, however, they are more reliable in terms of implant failure.
- The reliability of PEEK rods have been still questionable, since the safety factor of a system may be indicative even the VMS remains under the yielding point.
- BalanC, BalanC +ADR and Mobile-PEEK+ADR including PEEK rods had higher tendency to the failure.

- Instrumenting more spine levels with longer rods reduced both the rod stress and the ROM of the spine model.
- Increasing the number of screws could help reduce the screw force since load was distributed to more screws.

To sum up;

- Mobile-PEEK and B-DYN+ADR represented reasonable results in terms of ROM, IDP and VMS and these HSSs may be viable and reliable solutions for multilevel disc degenerations.
- The outcomes of this thesis may bring a new perspective to the surgeons pre- and post-operations since some design limitations were pointed out.

For future work, further studies are needed whether both anterior and posterior surgeries for multilevel disc degeneration are applicable. Nonlinear mechanical properties can be included for FEA in order to close to the real anatomy and to investigate kinetic and kinematic behavior of lumbar spine in details. Besides, more complicated mathematical models can be studied in different loading conditions in order to strength the validation procedure. In addition to this, HSSs should be tested under cycling loading conditions to provide the knowledge about fatique failure of this mentioned systems. The number of clinical studies subjected to HSS is still limited and potential clinical translation will require further investigation of the long-term effects.

# REFERENCES

[1] Aunoble, S., Meyrat, R., Al Sawad, Y., Tournier, C., Leijssen, P., et al. Hybrid construct for two levels disc disease in lumbar spine. European Spine Journal, 19(2), 290-296, 2010.

[2] Qian, J., Bao, Z., Li, X., Zou, J., & Yang, H. Short-term therapeutic efficacy of the isobar TTL dynamic internal fixation system for the treatment of lumbar degenerative disc diseases. Pain Physician, 19(6), E853-861, 2016.

[3] Hudson, W. R., Gee, J. E., Billys, J. B., & Castellvi, A. E. Hybrid dynamic stabilization with posterior spinal fusion in the lumbar spine. SAS Journal, 5(2), 36-43, 2011.

[4] Schwarzenbach, O., Rohrbach, N., & Berlemann, U. Segment-by-segment stabilization for degenerative disc disease: a hybrid technique. European Spine Journal, 19(6), 1010-1020, 2010.

[5] Jiang, S. & Li, W. Biomechanical study of proximal adjacent segment degeneration after posterior lumbar interbody fusion and fixation: a finite element analysis. Journal of Orthopaedic Surgery and Research, 14(1), 1-7, 2019.

[6] Park, P., Garton, H. J., Gala, V. C., Hoff, J. T., & McGillicuddy, J. E. Adjacent segment disease after lumbar or lumbosacral fusion: review of the literature. Spine, 29(17), 1938-1944, 2004.

[7] Rahm, M. D. & Hall, B. B. Adjacent-segment degeneration after lumbar fusion with instrumentation: a retrospective study. Journal of Spinal Disorders, 9(5), 392-400, 1996.

[8] Rijsbergen, M. V., van Rietbergen, B., Barthelemy, V., Eltes, P., Lazáry, Á., Lacroix, D., et al. Comparison of patient-specific computational models vs. clinical follow-up, for adjacent segment disc degeneration and bone remodelling after spinal fusion. PLoS One, 13(8), e0200899, 2018.

[9] Castellvi, A. E. & Andrew, S. A. Scient'x IsoBar TTL dynamic rod stabilization. Motion Preservation Surgery of the Spine. 3rd ed. Philadelphia: Saunders Elsevier, 483-9, 2008.

[10] Más, Y., Gracia, L., Ibarz, E., Gabarre, S., Peña, D., & Herrera, A. Finite element simulation and clinical follow-up of lumbar spine biomechanics with dynamic fixations. PloS One, 12(11), e0188328, 2017.

[11] Mageswaran, P., Techy, F., Colbrunn, R. W., Bonner, T. F., & McLain, R. F. Hybrid dynamic stabilization: a biomechanical assessment of adjacent and supraadjacent levels of the lumbar spine. Journal of Neurosurgery: Spine, 17(3), 232-242, 2012.

[12] Maserati, M. B., Tormenti, M. J., Panczykowski, D. M., et al. The use of a hybrid dynamic stabilization and fusion system in the lumbar spine: preliminary experience. Neurosurgical Focus, 28(6): E2, 2010.

[13] Panjabi, M., Henderson, G., Abjornson, C., & Yue, J. Multidirectional testing of one-and two-level ProDisc-L versus simulated fusions. Spine, 32(12), 1311-1319, 2007.

[14] Auerbach, J. D., Wills, B. P., McIntosh, T. C., & Balderston, R. A. Evaluation of spinal kinematics following lumbar total disc replacement and circumferential fusion using in vivo fluoroscopy. Spine, 32(5), 527-536, 2007.

[15] Gan, T., Rickenbach, A., Scott-Young, M. Artificial Disc Replacement Surgery in a Professional Australian Rugby League Player: A Case Report. Clinical Journal of Sport Medicine, 30(1):e5-e7, 2010.

[16] Bertagnoli, R., Tropiano, P., Zigler, J., Karg, A., & Voigt, S. Hybrid constructs. Orthopedic Clinics, 36(3), 379-388, 2005.

[17] Lee, S. E., Jahng, T. A., & Kim, H. J. Hybrid surgery combined with dynamic stabilization system and fusion for the multilevel degenerative disease of the lumbosacral spine. International Journal of Spine Surgery, 9, 2015.

[18] Retrieved on September 6, 2021, from https://calspinemd.com/spinal-fractures/.

[19] Herkowitz, H. N. (Ed.). The lumbar spine. Lippincott Williams & Wilkins. 2004.

[20] Bogduk, N. Clinical and Radiological Anatomy of the Lumbar Spine E-Book. Elsevier Health Sciences. 2012.

[21] Patel, V. V., Patel, A., Harrop, J. S., & Burger, E. (Eds.). Spine surgery basics. Springer Berlin Heidelberg. 2014.

[22] Cooper, G. Non-operative treatment of the lumbar spine. Springer. 2015.

[23] Asfour, S. Spine Biomechanics: A Review of Current Approaches. Spine, 1(1), 4. 2015.

[24] Humzah, M. D., & Soames, R. W. Human intervertebral disc: structure and function. The Anatomical Record, 220(4), 337-356, 1988.

[25] Farfan, H. F., Cossette, J. W., Robertson, G. H., Wells, R. V., & Kraus, H. T. The effects of torsion on the lumbar intervertebral joints: the role of torsion in the production of disc degeneration. The Journal of Bone and Joint Surgery, JBJS, 52(3), 468-497, 1970.

[26] Netter, F. H. Atlas of human anatomy, Professional Edition E-Book: including NetterReference. com Access with full downloadable image Bank. Elsevier health sciences. 2014.

[27] Vital, J. M., & Cawley, D. T. (Eds.). Spinal Anatomy: Modern Concepts. Berlin. Springer. 2016.

[28] Hadjipavlou, A. G., Simmons, J. W., Pope, M. H., Necessary, J. T., & Goel, V. K. Pathomechanics and clinical relevance of disc degeneration and annular tear: a point-of-view review. American Journal of Orthopedics (Belle Mead, NJ), 28(10), 561-571, 1999.

[29] Inoue, H. A. J. I. M. E. Three-dimensional architecture of lumbar intervertebral discs. Spine, 6(2), 139-146, 1981.

[30] Iatridis, J. C., Setton, L. A., Weidenbaum, M., & Mow, V. C. Alterations in the mechanical behavior of the human lumbar nucleus pulposus with degeneration and aging. Journal of Orthopaedic Research, 15(2), 318-322, 1997.

[31] Frobin, W., Brinckmann, P., Kramer, M., & Hartwig, E. Height of lumbar discs measured from radiographs compared with degeneration and height classified from MR images. European Radiology, 11(2), 263-269, 2001.

[32] Pollintine, P., Dolan, P., Tobias, J. H., & Adams, M. A. Intervertebral disc degeneration can lead to “stress-shielding” of the anterior vertebral body: a cause of osteoporotic vertebral fracture? Spine, 29(7), 774-782, 2004.

[33] Ozgur, B., Benzel, E., & Garfin, S. (Eds.). Minimally invasive spine surgery: a practical guide to anatomy and techniques. Springer Science and Business Media, 2009.

[34] Weinstein, J. N., Tosteson, T. D., Lurie, J. D., Tosteson, A. N., Blood, E., Hanscom, B., et al. Surgical versus nonsurgical therapy for lumbar spinal stenosis. New England Journal of Medicine, 358(8), 794-810, 2008.

[35] Gionis, T. A., & Groteke, E. Spinal decompression. Orthopedic Technology Review, 5, 36-39, 2003.

[36] Eyerman, E. MRI evidence of mechanical reduction and repair of the torn annulus disc. International Society of Neuroradiologists, 1998.

[37] Chen, C. S., Cheng, C. K., Liu, C. L., & Lo, W. H. Stress analysis of the disc adjacent to interbody fusion in lumbar spine. Medical Engineering and Physics, 23(7), 485-493, 2001.

[38] Mummaneni, P. V., Haid, R. W., & Rodts, G. E. Lumbar interbody fusion: state-of-the-art technical advances: invited submission from the Joint Section Meeting on Disorders of the Spine and Peripheral Nerves, March 2004. Journal of Neurosurgery: Spine, 1(1), 24-30, 2004.

[39] Lehmann, T. R., Spratt, K. F., Tozzi, J. E., Weinstein, J. N., Reinarz, S. J., El-Khoury, et al. Long-term follow-up of lower lumbar fusion patients. Spine, 12(2), 97-104, 1987.

[40] Hilibrand, A. S., & Robbins, M. Adjacent segment degeneration and adjacent segment disease: the consequences of spinal fusion?. The Spine Journal, 4(6), S190-S194, 2004.

[41] Kaner, T., Dalbayrak, S., Oktenoglu, T., Sasani, M., Aydin, A. L., & Ozer, A. F. Comparison of posterior dynamic and posterior rigid transpedicular stabilization with fusion to treat degenerative spondylolisthesis. Orthopedics (Online), 33(5), 2010.

[42] Cunningham, B. W. Basic scientific considerations in total disc arthroplasty. The Spine Journal, 4(6), S219-S230, 2004.

[43] Lee, C. K. Accelerated degeneration of the segment adjacent to a lumbar fusion. Spine, 13(3), 375-377, 1988.

[44] Kim, Y. S., Zhang, H. Y., Moon, B. J., Park, K. W., Ji, K. Y., Lee, et al. Nitinol spring rod dynamic stabilization system and Nitinol memory loops in surgical treatment for lumbar disc disorders: short-term follow-up. Neurosurgical Focus, 22(1), 1-9, 2007.

[45] Retrieved on September 6, 2021, from https://www.esp-disc.com/lombar-prosthesis/

[46] Lazennec, J. Y., Even, J., Skalli, W., Rakover, J. P., Brusson, A., & Rousseau, M. A. Clinical outcomes, radiologic kinematics, and effects on sagittal balance of the 6 df LP-ESP lumbar disc prosthesis. The Spine Journal, 14(9), 1914-1920, 2014.

[47] Lazennec, J. Y., Aaron, A., Brusson, A., Rakover, J. P., & Rousseau, M. A. The LP-ESP® lumbar disc prosthesis with 6 degrees of freedom: development and 7 years of clinical experience. European Journal of Orthopaedic Surgery and Traumatology, 23(2), 131-143, 2013.

[48] Lazennec, J. Y., Rakover, J. P., & Rousseau, M. A. Five-year follow-up of clinical and radiological outcomes of LP-ESP elastomeric lumbar total disc replacement in active patients. The Spine Journal, 19(2), 218-224, 2019.

[49] Mulholland, R. C., & Sengupta, D. K. Rationale, principles and experimental evaluation of the concept of soft stabilization. Arthroplasty of the Spine, 142-149, 2004.

[50] Jahng, T. A., Kim, Y. E., & Moon, K. Y. Comparison of the biomechanical effect of pedicle-based dynamic stabilization: a study using finite element analysis. The Spine Journal, 13(1), 85-94, 2013.

[51] Erbulut, D. U., Kiapour, A., Oktenoglu, T., Ozer, A. F., & Goel, V. K. A computational biomechanical investigation of posterior dynamic instrumentation: combination of dynamic rod and hinged (dynamic) screw. Journal of Biomechanical Engineering, 136(5), 051007, 2014.

[52] Ozer, A. F. Dynamic stabilization of the spine: a new classification system. Turkish Neurosurgery, 20(2), 205-15, 2010.

[53] Kaner, T., & Ozer, A. F. Dynamic stabilization for challenging lumbar degenerative diseases of the spine: a review of the literature. Advances in Orthopedics, 2013.

[54] Kashkoush, A., Agarwal, N., Paschel, E., Goldschmidt, E., & Gerszten, P. C. Evaluation of a hybrid dynamic stabilization and fusion system in the lumbar spine: a 10 year experience. Cureus, 8(6), 2016.

[55] Retrieved on September 6, 2021, from https://www.vasculart.com.ar/product-page/sistema-de-columna-din%C3%A1mico-bdyn-s14

[56] Oikonomidis, S., Ashqar, G., Kaulhausen, T., Herren, C., Siewe, J., & Sobottke, R. Clinical experiences with a PEEK-based dynamic instrumentation device in lumbar spinal surgery: 2 years and no more. Journal of Orthopaedic Surgery and Research, 13(1), 1-10, 2018.

[57] Herren, C., Beckmann, A., Meyer, S., Pishnamaz, M., Mundt, M., Sobottke, et al. Biomechanical testing of a PEEK-based dynamic instrumentation device in a lumbar spine model. Clinical Biomechanics, 44, 67-74, 2017.

[58] Formica, M., Cavagnaro, L., Basso, M., Zanirato, A., Felli, L., & Formica, C. Is it possible to preserve lumbar lordosis after hybrid stabilization? Preliminary results of a novel rigid–dynamic stabilization system in degenerative lumbar pathologies. European Spine Journal, 24(7), 849-854, 2015.

[59] Baioni, A., Di Silvestre, M., Greggi, T., Vommaro, F., Lolli, F., & Scarale, A. Does hybrid fixation prevent junctional disease after posterior fusion for degenerative lumbar disorders? A minimum 5-year follow-up study. European Spine Journal, 24(7), 855-864, 2015.

[60] Fu, L., France, A., Xie, Y., Fang, K., Gan, Y., & Zhang, P. Functional and radiological outcomes of semi-rigid dynamic lumbar stabilization adjacent to single-level fusion after 2 years. Archives of Orthopaedic and Trauma Surgery, 134(5), 605-610, 2014.

[61] Barrey, C., Perrin, G., & Champain, S. Pedicle-screw-based dynamic systems and degenerative lumbar diseases: biomechanical and clinical experiences of dynamic fusion with isobar TTL. International Scholarly Research Notices, 2013.

[62] Tegos, S., Charitidis, C., & Korovessis, P. G. Hybrid Circumferential Fixation for Degenerative Lumbosacral Spine Disease: Posterior Lumbar Interbody Fusion Plus Universal Clamp Rod-Band InstrumentationA Novel Technique for Lumbosacral Fixation. Spine, 39(7), E441-E449, 2014.

[63] Siewe, J., Bredow, J., Oppermann, J., Koy, T., Delank, S., Knoell, P., et al. Evaluation of efficacy of a new hybrid fusion device: a randomized, two-centre controlled trial. BMC Musculoskeletal Disorders, 15(1), 1-9, 2014.

[64] Castelli, R., & Steverlynck, A. Hybrid constructions of the lumbosacral spine: preliminary work-20 cases. Coluna/Columna, 12, 300-303, 2013.

[65] Strube, P., Tohtz, S., Hoff, E., Gross, C., Perka, C., & Putzier, M. Dynamic stabilization adjacent to single-level fusion: part I. Biomechanical effects on lumbar spinal motion. European Spine Journal, 19(12), 2171-2180, 2010.

[66] Tsai, T. H., Kung, S. S., Huang, T. Y., Hwang, Y. F., Chang, C. H., & Hwang, S. L. Posterior dynamic stabilization system (Dynesys) with interbody fusion for treating two-segment lumbar degenerative disc disease. Formosan Journal of Surgery, 46(4), 116-122, 2013.

[67] Kumar, A., Beastall, J., Hughes, J., Karadimas, E. J., Nicol, M., Smith, F., & Wardlaw, D. Disc changes in the bridged and adjacent segments after Dynesys dynamic stabilization system after two years. Spine, 33(26), 2909-291, 2008.

[68] Cheng, B. C., Gordon, J., Cheng, J., & Welch, W. C. Immediate biomechanical effects of lumbar posterior dynamic stabilization above a circumferential fusion. Spine, 32(23), 2551-2557, 2007.

[69] Putzer, M., Ehrlich, I., Rasmussen, J., Gebbeken, N., & Dendorfer, S. Sensitivity of lumbar spine loading to anatomical parameters. Journal of Biomechanics, 49(6), 953-958, 2016.

[70] Dall'Ara, E., Schmidt, R., Pahr, D., Varga, P., Chevalier, Y., Patsch, J., et al. A nonlinear finite element model validation study based on a novel experimental technique for inducing anterior wedge-shape fractures in human vertebral bodies in vitro. Journal of Biomechanics, 43(12), 2374-2380, 2010.

[71] Castro, A. P. G., Paul, C. P. L., Detiger, S. E. L., Smit, T. H., Van Royen, B. J., Pimenta Claro, et al. Long-term creep behavior of the intervertebral disk: comparison between bioreactor data and numerical results. Frontiers in Bioengineering and Biotechnology, 2, 56, 2014.

[72] Shin, D. S., Lee, K., & Kim, D. Biomechanical study of lumbar spine with dynamic stabilization device using finite element method. Computer-Aided Design, 39(7), 559-567, 2007.

[73] Rohlmann, A., Zander, T., Rao, M., & Bergmann, G. Realistic loading conditions for upper body bending. Journal of Biomechanics, 42(7), 884-890, 2009.

[74] Noailly, J., Lacroix, D., & Planell, J. A. Finite element study of a novel intervertebral disc substitute. Spine, 30(20), 2257-2264, 2005.

[75] Zhong, Z. C., Wei, S. H., Wang, J. P., Feng, C. K., Chen, C. S., & Yu, C. H. Finite element analysis of the lumbar spine with a new cage using a topology optimization method. Medical Engineering and Physics, 28(1), 90-98, 2006.

[76] Liu, C. L., Zhong, Z. C., Shih, S. L., Hung, C., Lee, Y. E., et al. Influence of Dynesys system screw profile on adjacent segment and screw. Clinical Spine Surgery, 23(6), 410-417, 2010.

[77] Retrieved on September 6, 2021, from https://www.azom.com

[78] Biswas, J. K., Rana, M., Majumder, S., Karmakar, S. K., & Roychowdhury, A. Effect of two-level pedicle-screw fixation with different rod materials on lumbar spine: a finite element study. Journal of Orthopaedic Science, 23(2), 258-265, 2018.

[79] Liu, C. L., Zhong, Z. C., Hsu, H. W., Shih, S. L., Wang, S. T., Hung, C., et al. Effect of the cord pretension of the Dynesys dynamic stabilisation system on the biomechanics of the lumbar spine: a finite element analysis. European Spine Journal, 20(11), 1850-1858, 2011.

[80] Chen, C. S., Huang, C. H., & Shih, S. L. Biomechanical evaluation of a new pedicle screw-based posterior dynamic stabilization device (Awesome Rod System)-a finite element analysis. BMC Musculoskeletal Disorders, 16(1), 1-8, 2015.

[81] Lin, H. M., Pan, Y. N., Liu, C. L., Huang, L. Y., Huang, C. H., & Chen, C. S. Biomechanical comparison of the K-ROD and Dynesys dynamic spinal fixator systems–a finite element analysis. Bio-medical Materials and Engineering, 23(6), 495-505, 2013.

[82] Kim, H. J., Chun, H. J., Kang, K. T., Moon, S. H., Kim, H. S., Park, et al. The biomechanical effect of pedicle screws' insertion angle and position on the superior adjacent segment in 1 segment lumbar fusion. Spine, 37(19), 1637-1644, 2012.

[83] Dreischarf, M., Schmidt, H., Putzier, M., & Zander, T. Biomechanics of the L5–S1 motion segment after total disc replacement–Influence of iatrogenic distraction, implant positioning and preoperative disc height on the range of motion and loading of facet joints. Journal of Biomechanics, 48(12), 3283-3291, 2015.

[84] Ruberté, L. M., Natarajan, R. N., & Andersson, G. B. Influence of single-level lumbar degenerative disc disease on the behavior of the adjacent segments—a finite element model study. Journal of Biomechanics, 42(3), 341-348, 2009.

[85] Keller, T. S, & Colloca, C. J. A rigid body model of the dynamic posteroanterior motion response of the human lumbar spine. Journal of Manipulative and Physiological Therapeutics. 25, 485-496, 2002.

[86] Keller, T. S., Colloca, C. J. & Béliveau, J. Force-deformation response of the lumbar spine: A sagittal plane model of posteroanterior manipulation and mobilization, Clin. Biomech., 17: 185-196, 2002.

[87] Yamamoto, I. S. A. O., Panjabi, M. M., Crisco, T. R. E. Y., & Oxland, T. O. M. Three-dimensional movements of the whole lumbar spine and lumbosacral joint. Spine, 14(11), 1256-1260, 1989.

[88] Schmoelz, W., Huber, J. F., Nydegger, T., Claes, L., & Wilke, H. J. Dynamic stabilization of the lumbar spine and its effects on adjacent segments: an in vitro experiment. Spine, 28, 418-423, 2003.

[89] Dreischarf, M., Zander, T., Shirazi-Adl, A., Puttlitz, C. M., Adam, C. J., Chen, C. S., et al. Comparison of eight published static finite element models of the intact lumbar spine: predictive power of models improves when combined together. Journal of Biomechanics. 47(8), 1757-1766, 2014.

[90] Rohlmann, A., Neller, S., Claes, L., Bergmann, G., & Wilke, H. J. Influence of a follower load on intradiscal pressure and intersegmental rotation of the lumbar spine. Spine, 26(24), E557-E561, 2001.

[91] Rohlmann, A., Neller, S., Bergmann, G., Graichen, F., Claes, L., & Wilke, H. J. Effect of an internal fixator and a bone graft on intersegmental spinal motion and intradiscal pressure in the adjacent regions. European Spine Journal, 10(4), 301-308, 2001.

[92] Wilke, H. J., Drumm, J., Häussler, K., Mack, C., Steudel, W. I., & Kettler, A. Biomechanical effect of different lumbar interspinous implants on flexibility and intradiscal pressure. European Spine Journal, 17(8), 1049-1056, 2008.

[93] Heuer, F., Schmidt, H., Claes, L., & Wilke, H. J. Stepwise reduction of functional spinal structures increase vertebral translation and intradiscal pressure. Journal of Biomechanics, 40(4), 795-803, 2007.

[94] Castro, A. P. G., & Alves, J. L. Numerical implementation of an osmo-poro-visco-hyperelastic finite element solver: application to the intervertebral disc. Computer Methods in Biomechanics and Biomedical Engineering, 24(5), 538-550, 2021.

[95] Wedemeyer, M., Parent, S., Mahar, A., Odell, T., Swimmer, T., & Newton, P. Titanium versus stainless steel for anterior spinal fusions: an analysis of rod stress as a predictor of rod breakage during physiologic loading in a bovine model. Spine, 32(1), 42-48, 2007.

[96] de Ruiter, L., Janssen, D., Briscoe, A., & Verdonschot, N. The mechanical response of a polyetheretherketone femoral knee implant under a deep squatting loading condition. Proceedings of the Institution of Mechanical Engineers, Part H: Journal of Engineering in Medicine, 231(12), 1204-1212, 2017.

[97] Eberlein, R., Holzapfel, G. A., & Fröhlich, M. Multi-segment FEA of the human lumbar spine including the heterogeneity of the annulus fibrosus. Computational Mechanics, 34(2), 147-163, 2004.

[98] Miyakoshi, N., Abe, E., Shimada, Y., Okuyama, K., Suzuki, T., & Sato, K. Outcome of one-level posterior lumbar interbody fusion for spondylolisthesis and postoperative intervertebral disc degeneration adjacent to the fusion. Spine, 25(14), 1837-1842, 2000.

[99] Ishihara, H., Osada, R., Kanamori, M., Kawaguchi, Y., Ohmori, K., Kimura, T., et al. Minimum 10-year follow-up study of anterior lumbar interbody fusion for isthmic spondylolisthesis. Clinical Spine Surgery, 14(2), 91-99, 2001.

[100] Glaser, J., Stanley, M., Sayre, H., Woody, J., Found, E., & Spratt, K. A 10-year follow-up evaluation of lumbar spine fusion with pedicle screw fixation. Spine, 28(13), 1390-1395, 2003.

[101] Niosi, C. A., Zhu, Q. A., Wilson, D. C., Keynan, O., Wilson, D. R., & Oxland, T. R. Biomechanical characterization of the three-dimensional kinematic behaviour of the Dynesys dynamic stabilization system: an in vitro study. European Spine Journal, 15(6), 913-922, 2006.